“Never underestimate the importance of having fun.
[…] I'm going to keep having fun every day
because there's no other way to play it.”

Prof. Randy Pausch

UNIVERSITA' DI ROMA "LA SAPIENZA"

Facoltà di medicina e psicologia

Dottorato in oncologia digestiva

XXV ciclo

Molecular mechanisms involved in the acquisition of drug resistance in pancreatic cancer cells

Sara Calabretta

Docente guida / Tutor:

Prof. Claudio Sette

Coordinatore:

Prof. Gianfranco Delle Fave

Anno Accademico 2011-2012

INDEX

CHAPTER I

Pancreatic ductal adenocarcinoma (PDAC)

Pancreatic cancer is a neoplastic malignant disease characterized by atypical growth of cells in the pancreas, a glandular organ that is part of the digestive system and endocrine system. The pancreas composed by two different tissues with distinct functions: the exocrine tissue, which is dedicated to the secretion of the enzymes into the digestive tract, helping the digestions of carbohydrates, lipids and proteins; and the endocrine tissue, which produces and release into the blood stream several hormones, including glucagon, insulin and somatostatin. The most common type of pancreatic cancer, accounting for 95% of these tumors, is pancreatic ductal adenocarcinoma (PDAC), which derives from the exocrine component of the pancreas. The remaining 5% originate from islet cells and are classified as neuroendocrine tumors.

PDAC is a common cause of death among solid cancers worldwide (Ferlay J *et al.*, 2010; Siegel R *et al.*, 2012), representing one of the most lethal malignancies. This poor outcome is due to late diagnosis, which often occurs when the disease is locally advanced or metastatic, thus excluding almost any possibility of a curative resection. Moreover, PDAC is an aggressive tumour and displays resistance to current medical treatment, resulting in rapidly spreading and metastatic disease (Vincent A *et al*., 2011). The median survival period is extremely low (Cunningham D *et al*., 2009; Stathis A and Moore MJ, 2010), emphasizing the need for improvement in diagnosis and treatment of this disease.

1.1 Molecular characteristics of PDAC carcinogenesis

The development of PDAC is a stepwise process, involving accumulation of genetic mutations that results in a gain of cell growth, proliferation, and metastatic dissemination. Non-invasive stages of duct lesions have been identified in PDAC preceding invasive carcinoma (Singh M and Maitra A, 2007). The three main premalignant epithelial lesions recognized are pancreatic intraepithelial neoplasia (PanIN), mucinous cystic neoplasia (MCN), and intraductal pancreatic mucinous neoplasia (IPMN). PanIN lesions can be classified in four grades, based on the degree of dysplasia reflected in cytonuclear atypia and architectural change: PanIN-1A, PanIN-1B, PanIN-2, and PanIN-3. PanIN-3 lesions also known as carcinoma-*in-situ*, own all of the characteristics of cancer, like loss of cell polarity, atypical nuclei, frequent mitoses and budding of neoplastic cells in the lumen. However, the growth of the premalignant lesion is non invasive

and remains confined within the basement membrane (Hruban RH *et al*., 2004). The increasing grade of dysplasia of the PanIN lesions manifests the morphological steps that precedes invasive PDAC and are genetically accompanied by genetic alterations in tumor suppressor genes, oncogenes and genes involved in the maintenance of genome stability. An early event in PDAC development is the mutation of the KRAS2 oncogene which is found mutated in 20% of PanIN-1 lesions and this percentage increases with PDAC until 95%. Other genetics alterations concern HER-2/neu, p16, p53, SMAD4, cyclin D1, Ki-67 and *BRCA2* genes, indicating that they are involved in the evolution from preneoplastic to infiltrating ductal carcinoma (Feldmann G *et al*., 2007). (Fig 1).

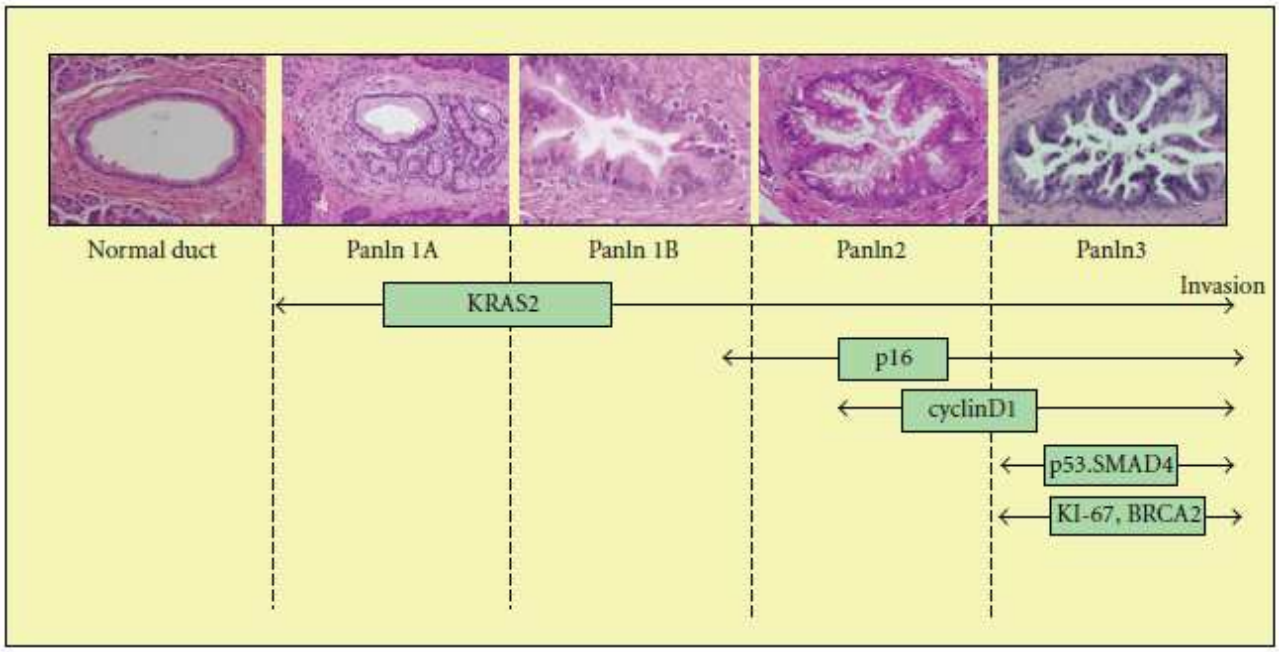

Figure 1: Progression model of PDAC from normal duct to invasive cancer.
The morphological evolution of the neoplasia correlates with the progressive accumulation of specific genetic alterations, highlighted below the pictures. (Ottenhof NA *et al.*, 2011)

Screening of PDAC samples revealed the alterations of five major pathways involved in crucial cellular functions: apoptosis, repair of DNA damage, G1/S phase cell cycle progression, cell adhesion and invasion (Jones S et al., 2008). Despite the increasing evidence that underline the involvement of epigenetics changes (Omura N *et al*., 2009) and alteration of microRNA expression (Szafranska AE *et al*., 2008) in pancreatic carcinogenesis, the hallmark mutations that describe advanced pancreatic intraepithelial neoplasias and invasive carcinomas remain the constitutive activation of KRAS2 oncogene and the inactivation or deletion of the p53 and SMAD4 tumor suppression genes (Ottenhof NA *et al*., 2011).

1.2 Symptoms and risk factors

Early stages of PDAC are usually clinically silent and the symptoms emerge only when the cancer has advanced to a late stage. Typical initial symptoms are abdominal pain, weight loss caused by difficulty in digestion and problems with sugar metabolism. Moreover, as the tumour grows, its mass may block the bile duct, leading to an accumulation of bilirubin in the blood and causing obstructive jaundice.

The etiology of PDAC is still unknown, even though numerous risk factors have been identified, including smoking, alcohol assumption, family history of chronic pancreatitis and pancreatic cancer, advancing age, male sex, diabetes mellitus and central obesity (abdominal obesity), (Zheng W *et al*., 1993). Diet also contributes to cancer risk, in particular the assumption of animal products rich in red meat, while consumption of vegetables and fruits has been suggested as preventive measure. Some genetic syndromes are been described as risk factors for PDAC as Peutz-Jeghers syndrome, familial atypical multiple mole melanoma, ataxia-telangiectasia and hereditary nonpolyposis colon cancer.

1.3 Diagnosis and prognosis

The analysis of pancreatic and liver functions may indicate a possible PDAC, combined with the analysis of the level of CA19-9 (carbohydrate antigen 19.9), a marker that is frequently elevated in pancreatic cancer. To construct a diagnosis and to establish the stage of the disease, multiple imaging techniques can be used to identify the location, the form and the stage of the PDAC. As first line approach, ultrasonography is the diagnostic method most frequently used to search liver alterations while the best initial diagnostic test for pancreatic cancer is computed tomography (CT) scan. Nonetheless, the accuracy of this screening is only about 65% for the lesions up to 2 cm in diameter. Additional imaging techniques can be used to determine possible obstructions of bile ducts and levels of the spreading of the cancer. In order to obtain accurate diagnosis, endoscopic ultrasound is performed, allowing the identification of small neoplastic lesions. This technique is accompanied by a needle biopsy to examine pancreatic cells for signs of cancer, increasing the diagnostic sensitivity up to 80%. However, these procedures still remain vary invasive and bring about risks of developing complications. Positron Emission Tomography/Computed Tomography (PET/CT) is not currently part of routine staging but can

be helpful for the identification of metastatic disease. The early diagnosis of PDAC could be crucial for the cure of the patients, thus searching for innovative markers detectable in bloodstream or biopsy is currently ongoing (McCarthy DM *et al*., 2003).

After diagnosis, the stage of PDAC is determined on the basis of the cancer progression: there are currently four different stages that describes cancer size, lymph node invasion, metastasis and clinical criteria (Varadhachary GR *et al*., 2006). Stage I are the local and resectable cancers, confined to the pancreas and not spread to other tissues, with a median survival period of 17/23 months. Stage II cancers have spread locally with signs of vascularization without reaching the lymph nodes or other tissues, with a median survival period up to 20 months. Currently, the clinical approach of this stage consists in a radiochemotherapy treatment in order to evaluate if cancer may regress to a resectable state. Stage III are the locally advanced or unresectable cancer, which have reached the lymph nodes but have not invaded other tissues whereas the stage IV presents with metastasis. The median survival period is 8–14 months for the stage III and decreases to 4–6 months for the stage IV, with no possibility of surgery.

1.4 Treatment

First line approach to treat PDAC is surgical resection whenever the cancer is confined to pancreas. However, this treatment is reserved to very few cases, due to the surgery-related complications. When cancer is spread to surrounding tissues or in metastasis, therapeutic approaches are aimed to solve the complication caused by the disease (Wray CJ *et al*., 2005). After surgery, adjuvant radiotherapy or chemotherapy has been shown in several large randomized studies to significantly increase the median survival period from approximately 10 to 20%. Chemotherapy is generally used if PDAC is spread and surgery is not suitable for intervention. In this case, palliative chemotherapy may be used to improve quality of life and to obtain a modest survival benefit. Gemcitabine represents the currently standard therapy for patients with advanced pancreatic cancer alone or in combination with other compounds (Burris HA 3rd *et al*., 1997; Storniolo AM *et al*., 1999), can induce a partial response and can alleviate symptoms due to advanced tumours.

Gemcitabine is a nucleoside analog that replaces one of the nucleic acids (cytidine) during DNA replication and it is incorporate into DNA chain. Thus, cancer cells are exposed to a genotoxic stress that arrest tumour growth and cause apoptotic cell death. However, significant results in improvement of survival have not been achieved due to the development of escape pathways that

lead to chemoresistance. Understanding the mechanisms of genotoxic stress resistance and discovery of new therapeutic targets is therefore of clinical importance.

1.5 Role of Epithelial to mesenchymal transition in PDAC

The Epithelial to Mesenchymal Transition (EMT) is a developmental process that allows polarized epithelial cells to undergo multiple changes that enable them to assume a mesenchymal phenotype, characterized by enhanced migratory ability, invasiveness and elevated resistance to apoptosis (Kalluri R *et al*; 2003). It is possible to distinguish epithelial from mesenchymal cells by analyzing specific markers. The epithelial cells are characterized by the expression of a cohort of specific proteins, among which are cytoskeletal proteins (i.e. E-cadherin, cytokeratin; Lee JM *et al*; 2006, Kalluri R *et al*; 2003) and epithelial specific RNA binding proteins (i.e. ESRP1, ESRP2; Warzecha CC *et al*, 2009; Horiguchi K *et al*., 2011). On the contrary, mesenchymal cells are characterized by expression of vimentin and fibronectin (Lee JM *et al*; 2006, Kalluri R *et al*; 2003) and of specific transcription factors that directly or indirectly inhibit the expression of E-cadherin (i.e. SLUG, SNAIL, ZEB1, ZEB2; Lee JM *et al*; 2006, Kalluri R *et al*; 2003) (Fig 2).

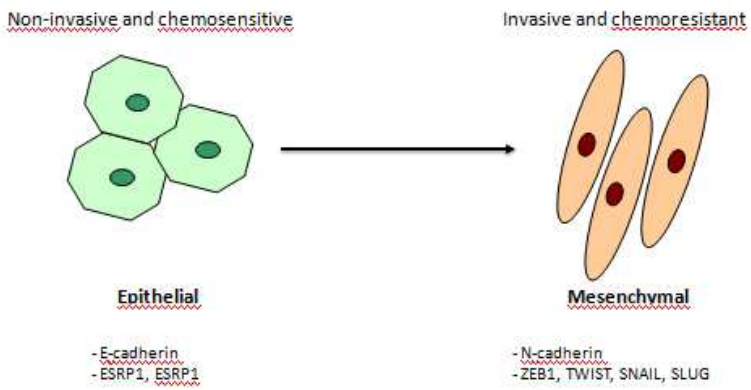

Figure 2: Schematic illustration of EMT rearrangements
Epithelial cells undergo multiple changes that cause their transformation from cobblestone, non invasive and chemosensitive cells to spindle-like, invasive and chemoresistant cells. Principal specific epithelial or mesenchymal markers are indicated.

The EMT process comprises deep rearrangements in gene expression resulting in a finely regulated circuit that involves multiple layers: regulation of gene expression mediated by specific transcription factors (Thiery JP *et al*., 2009), regulation of alternative splicing (De

Craene B *et al*., 2013; Warzecha CC and Carstens RP, 2012) and microRNA regulation (Gregory PA *et al.*, 2008; Cano A and Nieto MA, 2008.).

Neoplastic cells may undergo EMT, thus becoming invasive cells that can promote the onset of metastasis (Thiery JP., 2002). Indeed, spindle-like cells are typically seen at the invasive front of primary tumors and are considered to be responsible for cancer colonization (Thiery JP., 2002; 2009). Moreover, it has been demonstrated that multiple EMT regulators have the ability to enhance tumor formation and/or metastasis (Ren J *et al*., 2013; Naber HP *et al*., 2013; Ferrari-Amorotti G *et al*., 2013; Peinado H *et al*., 2007), strongly indicating that EMT regulates invasiveness and tumor aggressiveness.

It has been demonstrated that EMT has a central role in pancreatic carcinogenesis (Rhim AD *et al*., 2012). Indeed, in a mouse model of PDAC the dissemination of mesenchymal cells appear to occur at a very preliminary stage of the disease (Rhim AD *et al*., 2012), indicating that mesenchymal cells are able to reach and seed distant organs even before, or in parallel to, primary tumor formation. Moreover, the analysis of pathological specimens of PDAC revealed that the expression of EMT markers, in particular expression of the transcription factor ZEB1, correlates with advanced tumor grade and worse prognosis (Maier HJ *et al*., 2010).

EMT has been shown to contribute to drug resistance in several cancer, including PDAC (Shah AN *et al*., 2007). Gene expression profiling of PDAC cell lines demonstrated a strong association between the expression of mesenchymal genes and chemotherapy resistance (Arumugam T *et al*; 2009). In particular, in this study ZEB1 has emerged as upregulated in more resistant cell lines, whereas its silencing restored chemosensitivity and caused re-expression of some epithelial markers. All these observation suggest that the expression of mesenchymal markers may contribute to drug resistance in pancreatic cancer.

References

Arumugam T, Ramachandran V, Fournier KF, Wang H, Marquis L, Abbruzzese JL, Gallick GE, Logsdon CD, McConkey DJ, Choi W. Epithelial to mesenchymal transition contributes to drug resistance in pancreatic cancer. *Cancer Res*. 2009 Jul 15;69(14):5820-8.

Burris HA 3rd, Moore MJ, Andersen J, Green MR, Rothenberg ML, Modiano MR, Cripps MC, Portenoy RK, Storniolo AM, Tarassoff P, Nelson R, Dorr FA,Stephens CD, Von Hoff DD. Improvements in survival and clinical benefit with gemcitabine as first-line therapy for patients with advanced pancreas cancer: a randomized trial. *J Clin Oncol* 1997; 15: 2403–13.

Cano A, Nieto MA. Non-coding RNAs take centre stage in epithelial-to-mesenchymal transition. *Trends Cell Biol*. 2008 Aug;18(8):357-9.

Cunningham D, Chau I, Stocken DD, Valle JW, Smith D, Steward W, Harper PG, Dunn J, Tudur-Smith C, West J, Falk S, Crellin A, Adab F, Thompson J,Leonard P, Ostrowski J, Eatock M, Scheithauer W, Herrmann R, Neoptolemos JP, Phase III randomized comparison of gemcitabine versus gemcitabine plus capecitabine in patients with advanced pancreatic cancer. *J Clin Oncol. 2*009 Nov 20;27(33):5513-8.

De Craene B, Berx G. Regulatory networks defining EMT during cancer initiation and progression. *Nat Rev Cancer*. 2013 Feb;13(2):97-110.

Feldmann G, Beaty R, Hruban RH, Maitra A. Molecular genetics of pancreatic intraepithelial neoplasia. *J Hepatobiliary Pancreat Surg.* 2007;14(3):224-32.

Ferlay J, Parkin DM, Steliarova-Foucher E, Estimates of cancer incidence and mortality in Europe in 2008. *Eur J Cancer* 2010 Mar;46(4):765-81.

Ferrari-Amorotti G, Fragliasso V, Esteki R, Prudente Z, Soliera AR, Cattelani S, Manzotti G, Grisendi G, Dominici M, Pieraccioli M,Raschellà G, Chiodoni C, Colombo MP, Calabretta B. Inhibiting interactions of lysine demethylase LSD1 with snail/slug blocks cancer cell invasion. *Cancer Res.* 2013 Jan 1;73(1):235-45.

Gregory PA, Bracken CP, Bert AG, Goodall GJ. MicroRNAs as regulators of epithelial-mesenchymal transition. *Cell Cycle*. 2008 Oct;7(20):3112-8.

Horiguchi K, Sakamoto K, Koinuma D, Semba K, Inoue A, Inoue S, Fujii H, Yamaguchi A, Miyazawa K, Miyazono K, Saitoh M. TGF-β drives epithelial-mesenchymal transition through δEF1-mediated downregulation of ESRP. *Oncogene*. 2012 Jun 28;31(26):3190-201.

Hruban RH, Takaori K, Klimstra DS, Adsay NV, Albores-Saavedra J, Biankin AV, Biankin SA, Compton C, Fukushima N, Furukawa T, Goggins M, Kato Y, Klöppel G, Longnecker DS, Lüttges J, Maitra A, Offerhaus GJ, Shimizu M,Yonezawa S. An illustrated consensus on the classification of pancreatic intraepithelialneoplasia and intraductal papillary mucinous neopla sms. *Am J Surg Pathol*. 2004 Aug;28(8):977-87.

Jones S, Zhang X, Parsons DW, Lin JC, Leary RJ, Angenendt P, Mankoo P, Carter H, Kamiyama H, Jimeno A, Hong SM, Fu B, Lin MT, Calhoun ES, Kamiyama M, Walter K,

Nikolskaya T, Nikolsky Y, Hartigan J, Smith DR, Hidalgo M, Leach SD, Klein AP, Jaffee EM, Goggins M, Maitra A, Iacobuzio-Donahue C, Eshleman JR, Kern SE, Hruban RH, Karchin R, Papadopoulos N, ParmigianiG,VogelsteinB,VelculescuVE,KinzlerKW. Core signaling pathways in human pancreatic cancers revealed by global genomic analyses. *Science*. 2008 Sep 26;321(5897):1801-6.

Kalluri R, Neilson EG. Epithelial-mesenchymal transition and its implications for fibrosis. *J Clin Invest*. 2003 Dec;112(12):1776-84.

Lee JM, Dedhar S, Kalluri R, Thompson EW. The epithelial-mesenchymal transition: new insights in signaling, development, and disease. *J Cell Biol*. 2006 Mar 27;172(7):973-81.

Maier HJ, Schmidt-Strassburger U, Huber MA, Wiedemann EM, Beug H, Wirth T. NF-kappaB promotes epithelial-mesenchymal transition, migration and invasion of pancreatic carcinoma cells. *Cancer Lett.* 2010 Sep 28;295(2):214-28.

McCarthy DM, Maitra A, Argani P, et al. Novel markers of pancreatic adenocarcinoma in fine-needle aspiration: mesothelin and prostate stem cell antigen labeling increases accuracy in cytologically borderline cases. *Appl Immunohistochem Mol Morphol* 2003; 11: 238–43.

Naber HP, Drabsch Y, Snaar-Jagalska BE, Ten Dijke P, van Laar T. Snail and Slug, key regulators of TGF-β-induced EMT, are sufficient for the induction of single-cell invasion. *Biochem Biophys Res Commun.* 2013 May 24;435(1):58-63

Omura N, Goggins M. Epigenetics and epigenetic alterations in pancreatic cancer. *Int J Clin Exp Pathol* 2009; 2: 310–26

Ottenhof NA, de Wilde RF, Maitra A, Hruban RH, Offerhaus GJ. Molecular characteristics of pancreatic ductal adenocarcinoma. *Patholog Res Int*. 2011 Mar 27;2011:620601.

Peinado H, Olmeda D, Cano A. Snail, Zeb and bHLH factors in tumour progression: an alliance against the epithelial phenotype? *Nat Rev Cancer*. 2007 Jun;7(6):415-28.

Ren J, Chen Y, Song H, Chen L, Wang R. Inhibition of ZEB1 reverses EMT and chemoresistance in docetaxel-resistant human lung adenocarcinoma cell line. *J Cell Biochem.* 2013 Jun;114(6):1395-403.

Shah AN, Summy JM, Zhang J, Park SI, Parikh NU, Gallick GE. Development and characterization of gemcitabine-resistant pancreatic tumor cells. *Ann Surg Oncol.* 2007 Dec;14(12):3629-37.

Siegel R, Naishadham D, Jemal A, Cancer statistics, 2012. *CA Cancer J Clin*. 2012 Jan-Feb;62(1):10-29

Singh M and Maitra A, Precursor lesions of pancreatic cancer: molecular pathology and clinical implications, *Pancreatology*, 2007 7, 9–19

Stathis A, Moore MJ, Advanced pancreatic carcinoma: current treatment and future challenges. *Nat Rev Clin Oncol*. 2010 Mar;7(3):163-72

Storniolo AM, Enas NH, Brown CA, Voi M, Rothenberg ML, Schilsky R. An investigational new drug treatment program for patients with gemcitabine: results for over 3000 patients with pancreatic carcinoma. *Cancer* 1999; 85: 1261–68.

Szafranska AE, Doleshal M, Edmunds HS, et al. Analysis ofmicroRNAs in pancreatic fine-needle aspirates can classify benign and malignant tissues. *Clin Chem* 2008; 54: 1716–24.

Thiery JP. Epithelial-mesenchymal transitions in tumour progression. *Nat Rev Cancer*. 2002 Jun;2(6):442-54.

Varadhachary GR, Tamm EP, Abbruzzese JL, et al. Borderline resectable pancreatic cancer: definitions, management, and role of preoperative therapy. *Ann Surg Oncol* 2006; 13: 1035–46.

Vincent A, Herman J, Schulick R, Hruban RH, Goggins M, Pancreatic cancer. *Lancet*. 2011 Aug 13;378(9791):607-20.

Warzecha CC, Carstens RP. Complex changes in alternative pre-mRNA splicing play a central role in the epithelial-to-mesenchymal transition (EMT). *Semin Cancer Biol*. 2012 Oct;22(5-6):417-27.

Warzecha CC, Sato TK, Nabet B, Hogenesch JB, Carstens RP. ESRP1 and ESRP2 are epithelial cell-type-specific regulators of FGFR2 splicing. *Mol Cell*. 2009 Mar 13;33(5):591-601.

Wray CJ, Ahmad SA, Matthews JB, Lowy AM. Surgery for pancreatic cancer: recent controversies and current practice. *Gastroenterology*. 2005 May;128(6):1626-41.

Zheng W, McLaughlin JK, Gridley G, Bjelke E, Schuman LM, Silverman DT, Wacholder S, Co-Chien HT, Blot WJ, Fraumeni JF Jr, A cohort study of smoking, alcohol consumption, and dietary factors for pancreatic cancer (United States). *Cancer Causes Control*. 1993 Sep;4(5):477-82.

CHAPTER II

Genotoxic stress and pancreatic adenocarcinoma

Cancer cells have developed several escape pathways to cope with a wide range of stresses, adopting a series of mechanisms that allow cell survival even in the hostile environment. Among the various types of stresses, DNA damaging agents, which are able to affect the integrity of the genome, are widely studied, since they are commonly used in cancer therapy. Most chemotherapeutic drugs directly induce breaks in the genome that injure the DNA chain or damage the DNA indirectly, like the topoisomerase inhibitors that target DNA processing enzymes. Another class of DNA damaging agents are the antimetabolites, chemical compounds which mimic purines or pyrimidines. They are incorporated in the DNA during the S-phase (synthesis phase) of the cell cycle in which DNA is replicated, interfering with DNA production and therefore with normal cell division and growth. Since cancer cells grow faster than normal cells, the inhibition of DNA synthesis affects tumor cells more drastically. Although most cells are sensitive to DNA damaging agents, some cancer cells often escape to this damage thereby surviving to drug treatments. Thus, identification of the molecular mechanisms promoting cancer cell survival to genotoxic insults may represent a strategy for improving current therapies.

The first-line treatment of locally and advanced PDAC is gemcitabine (dFdC, 2',2'-difluorodeoxycytidine), a deoxycytidine nucleoside analogue (Burris HA 3rd *et al*., 1997). Like for other nucleoside analogues, the effect of gemcitabine is exerted by its phosphorylated metabolites. The transport of gemcitabine into the cell is due to nucleoside transporters, then the drug is phosphorylated to the monophosphate (dFdCMP) form by the deoxycytidine kinase (dCK). Then, other kinases further phosphorylate dFdCMP to its two active diphosphate and triphosphate (dFdCTP) forms (Plunkett W *et al*., 1995; Mini E *et al*., 2006). The resulting active form dFdCTP, competes with the natural deoxycytidine-triphosphate for incorporation in the nascent DNA and RNA chains causing premature termination (Huang P *et al*., 1991). The peculiar features that made gemcitabine the elective agent for the treatment of PDAC are the efficient intracellular phosphorylation and its slow rate of elimination (Gesto DS *et al*., 2012). Nevertheless, gemcitabine offers only a marginal benefit in terms of improvement in median survival of patients affected by locally advanced or metastatic cancer (Ying JE *et al*., 2012). Hence, PDACs show an initial response to chemotherapy followed by rapid development of drug

resistance that allows cancer survival. Although several molecular mechanisms to explain the acquired resistance have been proposed (Kim MP and Gallick GE, 2008), the full comprehension of the origins of this phenomenon is still lacking.

2.1 Role of RNA binding proteins in genotoxic stress response

In response to DNA damage, cells react by regulating gene expression at many levels. One of the most characterized ones is the inhibition of transcriptional activity that is accomplished through degradation of the RNA polymerase II (RNAPII) (Kleiman FE *et al*., 2005). This process allows cells to repair the damaged DNA and to overcome the injury. In addition to alteration of transcription, recent evidence shows that profound changes in post-trascriptional regulation of gene expression occurs in response of genotoxic stress. In particular, high-throughput screening of the mammalian transcriptome revealed that a large number of alternative splicing (AS) events are differentially regulated after genotoxic treatments (Muñoz MJ *et al*., 2009; Dutertre M *et al*., 2010; Paronetto MP *et al*., 2011), suggesting that AS may play an important role in cell response and survival to DNA damage. AS is one of the major molecular processes involved in the pre-mRNA maturation. It mediates the elimination of the intronic sequences and the inclusion or the exclusion of the exons in the mature mRNA transcript. The resulting differential assortment of exons contributes to genome plasticity, creating from a single precursor transcript different mRNAs that give rise to multiple protein isoforms with different chemical and biological activities (Wang ET *et al*, 2008). The macromolecular complex that operates the splicing reaction is the spliceosome. Its structure is mainly composed of five small nuclear ribonucleoprotein particles (snRNPs) and a great number of auxiliary proteins that cooperate with the spliceosome to accurately recognize the splice sites and to catalyze the splicing reaction (Black DL, 2003). Moreover, several RNA binding proteins (RBPs), also called splicing factors (SF), participate in the regulation of AS events, through the binding of specific sequence in the transcript. Two main families of SFs are: the serine/arginine-rich (SR) proteins, which generally act as positive regulators of exon inclusion (Manley JL and Tacke R, 1996) and the heterogeneous nuclear ribonucleoproteins (hnRNPs), which generally mediate exonic silencing (Krecic AM and Swanson MS, 1999).

As mentioned above, AS regulation is part of the cellular response to genotoxic stress. Indeed, it has been demonstrated that alterations in AS variants occurs in cancer cells in response to UV light, cisplatin or etoposide treatment (Muñoz MJ *et al*., 2009; Solier S *et al*., 2004; Paronetto et al., 2011). Interestingly, a group of genes that encode for apoptotic proteins are regulated by AS

after DNA damage. For instance treatment with inhibitors of topoisomerase I or II favors the inclusion of exon 9 in the caspase 2 transcript, thus promoting an anti-apoptotic isoform (Solier S *et al*., 2004). Treatment with DNA damaging agents also affects AS of transcript involved in cell motility (i.e. CD44, Filippov V *et al*., 2007) and proliferation (i.e. Cyclin D1b, Muñoz MJ *et al*., 2009; MDM2 and MDM4, Chandler DS *et al.*, 2006). Changes in AS in response to genotoxic stress are accompanied by modulation of SF activity, through the modulation of SF cellular localization or the regulation of their post-translational modifications. UV treatment causes a relocalization of hnRNPA1 from the nucleus to the cytoplasm, thereby probably affecting hnRNPA1 mediated splicing events (Guil S *et al*., 2006; Biamonti G and Caceres JF, 2009). Relocalization in nuclear compartments it is also been observed: after genotoxic stress the DDX5 and EWS RNA binding proteins move to nucleoli (Cohen AA *et al*., 2008; Paronetto et al., 2011) while a cohort of SFs localize to DNA repair foci where actively contributes to the repair of the damage (Gaudreault I *et al*., 2004; Mirkin N *et al*., 2008). Co-localization with foci of active RNAPII has also been observed for the splicing regulator SAM68 after genotoxic treatment, indicating that residual splicing activity still occurs when cancer cells undergo to hostile insults (Busà R *et al*., 2010).

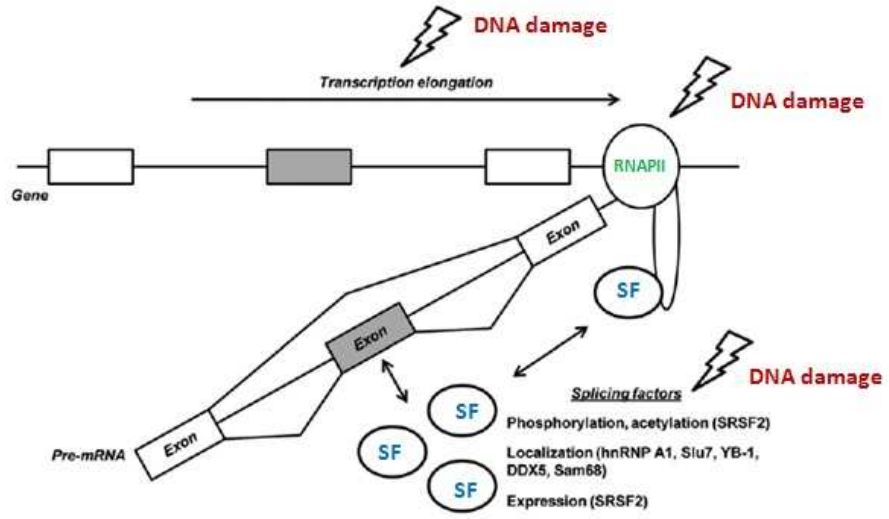

Figure 3: Impact of DNA damage on alternative splicing
Genotoxic stress cause an alteration of transcription by regulating RNAPII activity and stability, accompanied by changes in SF activity. Thus, in this way cancer cell are able to overcome hostile stimuli, surviving to drug treatments. (Modified by Dutertre M *et al*., 2011)

Phosphorylation, acetylation and general changes in protein expression of SFs were observed as consequences of DNA damage, thereby adding a further level of regulation of AS that might be involved in cancer cell escape to injury. Remarkably, significant cellular pathways that are activated after stress contributes to the regulation of SFs, like ATM/ATR protein kinases that tune the activity of many RBPs (Matsuoka S *et al*., 2007) and AKT that phoshorylates SRSF1 thereby regulating its splicing activity (Shultz JC *et al*., 2010). Collectively, all these observations demonstrate that cells respond to DNA damage adapting gene expression through changes in the regulation of AS (Fig 3). Thus, cancer cells are able to adapt themselves to hostile stimuli that cause genome instability in order to overcome stressful situations and thereby survive to genotoxic treatments. Targeting the activity of SFs involved in this escape pathway can be an important way to overcome the mechanisms of cell survival and might represent a suitable novel approaches to clinical treatments of cancer.

2.2 Role of eIF4E in genotoxic stress response

Stressful situations can lead to changes in translation initiation, a process that is strongly regulated since it has important regulatory functions in cell metabolism. The limiting step of the regulation of translation is the assembly of the eukaryotic initiation complex (eIF4F) on the mRNA 5' cap. This complex is composed by the eukaryotic translation initiation factor 4E (eIF4E), which binds to the 5' terminal 7-methyl-GTP (m7GTP) cap of all mRNAs; a scaffold protein named eukaryotic translation initiation factor 4 gamma (eIF4G) and the RNA helicase named eukaryotic initiation factor 4A (eIF4A), which allows melting of the secondary structure of mRNA. Immediately after eIF4F formation, additional factors and ribosomal components are recruited thereby allowing the initiation of translation from the nearest start codon (Aitken CE and Lorsch JR, 2012). The assembling of the eIF4F complex is strongly regulated. One important level of control lies in the availability of eIF4E, the limiting component for the initiation complex. The major regulation is due through translation repressor molecules: the eIF4E-binding proteins (4E-BPs), which are in turn regulated through phosphorylation by the mammalian target of rapamycin (mTOR) kinase (Fingar DC *et al.*, 2002). Phosphorylation of 4E-BPs causes their release from eIF4E, thus allowing recruitment of eIF4G and formation of eIF4F on the cap structure. An additional layer of regulation is represented by the phosphorylation of eIF4E on serine 209 by the MAP kinase signal-integrating kinases (MNK1/2) proteins. This event occurs in response to activation of the MAPK signal transduction pathways (p38 stress MAPK; extracellular regulated kinases ERK1/2) (Buxade M *et al*., 2008). A number

of observations link the eIF4E phosphorylation with cancerogenesis. Animal models demonstrated that the inhibition of eIF4E phosphorylation impairs tumor development (Furic L *et al*., 2010; Ueda T *et al*., 2010). Similar Importantly, in cancer cell several kinds of stresses cause eIF4E phosphorylation (Dolniak B *et al.*, 2008), including DNA damaging agents. (Zhang Y *et al.*, 2008). Regulation of translation is a key step that allows cells to overcome the insults posed by hostile environments. The phosphorylation of eIF4e may contribute to this finely tuned regulation, as suggested by the block of cell proliferation and decreased cell survival observed after inhibition of MNK activity in prostate, breast and lung cancer (Bianchini A *et al*., 2008; Wheater MJ *et al*., 2010; Konicek BW *et al*., 2011). Importantly, the regulation of eIF4E phosphorylation can also occur independently from external stimuli. Indeed, alternative splicing of the *MKNK1* and *MKNK2* genes yields four different splice variants: MNK1a/b and MNK2a/b. The different protein isoforms differ at their C-terminus: both b-isoforms possess a shorter C-terminal than the a-isoforms. These splicing events modulate MAPK regulation of MNK function, because the b-isoforms lack the MAPK-interacting domain (Scheper GC *et al*., 2003; O'Loghlen A *et al*., 2004). The different splicing isoforms also differ for intracellular localization and basal activity, MNK1a is prevalently localized in the cytoplasm and show low basal activity that is enhanced by different stimuli while MNK1b has high basal activity and is uniformly distributed throughout the cell (O'Loghlen A *et al*., 2007). MNK2a is cytoplasmatic whereas MNK2b is partially nuclear and, unlike MNK2a, it does not show high basal activity. Indeed, its intrinsic activity is low and is not increased by external cellular stimuli (Scheper GC *et al*., 2003). Remarkably, it has been demonstrated that several RNA binding proteins are substrates of MNKs, for instance hnRNPA1 (Buxadé M *et al*., 2005; Guil S *et al*., 2006) and the polypyrimidine-tract binding protein-associated splicing factor (PSF) (Buxadé M *et al*., 2007), underlying the importance of RNA metabolism in the response of cancer cells to various stresses.

References

Aitken CE, Lorsch JR. A mechanistic overview of translation initiation in eukaryotes. *Nat Struct Mol Biol*. 2012 Jun 5;19(6):568-76.

Biamonti G, Caceres JF. Cellular stress and RNA splicing. *Trends Biochem Sci*. 2009 Mar;34(3):146-53.

Bianchini A, Loiarro M, Bielli P, Busà R, Paronetto MP, Loreni F, Geremia R, Sette C.Phosphorylation of eIF4E by MNKs supports protein synthesis, cell cycle progression and proliferation in prostate cancer cells. *Carcinogenesis*. 2008 Dec;29(12):2279-88.

Black DL. Mechanisms of alternative pre-messenger RNA splicing. *Annu Rev Biochem.* 2003;72:291-336

Burris HA 3rd, Moore MJ, Andersen J, Green MR, Rothenberg ML, Modiano MR, Cripps MC, Portenoy RK, Storniolo AM, Tarassoff P, Nelson R, Dorr FA,Stephens CD, Von Hoff DD. Improvements in survival and clinical benefit with gemcitabine as first-line therapy for patients with advanced pancreas cancer: a randomized trial. *J Clin Oncol* 1997; 15: 2403–13.

Busà R, Geremia R, Sette C. Genotoxic stress causes the accumulation of the splicing regulator Sam68 in nuclear foci of transcriptionally active chromatin *Nucleic Acids Res*. 2010 May;38(9):3005-18

Buxadé M, Morrice N, Krebs DL, Proud CG The PSF.p54nrb complex is a novel Mnk substrate that binds the mRNA for tumor necrosis factor alpha. J Biol Chem. 2008 Jan 4;283(1):57-65

Buxadé M, Parra JL, Rousseau S, Shpiro N, Marquez R, Morrice N, Bain J, Espel E, Proud CG. The Mnks are novel components in the control of TNF alpha biosynthesis and phosphorylate and regulate hnRNP A1. *Immunity*. 2005 Aug;23(2):177-89.

Buxade M, Parra-Palau JL, Proud CG. The Mnks: MAP kinase-interacting kinases (MAP kinase signal-integrating kinases). *Front Biosci*. 2008 May 1;13:5359-73.

Chandler DS, Singh RK, Caldwell LC, Bitler JL, Lozano G. Genotoxic stress induces coordinately regulated alternative splicing of the p53 modulators MDM2 and MDM4. *Cancer Res*. 2006 Oct 1;66(19):9502-8.

Cohen AA, Geva-Zatorsky N, Eden E, Frenkel-Morgenstern M, Issaeva I, Sigal A, Milo R, Cohen-Saidon C, Liron Y, Kam Z, Cohen L, Danon T, Perzov N,Alon U. Dynamic proteomics of individual cancer cells in response to a drug. *Science*. 2008 Dec 5;322(5907):1511-6.

Dolniak B, Katsoulidis E, Carayol N, Altman JK, Redig AJ, Tallman MS, Ueda T, Watanabe-Fukunaga R, Fukunaga R, Platanias LC. Regulation of arsenic trioxide-induced cellular responses by Mnk1 and Mnk2. *J Biol Chem*. 2008 May 2;283(18):12034-42.

Dutertre M, Sanchez G, Barbier J, Corcos L, Auboeuf D. The emerging role of pre-messenger RNA splicing in stress responses: sending alternative messages and silent messengers *RNA Biol*. 2011 Sep-Oct;8(5):740-7

Dutertre M, Sanchez G, De Cian MC, Barbier J, Dardenne E, Gratadou L, Dujardin G, Le Jossic-Corcos C, Corcos L, Auboeuf D. Cotranscriptional exon skipping in the genotoxic stress response. *Nat Struct Mol Biol*. 2010 Nov;17(11):1358-66.

Filippov V, Filippova M, Duerksen-Hughes PJ. The early response to DNA damage can lead to activation of alternative splicing activity resulting in CD44 splice pattern changes. *Cancer Res*. 2007 Aug 15;67(16):7621-30.

Fingar DC, Salama S, Tsou C, Harlow E, Blenis J. Mammalian cell size is controlled by mTOR and its downstream targets S6K1 and 4EBP1/eIF4E. Genes Dev. 2002 Jun 15;16(12):1472-87.

Furic L, Rong L, Larsson O, Koumakpayi IH, Yoshida K, Brueschke A, Petroulakis E, Robichaud N, Pollak M, Gaboury LA, Pandolfi PP,Saad F, Sonenberg N. eIF4E phosphorylation promotes tumorigenesis and is associated with prostate cancer progression. *Proc Natl Acad Sci U S A*. 2010 Aug 10;107(32):14134-9.

Gaudreault I, Guay D, Lebel M. YB-1 promotes strand separation in vitro of duplex DNA containing either mispaired bases or cisplatin modifications, exhibits endonucleolytic activities and binds several DNA repair proteins. *Nucleic Acids Res*. 2004 Jan 12;32(1):316-27

Gesto DS, Cerqueira NM, Fernandes PA, Ramos MJ. Gemcitabine: a critical nucleoside for cancer therapy. *Curr Med Chem*. 2012;19(7):1076-87.

Graff JR, Konicek BW, Lynch RL, Dumstorf CA, Dowless MS, McNulty AM, Parsons SH, Brail LH, Colligan BM, Koop JW, Hurst BM, Deddens JA,Neubauer BL, Stancato LF, Carter HW, Douglass LE, Carter JH. eIF4E activation is commonly elevated in advanced human prostate cancers and significantly related to reduced patient survival. Cancer Res. 2009 May 1;69(9):3866-73

Guil S, Long JC, Cáceres JF. hnRNP A1 relocalization to the stress granules reflects a role in the stress response. *Mol Cell Biol*. 2006 Aug;26(15):5744-58.

Guil S, Long JC, Cáceres JF. hnRNP A1 relocalization to the stress granules reflects a role in the stress response. *Mol Cell Biol*. 2006 Aug;26(15):5744-58.

Huang P, Chubb S, Hertel LW, Grindey GB, Plunkett W. Action of 2',2'-difluorodeoxycytidine on DNA synthesis. *Cancer Res*. 1991 Nov 15;51(22):6110-7.

Kim MP and Gallick GE Gemcitabine Resistance in Pancreatic Cancer: Picking the Key Players, *Clin Cancer Res*, March 1, 2008 *14;*1284

Kleiman FE, Wu-Baer F, Fonseca D, Kaneko S, Baer R, Manley JL. BRCA1/BARD1 inhibition of mRNA 3' processing involves targeted degradation of RNA polymerase II. *Genes Dev*. 2005 May 15;19(10):1227-37.

Konicek BW, Stephens JR, McNulty AM, Robichaud N, Peery RB, Dumstorf CA, Dowless MS, Iversen PW, Parsons S, Ellis KE, McCann DJ, Pelletier J,Furic L, Yingling JM, Stancato LF, Sonenberg N, Graff JR. Therapeutic inhibition of MAP kinase interacting kinase blocks eukaryotic initiation factor 4Ephosphorylation and suppresses outgrowth of experimental lung metastases. Cancer Res. 2011 Mar 1;71(5):1849-57

Krecic AM, Swanson MS. hnRNP complexes: composition, structure, and function. *Curr Opin Cell Biol*. 1999 Jun;11(3):363-71.

Manley JL, Tacke R. SR proteins and splicing control. *Genes Dev*. 1996 Jul 1;10(13):1569-79.

Matsuoka S, Ballif BA, Smogorzewska A, McDonald ER 3rd, Hurov KE, Luo J, Bakalarski CE, Zhao Z, Solimini N, Lerenthal Y, Shiloh Y, Gygi SP, Elledge SJ. ATM and ATR substrate analysis reveals extensive protein networks responsive to DNA damage. *Science*. 2007 May 25;316(5828):1160-6.

Mini E, Nobili S, Caciagli B, Landini I, Mazzei T. Cellular pharmacology of gemcitabine. *Ann Oncol.* 2006 May;17 Suppl 5:v7-12.

Mirkin N, Fonseca D, Mohammed S, Cevher MA, Manley JL, Kleiman FE. The 3' processing factor CstF functions in the DNA repair response. *Nucleic Acids Res*. 2008 Apr;36(6):1792-804

Muñoz MJ, Pérez Santangelo MS, Paronetto MP, de la Mata M, Pelisch F, Boireau S, Glover-Cutter K, Ben-Dov C, Blaustein M, Lozano JJ, Bird G, Bentley D, Bertrand E, Kornblihtt AR. DNA damage regulates alternative splicing through inhibition of RNA polymerase II elongation. *Cell*. 2009 May 15;137(4):708-20.

O'Loghlen A, González VM, Piñeiro D, Pérez-Morgado MI, Salinas M, Martín ME Identification and molecular characterization of Mnk1b, a splice variant of human MAP kinase-interacting kinase Mnk1. *Exp Cell Res*. 2004 Oct 1;299(2):343-55.

O'Loghlen A, González VM, Jurado T, Salinas M, Martín ME. Characterization of the activity of human MAP kinase-interacting kinase Mnk1b. *Biochim Biophys Acta.* 2007 Sep;1773(9):1416-27.

Paronetto MP, Miñana B, Valcárcel J.The Ewing sarcoma protein regulates DNA damage-induced alternative splicing. *Mol Cell*. 2011 Aug 5;43(3):353-68.

Plunkett W, Huang P, Xu YZ, Heinemann V, Grunewald R, Gandhi V. Gemcitabine: metabolism, mechanisms of action, and self-potentiation. *Semin Oncol*. 1995 Aug;22(4 Suppl 11):3-10.

Scheper GC, Parra JL, Wilson M, Van Kollenburg B, Vertegaal AC, Han ZG, Proud CG. The N and C termini of the splice variants of the human mitogen-activated protein kinase-interacting kinase Mnk2 determine activity and localization. *Mol Cell Biol*. 2003 Aug;23(16):5692-705.

Shultz JC, Goehe RW, Wijesinghe DS, Murudkar C, Hawkins AJ, Shay JW, Minna JD, Chalfant CE. Alternative splicing of caspase 9 is modulated by the phosphoinositide 3-kinase/Akt pathway via phosphorylation of SRp30a. *Cancer Res*. 2010 Nov 15;70(22):9185-96.

Solier S, Lansiaux A, Logette E, Wu J, Soret J, Tazi J, Bailly C, Desoche L, Solary E, Corcos L. Topoisomerase I and II inhibitors control caspase-2 pre-messenger RNA splicing in human cells. *Mol Cancer Res*. 2004 Jan;2(1):53-61.

Ueda T, Sasaki M, Elia AJ, Chio II, Hamada K, Fukunaga R, Mak TW. Combined deficiency for MAP kinase-interacting kinase 1 and 2 (Mnk1 and Mnk2) delays tumor development. *Proc Natl Acad Sci U S A*. 2010 Aug 10;107(32):13984-90

Wang ET, Sandberg R, Luo S, Khrebtukova I, Zhang L, Mayr C, Kingsmore SF, Schroth GP, Burge CB. Alternative isoform regulation in human tissue transcriptomes. *Nature*. 2008 Nov 27;456(7221):470-6.

Wheater MJ, Johnson PW, Blaydes JP. The role of MNK proteins and eIF4E phosphorylation in breast cancer cell proliferation and survival. *Cancer Biol Ther*. 2010 Oct;10(7):728-35.

Yamasaki S, Anderson P. Reprogramming mRNA translation during stress. *Curr Opin Cell Biol*. 2008 Apr;20(2):222-6.

Ying JE, Zhu LM, Liu BX. Developments in metastatic pancreatic cancer: is gemcitabine still the standard? *World J Gastroenterol*. 2012 Feb 28;18(8):736-45.

Yoshizawa A, Fukuoka J, Shimizu S, Shilo K, Franks TJ, Hewitt SM, Fujii T, Cordon-Cardo C, Jen J, Travis WD. Overexpression of phospho-eIF4E is associated with survival through AKT pathway in non-small cell lung cancer. *Clin Cancer Res*. 2010 Jan 1;16(1):240-8

Zhang Y, Li Y, Yang DQ. Phosphorylation of eIF-4E positively regulates formation of the eIF-4F translation initiation complex following DNA damage. *Biochem Biophys Res Commun*. 2008 Feb 29;367(1):54-9

CHAPTER III

Gemcitabine triggers a pro-survival response in pancreatic cancer cells through activation of the MNK2/eIF4E pathway

Cancer cells are prone to develop escape pathways in order to survive to drug treatments. The study presented in this chapter aimed at investigating the involvement of mitogenic activating protein kinase interacting kinase (MNK/eIF4E pathway) in the acquisition of gemcitabine resistance of PDAC cells.

The screening of cohort of PDAC patients pointed out a correlation between the phosphorylation of eIF4E and disease grade, early onset and worse prognosis. Thus, we investigated the involvement of MNK/eIF4E pathway in the pro-survival response of PDAC cells. Interestingly, chemotherapeutic drug treatments promoted MNK-dependent phosphorylation of eIF4E and MNK inhibition enhanced cell death induced by gemcitabine treatment. Our study revealed that MNK2 is primary responsible for the phosphorylation of eIF4E and the survival of PDAC cells under genotoxic stress. MNK2 transcript is regulated by alternative splicing producing two isoforms: MNK2a and MNK2b. Importanly, the analysis of the expression of these splice variants revealed that gemcitabine treatment promotes splicing of MNK2b through the upregulation of the SRSF1 proto-oncogene. Importantly, MNK2b overrides the control of upstream pathways and its overexpression caused increased resistance to drug treatment. Depletion of SRSF1 impaired the effect of this pro-survival pathway. Thus, the results obtained in our study identify a novel escape strategy triggered by genotoxic stress in PDAC cells, which causes upregulation of the splicing factor SRSF1 and splicing of the MNK2b variant, thus allowing phosphorylation of eIF4E independently of external cues.

Oncogene (2012), 1–10

www.nature.com/onc

ORIGINAL ARTICLE

Gemcitabine triggers a pro-survival response in pancreatic cancer cells through activation of the MNK2/eIF4E pathway

L Adesso[1,2], S Calabretta[1,2], F Barbagallo[1,3], G Capurso[2], E Pilozzi[2], R Geremia[1], G Delle Fave[1,2] and C Sette[1,3]

Pancreatic ductal adenocarcinoma (PDAC) is an aggressive neoplastic disease. Gemcitabine, the currently used chemotherapeutic drug for PDAC, elicits only minor benefits, because of the development of escape pathways leading to chemoresistance. Herein, we aimed at investigating the involvement of the mitogen activating protein kinase interacting kinase (MNK)/eIF4E pathway in the acquired drug resistance of PDAC cells. Screening of a cohort of PDAC patients by immunohistochemistry showed that eIF4E phosphorylation correlated with disease grade, early onset of disease and worse prognosis. In PDAC cell lines, chemotherapeutic drugs induced MNK-dependent phosphorylation of eIF4E. Importantly, pharmacological inhibition of MNK activity synergistically enhanced the cytostatic effect of gemcitabine, by promoting apoptosis. RNA interference (RNAi) experiments indicated that MNK2 is mainly responsible for eIF4E phosphorylation and gemcitabine resistance in PDAC cells. Furthermore, we found that gemcitabine induced the expression of the oncogenic splicing factor SRSF1 and splicing of MNK2b, a splice variant that overrides upstream regulatory pathways and confers increased resistance to the drug. Silencing of SRSF1 by RNAi abolished this splicing event and recapitulated the effects of MNK pharmacological or genetic inhibition on eIF4E phosphorylation and apoptosis in gemcitabine-treated cells. Our results highlight a novel pro-survival pathway triggered by gemcitabine in PDAC cells, which leads to MNK2-dependent phosphorylation of eIF4E, suggesting that the MNK/eIF4E pathway represents an escape route utilized by PDAC cells to withstand chemotherapeutic treatments.

Oncogene advance online publication, 16 July 2012; doi:10.1038/onc.2012.306

Keywords: eIF4E phosphorylation; MNK2 alternative splicing; drug resistance

INTRODUCTION

Pancreatic ductal adenocarcinoma (PDAC) is a highly malignant neoplastic disease.[1] Gemcitabine, the elective agent used in PDAC chemotherapy, exerts only marginal survival benefits,[1] urging for the identification of new agents and/or therapeutic targets. In this regard, as the PI3K/AKT/mTOR (mammalian target of rapamycin) pathway is activated in approximately half of PDACs, correlating with poor prognosis,[2] mTOR inhibitors are being considered as possible therapeutic agents in combination with chemotherapy. Nevertheless, their efficacy is often limited by activation of escape pathways leading to phosphorylation of AKT and eIF4E in response to mTOR inhibition.[3,4] For these reasons, characterization of the molecular mechanisms involved in the acquisition of drug resistance represents a clinical priority.

The mTOR serine/threonine kinase is a central regulator of protein synthesis and cell growth.[5] mTOR modulates the activity of eIF4E, the core component of the translation initiation complex eIF4F that assembles at the 5′ cap of eukaryotic mRNAs.[5] In quiescent cells, eIF4E activity is restricted by the 4EBPs (eIF4E-binding proteins).[5–7] Nutrients induce phosphorylation of 4EBPs by mTOR, thereby causing their release from eIF4E and assembly of eIF4F.[5] Furthermore, eIF4E indirectly stimulates translation by favoring nuclear export of selected mRNAs.[6] In line with its central role in cell growth, increased eIF4E levels can promote neoplastic transformation.[7]

An additional layer of regulation of eIF4E is provided by its phosphorylation in serine 209 by the mitogen activated protein kinase (MAPK) interacting kinases (MNK) MNK1 and MNK2,[8,9] which are activated by ERK1/2 and p38.[9] Phosphorylation of eIF4E occurs in cells exposed to growth factors and chemotherapeutic agents,[9,10] and its pharmacological inhibition was shown to reduce proliferation in cancer cells.[11–13] Importantly, although phosphorylation of eIF4E by MNKs is dispensable for basal protein synthesis and cell viability,[8] it is essential for the transforming activity of eIF4E in mouse models of cancer,[14–16] and it positively correlates with poor prognosis and disease grade in human prostate and lung cancers.[17,18] These observations point to eIF4E phosphorylation as a key step in oncogenic transformation. Noteworthy, as suppression of eIF4E phosphorylation sensitizes cancer cells to growth arrest[11] and stress-induced death[19] without affecting normal development or lifespan in animal models,[8] the MNK/eIF4E pathway appears as a promising pharmacological target for cancer treatment.

Herein, we have investigated the regulation and function of the MNK/eIF4E pathway in PDAC. Phosphorylation of eIF4E positively correlated with grade, and was associated with worse prognosis and earlier disease onset in PDAC patients. MNK2-dependent phosphorylation of eIF4E was induced by gemcitabine in PDAC cells. The drug also promoted upregulation of the splicing factor SRSF1 and splicing of MNK2b, a splice variant that overrides upstream regulatory pathways[9,20] and confers increased resistance to gemcitabine. Suppression of this pathway by pharmacological or genetic inhibition of either MNKs or SRSF1

[1]Department of Biomedicine and Prevention, University of Rome 'Tor Vergata', Rome, Italy; [2]Digestive and Liver Disease Unit, II Medical School, University of Rome La Sapienza, Rome, Italy and [3]Laboratory of Neuroembryology, Fondazione Santa Lucia, Rome, Italy. Correspondence: Professor G Delle Fave, Digestive and Liver Disease Unit, II Medical School, University of Rome La Sapienza, Rome 00133, Italy or Professor C Sette, Department of Biomedicine and Prevention, University of Rome 'Tor Vergata', Via Montpellier 1, Rome 00133, Italy.
E-mail: gianfranco.dellefave@uniroma1.it or claudio.sette@uniroma2.it
Received 26 December 2011; revised 7 May 2012; accepted 5 June 2012

synergistically enhanced the cytotoxic effects of gemcitabine. Our results highlight a novel pro-survival pathway triggered by gemcitabine in PDAC cells, which leads to MNK2-dependent phosphorylation of eIF4E, suggesting that the MNK/eIF4E pathway might represent a promising therapeutic target for PDAC.

RESULTS

Increased phosphorylation of eIF4E in PDAC correlates with worse prognosis

A cohort of 32 patients diagnosed with primary PDAC in the absence of metastases, who received surgery with radical intent (see Supplementary Table 1), was analyzed for the levels of the phosphorylated form of eIF4E (p-eIF4E) by immunohistochemistry. We found that 27 samples (84.3%) stained positive for p-eIF4E (Figure 1a, Supplementary Table 1). A linear score of staining (range 0–5) was assigned to the samples (Figure 1a; see Materials and methods), and patients were subdivided in two groups: group 0 comprised eight samples displaying no staining (score 0) or low p-eIF4E staining (that is, $\leqslant 2$), whereas group 1 comprised 24 samples displaying strong p-eIF4E staining (that is, $\geqslant 3$) (Figure 1b). The two groups displayed statistically significant differences only for age at diagnosis, grading, progression-free survival and overall survival (Figure 1b). Group 1 patients had a mean age at diagnosis of 64.5, with 95% confidence interval (CI) 59.8–69.2, whereas patients with a low p-eIF4E score (group 0) had a significantly higher mean age at diagnosis of 74.2 (95% CI: 71.9–76.5; $P = 0.02$) (Figure 1b). Notably, of the eight patients diagnosed at age $\leqslant 60$, four had a p-eIF4E score of 5, three had a score of 4 and one a score of 3 (Supplementary Table 1). Furthermore, the p-eIF4E score was positively correlated with tumor grade (G grade, range 1–3; Spearman's coefficient of rank correlation (ρ) = 0.6, $P = 0.0008$).

The high p-eIF4E score was also associated with worse survival probability (log-rank test $P = 0.02$, Figure 1c). Similarly, in a Cox-proportional hazards regression model, high p-eIF4E score was associated with worse survival (hazard ratio 4.6; 95% CI: 1–20.1). Adjuvant therapy (gemcitabine) was associated with a better overall survival in the Cox-proportional hazards regression model (hazard ratio 0.3; 95% CI: 0.12–0.85), whereas neither the resection margins (R status), nor the lymph node status (N stage or lymph node ratio) were. The mean survival of group 0 patients was 25.1 months (95% CI: 11.3–38.8) as compared with 13 months (95% CI: 8.2–17.8) in group 1 patients ($P = 0.04$) (Figure 1b). Elevated p-eIF4E was also associated with shorter 'recurrence-free survival' (log-rank test $P = 0.018$). Accordingly, the mean time to tumor recurrence was 20.6 months for group 0 and 9 months for group 1 ($P = 0.02$) (Figure 1b). Collectively, these data suggest that eIF4E phosphorylation is directly correlated with tumor grade and associated with worse survival probability.

Therapeutic drugs induce eIF4E phosphorylation in PDAC cells

The marginal survival benefits observed in patients[1] may suggest that chemotherapeutic treatments trigger the activation of pro-survival pathways in PDAC cells. The MNK/eIF4E and the AKT/mTOR pathways are two pro-survival routes frequently activated in cancer.[3,4] To test whether they contribute to drug resistance in PDAC cells, we analyzed activation of key proteins in these pathways. Phosphorylation of eIF4E was induced by treatment with gemcitabine in several poorly differentiated PDAC cell lines, such as MiaPaCa2 (Figure 2a), PT45P1 (Figure 2b) and PANC-1 cells (Supplementary Figure S1A), as well as in the well-differentiated HPAF2 cells (Supplementary Figure S1A). Activation of the MNK/eIF4E pathway was a specific response, as no increase in AKT phosphorylation occurred under these conditions (data not shown), whereas the decreased phosphorylation of the ribosomal protein rpS6 indicated that the mTOR pathway was inhibited by gemcitabine (Figures 2a,b).

Next, we tested whether activation of the MNK/eIF4E pathway was triggered by other chemotherapeutic treatments. eIF4E phosphorylation was also increased in response to cisplatin in PDAC cells (Supplementary Figure S1B), whereas neither phosphorylation of AKT (data not shown) nor activation of the mTOR pathway were observed (Supplementary Figure S1B). PDAC cells were also treated with the mTOR inhibitor rapamycin (1 and 10 nM) for up to 24 h. As for other cancer cells,[3,4] mTOR inhibition caused an increase in phosphorylation of both AKT and eIF4E in PDAC cells (Supplementary Figures S1C, D). However, AKT phosphorylation returned to basal levels by 4–24 h of treatment with the higher dose of rapamycin, whereas eIF4E phosphorylation persisted for the whole duration of the experiment, regardless of the dose used (Supplementary Figures S1C, D). These results suggest that eIF4E phosphorylation is a general, long-lasting feedback response of PDAC cells to therapeutic treatments.

Inhibition of eIF4E phosphorylation enhances the cytostatic effect of therapeutic drugs

To test the most effective tool to interfere with eIF4E phosphorylation in PDAC cells, we treated them with inhibitors of kinases acting upstream of the MAPK/MNK pathway.[9] The PI3K inhibitor (LY294002), MEK1/2 inhibitor (U0126) and p38 inhibitor (SB202190), alone or in combination, only partially reverted the increased phosphorylation of eIF4E induced by gemcitabine and rapamycin in the poorly differentiated MiaPaCa2 and PT45P1 cell lines (Supplementary Figures S2A, B). However, direct inhibition of MNKs by their chemical inhibitor MNK-I completely abolished eIF4E phosphorylation under all treatments (Supplementary Figure S2A,B). Moreover, MNK-I also strongly reduced gemcitabine-induced eIF4E phosphorylation in the well-differentiated HPAF2 cells (Supplementary Figure S2C). Thus, MNK-I was selected for further studies.

Dose-response experiments showed that MiaPaCa2 cells were highly resistant to gemcitabine, with less than 50% growth inhibition at 100 nM (Supplementary Figure S3A), whereas an almost complete suppression of PT45P1 cell growth was achieved at 30 nM (Supplementary Figure S3B). Thus, to test the effect of MNK-I on PDAC cell growth, we used sub-optimal doses of gemcitabine (30 nM for MiaPaCa2 and 0.1 nM for PT45P1). MNK-I alone slightly reduced growth of both cell lines (Figures 2c, d), to an extent similar to the sub-optimal doses of gemcitabine. However, the combined treatment with the two drugs synergistically inhibited PDAC cell growth, with an almost complete block achieved in PT45P1. A similar synergic effect was also observed in the well-differentiated HPAF2 cells (Supplementary Figure S3C). Furthermore, inhibition of eIF4E phoshorylation by MNK-I significantly augmented the cytostatic effects of cisplatin and rapamycin (Supplementary Figures S3D, E), indicating that activation of this pathway exerts a general positive effect in the stress response of PDAC cells.

Inhibition of MNK activity enhances gemcitabine-induced apoptosis in MiaPaCa2 cells

Clonogenic assays were performed to directly test whether MNK-I enhanced the cytotoxic activity of gemcitabine. MiaPaCa2 cells, which were chosen for their higher resistance to the drug, were cultured for 24 h with sub-optimal doses of gemcitabine (0.1–0.3 nM) with or without MNK-I (10 μM) and then grown for 10 days in complete medium (± 5 μM MNK-I). Under these conditions, MNK-I suppressed eIF4E phosphorylation in the large majority of the cells (Supplementary Figure S4A). Gemcitabine reduced the number of colonies in a dose-dependent manner, whereas MNK-I did not significantly affect their number (Figure 3b), even though it reduced the size of colonies

A

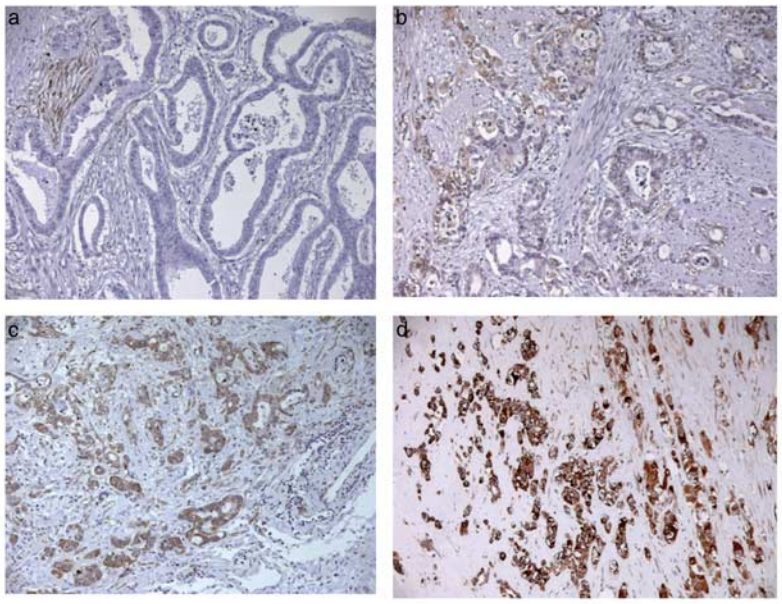

B

p-eIF4E score	Grading (G1 or G2) n patients	age at diagnosis	survival (months)	time of recurrence (months)	N stage 1 (n patients)	Resection margin (R1)	Adiuvant treatment (n patients)
GROUP 0 (≤2) n=8	6 (75%)	74.2	25.1	20.6	6 (75%)	3 (37,5%)	6 (75%)
GROUP 1 (≥3) n=24	5 (20,8%)	64.5	13	9	17 (70,9%)	13 (54,2%)	18 (75%)
p value	0.004	0.02	0.04	0.02	1	0.4	1

C

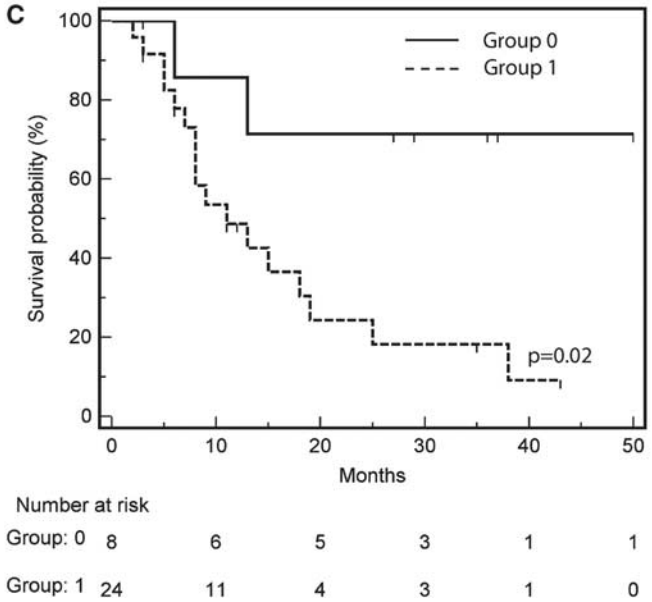

Figure 1. Phosphorylation of eIF4E in PDAC. (**A**) Examples of p-eIF4E immunohistochemistry of PDAC tissues. Panels (a–d) show different intensity of staining. (a) Well-differentiated PDAC with no p-eIF4E staining in the gland and few positive stromal cells (score 0); (b) moderately differentiated (G2) PDAC tissue with mild cytoplasmic staining in few neoplastic glands (score 1); (c) moderately differentiated (G2) PDAC tissue showing cytoplasmic staining in most glands (score 2); (d) poorly differentiated (G3) PDAC tissue with strong cytoplasmic staining (score 3). (**B**) Summary of the clinical-pathological features associated with patients in group 0 (low p-eIF4E) and group 1 (high p-eIF4E). Categorical variables were analyzed by Fisher's test, continuous variables by *t*-test for independent samples. (**C**) Survival likelihood of PDAC patients. Group 0 comprised 8 patients with low p-eIF4E staining (score $\leqslant 2$), group 1 comprised 24 patients with high p-eIF4E (score $\geqslant 3$); $P = 0.02$ at log-rank test. Patients lost at follow-up are 'censored' and marked as small vertical lines.

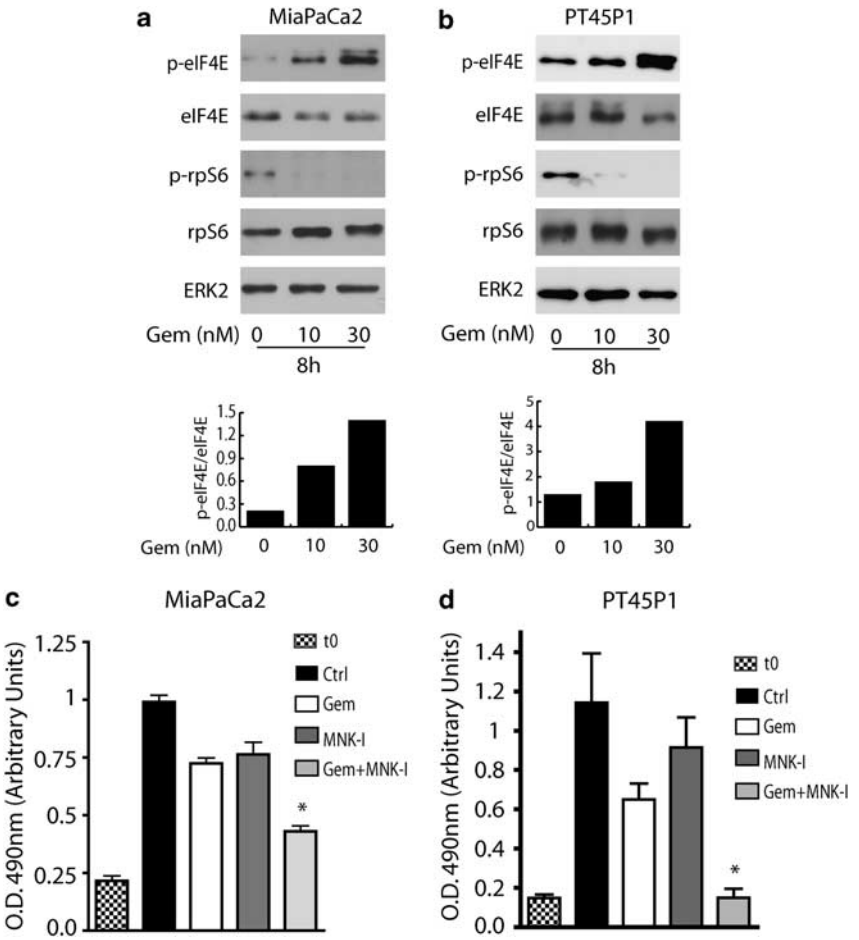

Figure 2. MNK-dependent phosphorylation of eIF4E supports growth of PDAC cells exposed to gemcitabine. Western blot analysis with antibodies for the total or phosphorylated forms of the indicated proteins in MiaPaCa2 (**a**) and PT45P1 (**b**) cells treated for 8 h with 10 and 30 nM gemcitabine. ERK2 was used as loading control. Histograms represent densitometric analysis of p-eIF4E/eIF4E ratio of the gels shown. Viability of MiaPaCa2 (**c**) and PT45P1 (**d**) cell lines was measured by MTS assay after 72 h of exposure to 30 nM gemcitabine alone or in combination with 10 μM MNK-I. Mean ± s.d. of three experiments performed in triplicate; $*P < 0.01$ in paired *t*-test.

(Figure 3a). Notably, the combined treatment with the two drugs almost completely suppressed colony formation (Figures 3a, b), confirming a synergic effect.

To understand whether MNK-I affected cell proliferation and/or death, we analyzed cell cycle progression and apoptosis. Treatment of MiaPaCa2 cells with MNK-I and gemcitabine for 72 h caused a slight increase in the percentage of cells in G1 (Supplementary Figure S4B). The combined treatment exerted an additive effect, which was, however, not statistically significant. By contrast, immunofluorescence analysis of the cleaved/activated form of caspase-3 (Figure 3c, Supplementary Figure S4C) and TUNEL assays (Figure 3d, Supplementary Figure S4C) documented that MNK-I significantly increased cell death in cells exposed to gemcitabine, even though it did not trigger apoptosis when it was administered alone (Figures 3c, d). Notably, MNK-I also enhanced the cytotoxic effects of cisplatin in MiaPaCa2 cells (Supplementary Figure S4D). These results suggest that the synergic inhibitory effect on cell growth and colony formation exerted by MNK-I is mainly because of enhanced apoptosis in gemcitabine-treated cells.

MNK2 is required for resistance of MiaPaCa2 cells to gemcitabine

To overcome possible off-target effects of MNK-I, we set out to interfere with MNK1/2 function by other means. MiaPaCa2 cells were transfected with MNK1 and MNK2 siRNAs (small interference RNAs) and depletion of the mRNAs corresponding to both splice variants was determined by RT–PCR (Figure 4a). Decreased expression of either MNK1 or MNK2 protein (Figure 4b) reduced eIF4E phosphorylation under basal conditions, with MNK2 exerting a stronger effect (Figure 4c). Furthermore, the increased phosphorylation of eIF4E triggered by gemcitabine was completely suppressed after silencing of MNK2, whereas MNK1 depletion only slightly reduced it (Figure 4c). Silencing of MNK2 suppressed gemcitabine-induced eIF4E phosphorylation also in PT45P1 and HPAF2 cells (Supplementary Figure S5A). These results suggest that MNK2 is predominantly responsible for eIF4E phosphorylation in PDAC cells treated with gemcitabine.

Next, MiaPaCa2 cells transfected with si-MNK1 and si-MNK2 were cultured with or without gemcitabine for 48 h. In the absence of the drug, silencing of either MNK1 or MNK2 caused a small reduction of cell growth (15–20%) compared with cells transfected with a control siRNA, whereas concomitant silencing of both MNKs elicited an additive effect (40% inhibition) (Figure 4d). However, in the presence of gemcitabine, which caused a 40% reduction in cell growth *per se* (Figure 4d), the effect of MNK2 depletion was significantly stronger than MNK1 depletion (75% inhibition vs 60% inhibition). Moreover, depletion of both kinases did not significantly increase the effect of MNK2 depletion alone in cells treated with gemcitabine (Figure 4d).

To investigate whether reduced growth was ascribable to increased cell death, as in the case of the MNK-I, we analyzed

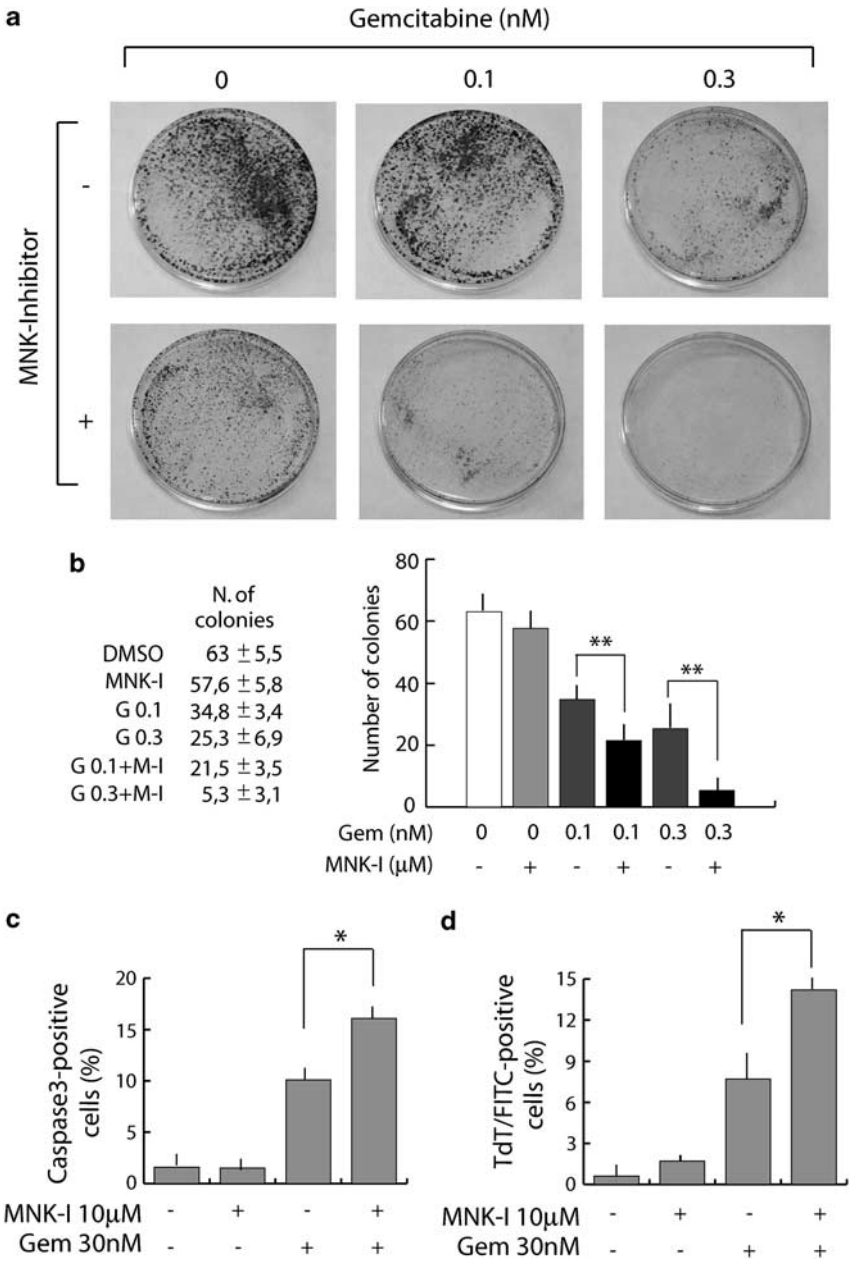

Figure 3. Inhibition of MNK activity enhances the cytotoxic effect of gemcitabine. (**a**) Representative images of colonies of clonogenic assays. (**b**) Histogram shows colony numbers from three experiments (mean ± s.d.). Actual numbers are reported to the left of the histogram. $^{**}P < 0.005$ in paired *t*-test. (**c**, **d**) Results of the immunofluorescence analyses of the cleaved form of caspase-3 (**c**) and TUNEL (**d**) in MiaPaCa2 cells treated as indicated. Histograms represent mean ± s.d. of three experiments; $^{*}P < 0.01$ in paired *t*-test.

apoptosis. We found that silencing of neither MNK1 nor MNK2 affected the viability of control cells (Figure 4e). However, depletion of MNK2, but not MNK1, significantly augmented apoptosis in the presence of gemcitabine (Figure 4e), thus recapitulating the effect of MNK-I. Importantly, similar results were also obtained in PT45P1 and HPAF2 cells (Supplementary Figures S5B, C). These results strongly suggest that MNK2-dependent phosphorylation of eIF4E contributes to the protective response of PDAC cells to gemcitabine.

SRSF1 promotes splicing of the MNK2b variant in gemcitabine-treated MiaPaCa2 cells

On the basis of its prominent role in the response of PDAC cells to gemcitabine, we focused on MNK2. The *MKNK2* gene encodes two splice variants, named MNK2a and MNK2b.[9] Notably, the b variant lacks the MAPK-interacting domain,[20] which uncouples its activation from this upstream pathway (Figure 5a).[9,20,21] Treatment with gemcitabine for 48 and 72 h modulated the expression of *MKNK2* in PDAC cells, by causing a reduction in expression of MNK2 (Figure 5b; Supplementary Figure S6A). Concomitantly with the reduction, gemcitabine also altered the ratio between the MNK2 splice variants in favor of MNK2b (Figure 5b; Supplementary Figure S6A). Importantly, we found that expression of recombinant GFP-MNK2b attenuated gemcitabine-dependent cell death in transfected MiaPaCa2 cells, whereas transfection of GFP-MNK2a did not exert any effect (Figure 5c; Supplementary Figure S6B). This result suggests that the shift toward the MNK2b variant in response to the treatment of MiaPaCa2 cells with gemcitabine contributes to reduce their sensitivity to the drug.

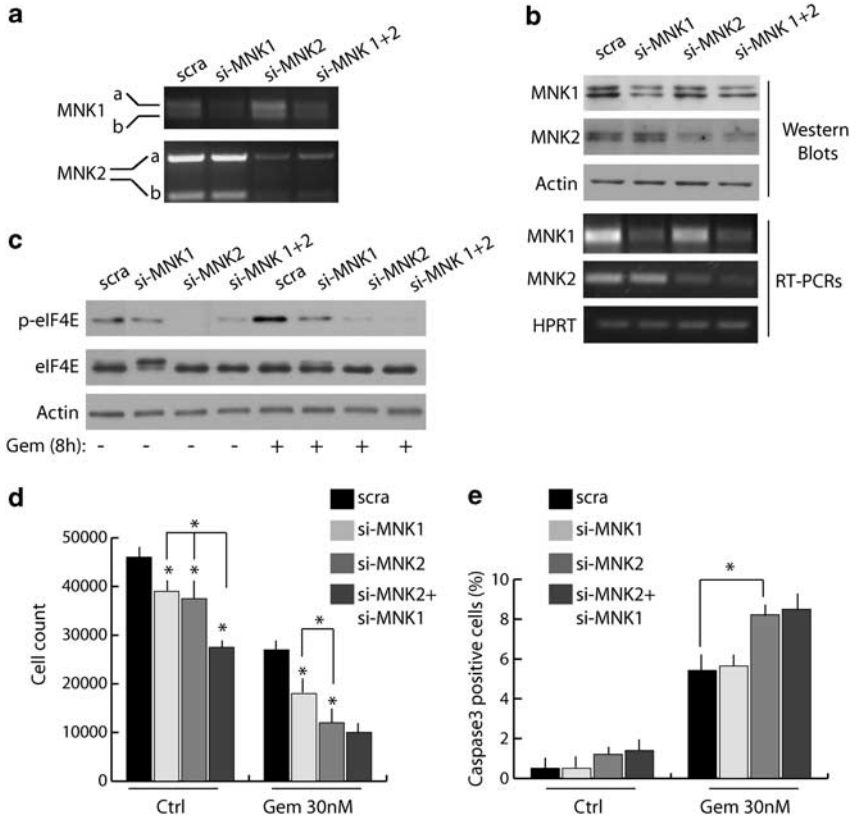

Figure 4. MNK2 promotes eIF4E phosphorylation and survival in gemcitabine-treated cells. (**a**) RT–PCR analysis of the transcripts encoding MNK1 and MNK2 using primers that distinguish between the a and b variants in MiaPaCa2 cells transfected with the indicated siRNAs. (**b**) Western blot and RT–PCR analyses of MNK1 and MNK2 protein and mRNA levels in MiaPaCa2 cells transfected with the indicated siRNAs. First and second panels show protein amounts of MNK1 or MNK2 after transfection. Actin was used as loading control. PCR amplifications were obtained with primers common to both splice variants of MNK1 (fourth panel) and MNK2 (fifth panel). (**c**) Western blot analyses of total and p-eIF4E levels in MiaPaCa2 cells transfected as in (**b**) and treated with or without 30 nM gemcitabine (8 h). (**d–e**) MiaPaCa2 cells transfected as in (**b**) were treated with 30 nM gemcitabine (48 h). The histogram in (**d**) represents cell number of three experiments (mean ± s.d.). The histogram in (**e**) represents the percentage of cleaved-caspase-3 positive cells of three experiments (mean ± s.d.). Statistical analysis was performed comparing values of cells silenced for MNKs with cells transfected with the scramble siRNA, or between the samples indicated by brackets; $*P < 0.05$ in paired *t*-test.

In other cell types splicing of MNK2b is promoted by SRSF1, a splicing factor of the SR protein family that functions as a proto-oncogene *in vitro* and *in vivo*.[21] Remarkably, gemcitabine induced expression of SRSF1 in MiaPaCa2 and PT45P1 cells (Figure 5d). SRSF1 upregulation was specific because other oncogenic splicing factors, such as hnRNPA1[22] and Sam68,[23] were not affected (Figure 5d). To investigate the role of SRSF1 in the alternative splicing of MNK2, we silenced it by RNAi. SRSF1 mRNA was decreased already at 24 h from transfection (Supplementary Figure S7), but SRSF1 protein depletion was only observed after 48 h and correlated with increased splicing of the MNK2a variant (Figure 6a). At this time-point, MiaPaCa2 cells were treated with gemcitabine for 48 h and analyzed for MNK2b expression and eIF4E phosphorylation levels. Although SRSF1 silencing did not affect eIF4E phosphorylation in cells growing in control medium (Figures 6a, b), it dramatically reduced it in gemcitabine-treated cells (Figure 6b). Moreover, SRSF1 depletion prevented the gemcitabine-induced shift of variants ratio toward MNK2b (Figure 6b), without affecting the reduction in the total levels of MNK2. These changes in MNK2 splicing and eIF4E phosphorylation were paralleled by reduced proliferation (Figure 6c) and increased death (Figure 6d) in SRSF1-depleted cells exposed to gemcitabine, similarly to what observed by MNK2 silencing and pharmacological inhibition of MNK activity.

Collectively, these observations strongly suggest that upon exposure to gemcitabine, PDAC cells activate a pro-survival pathway that involves upregulation of SRSF1, splicing of the MNK2b variant and increased phosphorylation of eIF4E.

DISCUSSION

PDAC is a non curable disease, mainly owing to late diagnosis and resistance to therapies, which results in rapid progression and metastatic spreading.[1] In this work, we found that various therapeutic treatments trigger MNK-dependent phosphorylation of eIF4E in PDAC cell models. The biological relevance of this phenomenon is indicated by the enhanced cell death in response to gemcitabine observed in PDAC cells in which eIF4E phosphorylation is prevented by pharmacological or genetic approaches. Furthermore, increased phosphorylation of eIF4E correlates with worse prognosis and disease grade in patients. Thus, these results suggest that the MNK/eIF4E pathway might represent a novel potential therapeutic target for PDAC.

Phosphorylation of eIF4E is associated with worse prognosis in lung cancer,[18] and it is required for the oncogenic properties of eIF4E in animal models.[14–16] To investigate whether phosphorylation of eIF4E displays clinical relevance in PDAC, we analyzed a cohort of 32 patients selected for the availability of detailed clinical and histopathological data and for the absence of metastases at diagnosis. We found that increased phosphorylation of eIF4E positively correlated with disease grade and was significantly associated with early disease onset in PDAC patients.

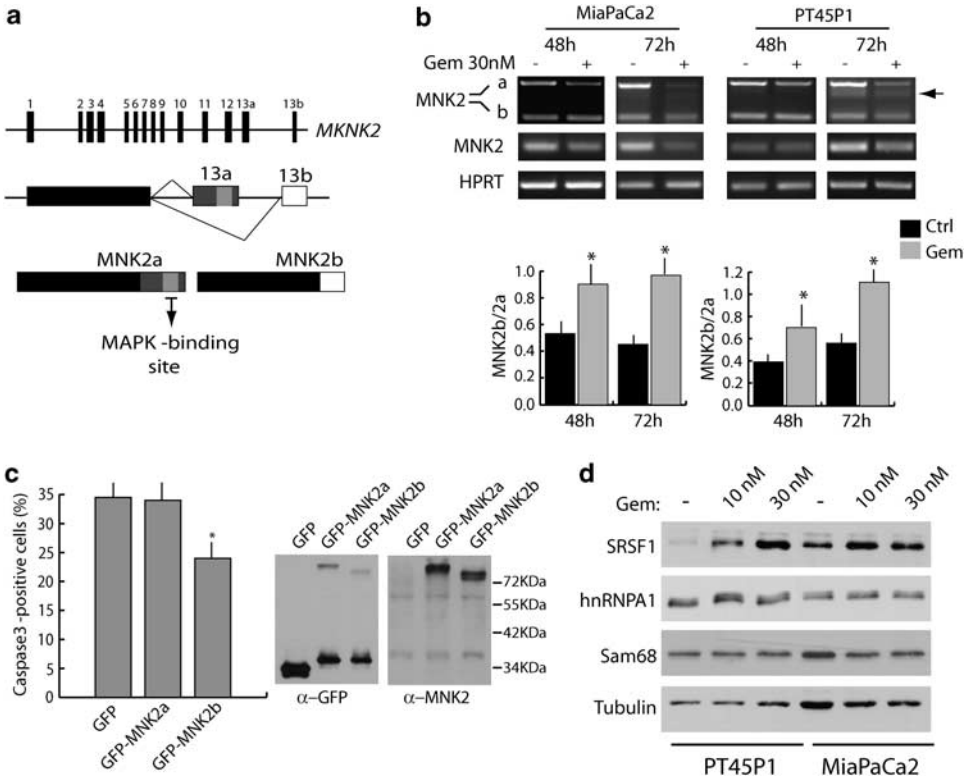

Figure 5. Gemcitabine affects the *MKNK2* splice variants ratio in PDAC cells. (**a**) Schematic representation of the *MKNK2* gene showing the mutually exclusive exons 13a and 13b. (**b**) RT–PCR analysis of MiaPaCa2 or PT45P1 cells treated with 30 nM gemcitabine. Panels show expression of splice variants (the arrow indicates a non specific band appearing with increased PCR cycles in PT45P1), total MNK2 levels and HPRT expression as internal control of the RNA quality. The histograms represent densitometric analysis of the MNK2b/a ratio from three experiments (mean ± s.d.); $*P<0.05$ in paired *t*-test. (**c**) Results of the immunofluorescence analyses of the cleaved form of caspase-3 in MiaPaCa2 cells overexpressing GFP, GFP-MNK2a or GFP-MNK2b vectors and treated with gemcitabine for 48 h. Bar graphs represent mean ± s.d. of three experiments. Statistical analysis was performed using the paired *t*-test; $*P<0.01$. Right panels represent western blots of the same samples using GFP or MNK2 antibody. (**d**) Western blot analysis of SRSF1, Sam68 and hnRNPA1 in MiaPaCa2 and PT45P1 cells after 72 h of treatment with the indicated doses of gemcitabine.

Furthermore, high eIF4E phosphorylation levels were also associated with worse survival and with a shorter mean time to tumor recurrence. Although the cohort examined in our study was relatively small, our results were statistically significant. However, as some of the patients were also lost to follow-up relatively early, more extensive analyses with larger patient numbers will be required to confirm that eIF4E phosphorylation may represent an important prognostic marker for PDAC. A larger cohort will also be necessary to determine whether increased eIF4E phosphorylation levels reflect an underlying biology associated with earlier onset and more aggressive disease.

Increased phosphorylation of eIF4E occurs in cancer cells of various organs after exposure to stress stimuli and chemotherapeutic treatments,[9–16] thus suggesting that this pathway allows cells to survive under adaptive pressures. Our results now indicate that MNK-dependent phosphorylation of eIF4E also promotes survival of PDAC cells exposed to therapeutic drugs. Although pharmacological inhibition of MNK activity had mild effects on cell growth, it strongly enhanced the cytostatic effect exerted by genotoxic stress and mTOR inhibition. Our studies indicate that MNK-I mainly affects cell survival in response to gemcitabine. Importantly, sub-optimal doses of gemcitabine combined with MNK-I were sufficient to completely prevent colony formation. As MNK activity and eIF4E phosphorylation are dispensable for normal organism development,[8] inhibition of this pathway might be well tolerated in combination with other therapeutic treatments. In this regard, it also appears promising the recent observation that inhibition of eIF4E activity by ribavirin exhibited substantial clinical benefits in acute myeloid leukemia patients without eliciting toxic responses.[24] As chemotherapeutic regimens exert only marginal effects in PDAC patients,[1] our findings on the possible role of eIF4E phosphorylation in drug sensitivity of PDAC cells suggest that targeting eIF4E phosphorylation might represent a novel strategy to improve therapeutic efficacy. Notably, this approach might also be useful in combination with other targeted therapies currently under evaluation in PDAC. For instance, RAD001 (Everolimus), a small-molecule mTOR inhibitor derived from rapamycin, exerted positive effects in combination with gemcitabine in preclinical and clinical studies with metastatic PDAC patients.[25] However, a side effect of blocking mTOR activity is the increased MNK-dependent phosphorylation of eIF4E.[3,4] As inhibition of MNK activity synergistically enhances the cytostatic effect of mTOR inhibitors in PDAC cells, it is possible that combined treatment with these molecules might exert beneficial effects.

Phosphorylation of eIF4E promotes tumor development in vivo.[14–16] The activation of MNKs and eIF4E phosphorylation reported in several human cancer cell lines further support the implication of this pathway in oncogenesis.[11–13] In line with this hypothesis, pharmacological inhibition of MNK activity was shown to reduce protein synthesis,[11] cancer cell proliferation[11–13] and development of tumors *in vivo*.[12] However, all these studies did not document a clear difference between the contribution of MNK1 and MNK2 to these processes. Our work now suggests that, although both kinases contribute to eIF4E phosphorylation and support PDAC cell proliferation under basal conditions, only MNK2

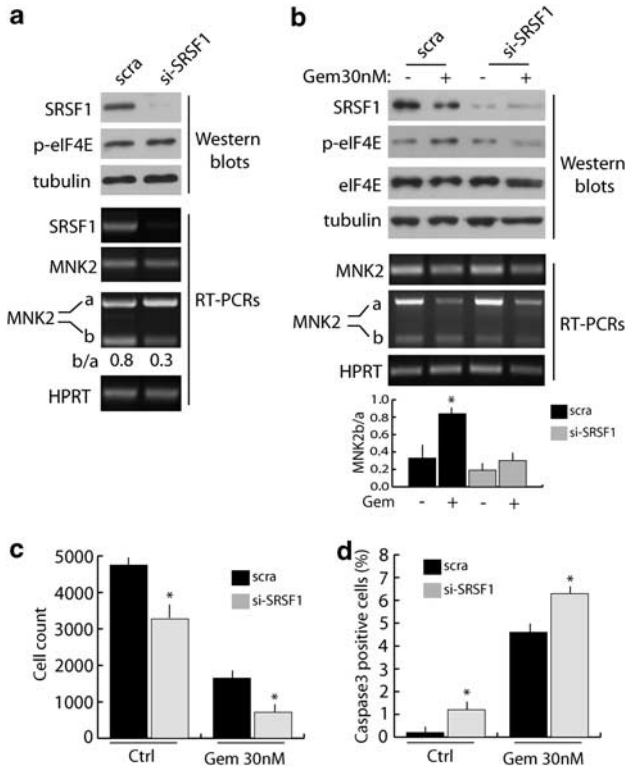

Figure 6. SRSF1 is required for the modulation of *MKNK2* splice variants by gemcitabine. (**a**) MiaPaCa2 cells transiently transfected with scrambled or SRSF1 siRNAs and analyzed after 48 h. Western blot analysis (first to third panel) of SRSF1, p-eIF4E and tubulin. RT–PCR analysis (fourth to seventh panel) of SRSF1, MNK2 total and splice variant mRNA levels (ratio quantified as in Figure 5. (**b**) MiaPaCa2 cells were transfected with control or SRSF1 siRNAs and treated with 30 nM gemcitabine for additional 48 h. Western blot analysis (first to fourth panel) of SRSF1, eIF4E, p-eIF4E and tubulin. RT–PCR analysis (fifth to seventh panel) of MNK2 and MNK2 splice variant mRNA levels as in (**a**). $*P<0.05$ in paired *t*-test. (**c**, **d**) MiaPaCa2 cells were transfected with scramble or SRSF1 siRNAs and treated with 30 nM gemcitabine for 48 h. The histogram in (**c**) represents cell number of three experiments (mean ± s.d.). The histogram in (**d**) represents the percentage of cleaved-caspase3-positive cells of three experiments (mean ± s.d.). Statistical analysis was performed comparing values of cells silenced for SRSF1 with cells transfected with the control siRNA; $*P<0.05$ in paired *t*-test.

is responsible for the pro-survival effects in cells treated with gemcitabine. Thus, our results uncover a new MNK2-specific function in PDAC cells, which confers resistance to a genotoxic treatment. As MNK2 was found to be upregulated in hormone-resistant prostate cancer,[12] it will be interesting to test whether it is more generally involved in the pro-survival responses of cells that develop resistance to chemotherapeutic treatments.

The *MKNK2* gene encodes two mRNA variants, through usage of alternative last exons named 13a (MNK2a) and 13b (MNK2b).[9,20] Gemcitabine caused a reduction in MNK2 expression, mainly affecting MNK2a levels and thereby altering the splice variant ratio in favor of MNK2b. We also found that MNK2b partially protected cells from gemcitabine-induced apoptosis, whereas MNK2a did not. MNK2b lacks the MAPK-interacting region and it is thereby uncoupled from upstream MAPK pathways.[9,20,21] Thus, it is possible that its expression in cells treated with gemcitabine allows higher levels of eIF4E phosphorylation independently from external cues, which might lead to progressive selection of chemoresistant cells. Splicing of MNK2b was previously shown to be regulated by the splicing factor SRSF1 in other cell types.[21] We found that gemcitabine induces the expression of SRSF1 in PDAC cells, which is necessary to favor MNK2b splicing under genotoxic stress. In the absence of SRSF1, gemcitabine still caused a reduction in MNK2 levels, but it did not alter the ratio between the two splice variants, indicating that SRSF1 is required to promote MNK2b splicing in PDAC cells exposed to the drug. Moreover, SRSF1 silencing impaired eIF4E phosphorylation and reduced viability of PDAC cells exposed to gemcitabine. These observations suggest that SRSF1 upregulation is part of the pro-survival response triggered by gemcitabine. Interestingly, *SRSF1* is an oncogene frequently upregulated in cancer.[21] More in general, splicing factors are emerging as novel regulators of oncogenic transformation, and increased expression of some of them was shown to correlate with malignancy and poor prognosis.[22] Furthermore, mutations that affect splicing of tumor suppressors, such as BRCA1/2 and APC, resulting in their inactivation, account for some types of inherited and sporadic susceptibility to cancer.[26,27] Our results now suggest that increased expression of splicing factors and changes in alternative splicing of target genes can also occur in response to chemotherapeutic treatment of cancer cells. Thus, targeting the activity of splicing factors might represent a novel approach for combined treatments of specific cancers. In this regard, it is noteworthy that the SR protein kinase 1, a key regulator of SRSF1 activity, is also upregulated in PDAC[28] and was proposed as a suitable target for novel therapies.[29]

In conclusion, our study identifies a novel pro-survival pathway triggered by gemcitabine in PDAC cells, which relies on MNK2-dependent phosphorylation of eIF4E, and suggests that targeting this pathway might represent a promising approach to enhance the response of PDAC cells to therapeutic agents.

MATERIALS AND METHODS

Tissue, histopathology and clinical information

Immunohistochemistry was performed with a rabbit polyclonal anti phospho-eIF4E antibody (1:200, Invitrogen, Rockville, MD, USA), as previously described,[18] on paraffin-embedded tissue samples from 32 primary non metastatic PDAC patients receiving surgery with radical intent. All but eight of these patients received gemcitabine-based adjuvant therapy after surgery. None of the patients received neoadjuvant treatment. Clinical and histopathological data for each patient were recorded (Supplementary Table 1). Scoring of p-eIF4E was based on distribution and intensity of staining in neoplastic cells.[18] Distribution was scored as 0 (0%), 1 (1–50%) and 2 (51–100%). Intensity was scored as 0 (no signal), 1 (mild), 2 (intermediate), 3 (strong) (Figure 1a). Values were summed in a total score from 0 to 5. Samples were classified as 'low p-eIF4E' expression when score was $\leqslant 2$ (group 0), and as 'high p-eIF4E' expression when score was $\geqslant 3$ (group 1). Statistical analysis was performed by MedCalc 9.6 (www.medcalc.be). Differences for continuous variables were evaluated by *t*-test and for categorical variables by Fisher's test. Correlation between the expression scores and pathological data was tested by Spearman's rank order correlation. Analysis of overall survival was performed by Kaplan–Meier method and analyzed by log-rank test. Patients lost at follow-up or whose follow-up ended before the outcome (death) was reached, are 'censored' and marked as small vertical lines in the survival curves. Univariate and multivariate analyses for risk factors affecting survival were performed by Cox-proportional hazards regression model test; a *P*-value <0.05 was considered as statistically significant.

Cell cultures, treatments and extract preparation

MiaPaCa2, PT45P1 and PANC-1 cells were obtained from the Cancer Research UK Cell Services (Clare Hall Laboratories, Potters Bar, UK); HPAF2 cells were purchased from American Type Culture Collection (ATCC, Rockville, MD, USA) and generously provided by Professor Aldo Scarpa (University of Verona). Cells were maintained in Dulbecco's modified Eagle's medium (GIBCO, Carlsbad, CA, USA) (MiaPaCa2) or RPMI 1640 (Lonza, Basel, Switzerland) (PT45P1, PANC-1, HPAF2) supplemented with 10% fetal bovine serum. MNK-Inhibitor (CGP57380), rapamycin, LY294002, U0126 and SB202190 (EMD Chemical Inc./Calbiochem, Darmstadt,

Germany) were dissolved in dimethyl sulfoxide and stored at $-20\,^{\circ}C$. Gemcitabine (Eli Lilly & Company, Indianapolis, IN, USA) was dissolved in water. Cisplatin (Sigma-Aldrich, St Louis, MO, USA) was dissolved in RPMI 1640. Stock solutions were diluted to the final concentrations in medium. After incubation, cells were washed with ice-cold phosphate buffered saline (PBS), resuspended in lysis buffer (100 mM NaCl, 15 mM $MgCl_2$, 30 mM Tris-HCl pH 7.5, 1 mM dithiothreitol, 2 mM Na-ortovanadate, 1% Triton X-100 and Protease-Inhibitor Cocktail (Sigma-Aldrich)) and kept on ice for 10 min. Cell extracts were separated by centrifugation at 12 000 r.p.m. for 10 min and diluted in SDS–PAGE sample buffer.

SDS–PAGE and western blot analyses

Western blot analyses of cell extracts (30 μg) were performed as previously described[11,30] using the following primary antibody: mouse anti beta tubulin (1:1000, Sigma-Aldrich); rabbit anti-4EBP1, anti-rpS6 and anti-eIF4E (1:1000, Cell Signaling Technology, Danvers, MA, USA); rabbit anti-p-rpS6 and anti p-eIF4E (1:1000, Biosource, Carlsbad, CA, USA); mouse anti-SRSF1 and anti-hnRNPA1, rabbit anti-Sam68 and anti-ERK2 (1:1000, SantaCruz Biotechnology, Santa Cruz, CA, USA). Secondary IgGs conjugated with horseradish peroxidase (1:10 000; Amersham Bioscience, Piscataway, NJ, USA) were incubated for 1 h at room temperature and signals were detected by enhanced chemiluminescence (SantaCruz Biotechnology).

Cell count and viability assays

MiaPaCa2 were seeded at 50 000 cells/plate in 24-well plate and treated as described in the text for 72 h, washed in PBS, trypsinized and counted using the Thoma's chamber. Cell viability was measured by the MTS Cell Titer 96 Aqueous Non-Radioactive Cell Proliferation Assay (Promega, Madison, WI, USA) according to manufacturer's instructions by plating 1500 cells (MiaPaCa2) or 3000 cells (PT45P1) per well. Results of cell count and cell viability assays represent mean ± s.d. of three experiments performed in triplicate.

Colony formation assay

Single-cell suspensions were plated in 100 mm plates (3500 cells/plate). After 1 day, cells were treated for 24 h with gemcitabine (0.1 and 0.3 nM) and MNK-I (10 μM) alone or in combination. At the end of the incubation, the medium was replaced every 24 h with or without addition of 5 μM MNK-I. After 10 days, cells were fixed in methanol for 10 min, stained overnight with 10% Giemsa, washed twice in PBS and dried. Pictures were taken using a digital camera to count the colonies. Results represent the mean ± s.d. of three experiments.

Immunofluorescence analysis

For eIF4E phosphorylation, MiaPaCa2 were seeded at 350 000 cells/plate in 35 mm dishes and treated with 30 nM gemcitabine with or without 10 μM MNK-I for 24 h. Cell lines were then fixed for 10 min in 4% paraformaldehyde (PFA), permeabilized with 0.1% Triton X-100, processed for immunofluorescence analysis using the anti p-eIF4E (1:200). For apoptotic markers, cells were seeded at 250 000 (MiaPaCa2, HPAF2) or 200 000 (PT45P1) cells/plate in 35 mm plates and treated with gemcitabine for 72 or 48 h. Immunofluorescence was performed as described above and cell were stained with anti-cleaved caspase-3 antibody (1:500; Sigma-Aldrich). For TUNEL assays, fixed cells were permeabilized in PBS containing 0.1% sodium citrate and 0.1% Triton X-100 and incubated with TUNEL reaction mixture containing terminal deoxynucleotidyltransferase and fluorescein-dUTPs at $37\,^{\circ}C$ for 60 min (In Situ Cell Death Detection Kit, Fluorescein, Roche, Penzberg, Germany). Four random fields were chosen for each treatment and at least 100 cells/field were counted. Results represent the mean ± s.d. of three experiments.

Cell transfection experiments

pEGFP MNK2a and pEGFP MNK2b vectors were obtained by subcloning the *Eco*RI/*Sal*I (MNK2a, 2b) fragments from pEBG (MNK2a) or pCMV5 (MNK2b) (generous gift of Dr CG Proud) in pEGFPC1 vector. MiaPaCa2 cells were transfected in 35 mM plates with 2 μg of plasmid using Lipofectamine 2000 (Invitrogen) by standard methods as described.[30,31]

MNK1 silencing was obtained using the Smart pool reagent mix from Dharmacon. MNK2 si-RNA 5′-GGAACGUCCUAGAGCUGAU-3′ (common to both splice variants of the gene) and SRSF1 si-RNA 5′-CCAAGGACAUU GAGGACGU-3′ were purchased from Sigma-Aldrich. Cells were transfected at 50% confluence in 35 mM plates with 30 nM of siRNAs using Lipofectamine RNAi MAX reagent (Invitrogen).[31]

RT–PCR analyses

RNA was extracted using the TRIzol reagent (Invitrogen) and following manufacturer's instruction. After digestion with RNase-free DNase (Roche Diagnostics GmbH), 1 μg of RNA was retro-transcribed (RT) using M-MLV reverse transcriptase (Invitrogen). PCR primers for MNK1 and MNK2 splice variants and PCR conditions were previously described.[21,32] For MNK1 and MNK2 expression we used primers that amplify both splice variants: MNK1 forward 5′-GAGGTTCCATCTTAGCCCACAT-3′, reverse 5′-ACGATGAGCAAT GCCTTTGGT-3′; MNK2 forward 5′-CGCCTTGGACTTTCTGCATAA-3′, reverse 5′-TCACAGATCTTCACGGGGGA-3′. For *SRSF1* expression, the following primers were used: forward 5′-ATGTCGGGAGGTGGTGTGATTCGT-3′, reverse 5′-TTATGT ACGAGAGCGAGATCTGCT-3′. Ten percent of the RT reaction was used for each PCR reaction.

CONFLICT OF INTEREST

The authors declare no conflict of interest.

ACKNOWLEDGEMENTS

We wish to thank Professor CG Proud for the generous gift of MNK2a and MNK2b plasmids, Professor A Scarpa for the gift of HPAF2 cells, Dr Enrica Bianchi for help with FACS analysis, Dr Maria Antonietta Talerico for technical support with immunohistochemistry and Dr Alessia Di Florio for helpful suggestions throughout the study. This work was supported by funds from the Associazione Italiana Ricerca sul Cancro (AIRC IG10348) and Association for International Cancer Research (AICR).

REFERENCES

1 Kern SE, Shi C, Hruban RH. The complexity of pancreatic ductal cancers and multidimensional strategies for therapeutic targeting. *J Pathol* 2011; **223**: 295–306.
2 Falasca M, Selvaggi F, Buus R, Sulpizio S, Edling CE. Targeting phosphoinositide 3-kinase pathways in pancreatic cancer--from molecular signaling to clinical trials. *Anticancer Agents Med Chem* 2011; **11**: 455–463.
3 Sun SY, Rosenberg LM, Wang X, Zhou Z, Yue P, Fu H *et al.* Activation of Akt and eIF4E survival pathways by rapamycin mediated mammalian target of rapamycin inhibition. *Cancer Res* 2005; **65**: 7052–7058.
4 Wang X, Yue P, Chan C, Ye K, Ueda T, Watanabe-Fukunaga R *et al.* Inhibition of Mammalian Target of Rapamycin Induces Phosphatidylinositol 3-Kinase Dependent and Mnk-Mediated Eukaryotic Translation Initiation Factor 4E Phosphorylation. *Mol Cell Biol* 2007; **27**: 7405–7413.
5 Zoncu R, Efeyan A, Sabatini DM. mTOR: from growth signal integration to cancer, diabetes and ageing. *Nat Rev Mol Cell Biol* 2011; **12**: 21–35.
6 Culjkovic B, Topisirovic I, Skrabanek L, Ruiz-Gutierrez M, Borden KL. eIF4E promotes nuclear export of cyclin D1 mRNAs via an element in the 3′ UTR. *J Cell Biol* 2005; **169**: 245–256.
7 Mamane Y, Petroulakis E, Rong L, Yoshida K, Ler LW, Sonenberg N. eIF4E – from translation to transformation. *Oncogene* 2004; **23**: 3172–3179.
8 Ueda T, Watanabe-Fukunaga R, Fukuyama H, Fukuyama H, Nagata S, Fukunaga R. Mnk2 and Mnk1 are essential for constitutive and inducible phosphorylation of eukaryotic initiation factor 4E but not for cell growth or development. *Mol Cell Biol* 2004; **24**: 6539–6654.
9 Buxade M, Parra-Palau JL, Proud CG. The Mnks: MAP kinase-interacting kinases (MAP kinase signal-integrating kinases). *Front Biosci* 2008; **13**: 5359–5373.
10 Zhang Y, Li Y, Yang D. Phosphorylation of eIF-4E positively regulates formation of the eIF-4F translation initiation complex following DNA damage. *Biochem Biophys Res Commun* 2008; **367**: 54–59.
11 Bianchini A, Loiarro M, Bielli P, Busà R, Paronetto MP, Loreni F *et al.* Phosphorylation of eIF4E supports protein synthesis, cell cycle progression and proliferation in prostate cancer cells. *Carcinogenesis* 2008; **29**: 2279–2288.
12 Konicek BW, Stephens JR, McNulty AM, Robichaud N, Peery RB, Dumstorf CA *et al.* Therapeutic inhibition of MAP kinase interacting kinase blocks eukaryotic initiation factor 4E phosphorylation and suppresses outgrowth of experimental lung metastases. *Cancer Res* 2011; **71**: 1849–1857.
13 Altman JK, Glaser H, Sassano A, Joshi S, Ueda T, Watanabe-Fukunaga R *et al.* Negative Regulatory Effects of Mnk Kinases in the Generation of Chemotherapy-Induced Antileukemic Responses. *Mol Pharmacol* 2010; **78**: 778–784.
14 Wendel HG, Silva RL, Malina A, Mills JR, Zhu H, Ueda T *et al.* Dissecting eIF4E action in tumorigenesis. *Genes Dev* 2007; **21**: 3232–3237.

15 Furic L, Rong L, Larsson O, Koumakpayi IH, Yoshida K, Brueschke A *et al.* eIF4E phopshorylation promotes tumorigenesis and is associated with prostate cancer progression. *Proc Natl Acad Sci USA* 2010; **107**: 14134–14139.
16 Ueda T, Sasaki M, Elia AJ, Chio II, Hamada K, Fukunaga R *et al.* Combined deficiency for MAP kinase-interacting kinase 1 and 2 (Mnk1 and Mnk2) delays tumor development. *Proc Natl Acad Sci USA* 2010; **107**: 13984–13990.
17 Graff JR, Konicek BW, Lynch RL, Dumstorf CA, Dowless MS, McNulty AM *et al.* eIF4E activation is commonly elevated in advanced human prostate cancers and significantly related to reduced patient survival. *Cancer Res* 2009; **69**: 3866–3873.
18 Yoshizawa A, Fukuoka J, Shimizu S, Shilo K, Franks TJ, Hewitt SM *et al.* Overexpression of phopsho-eIF4E is associated with survival through AKT pathway in non-small-cell lung cancer. *Clin Cancer Res* 2010; **16**: 240–248.
19 Chrestensen CA, Eschenroeder A, Ross WG, Ueda T, Watanabe-Fukunaga R, Fukunaga R *et al.* Loss of MNK function sensitizes fibroblasts to serum-withdrawal induced apoptosis. *Genes Cells* 2007; **12**: 1133–1140.
20 Scheper GC, Parra JL, Wilson M, Van Kollenburg B, Vertegaal AC, Han ZG *et al.* The N and C termini of the splice variants of the human mitogen-activated protein kinase-interacting kinase Mnk2 determine activity and localization. *Mol Cell Biol* 2003; **23**: 5692–5705.
21 Karni R, De Stanchina E, Lowe SW, Sinha R, Mu D, Krainer AR. The gene encoding the splicing factor SF2/ASF is a proto-oncogene. *Nat Struct Mol Biol* 2007; **14**: 185–193.
22 David CJ, Chen M, Assanah M, Canoll P, Manley JL. HnRNP proteins controlled by c-Myc deregulate pyruvate kinase mRNA splicing in cancer. *Nature* 2010; **463**: 364–368.
23 Bielli P, Busà R, Paronetto MP, Sette C. The RNA-binding protein Sam68 is a multifunctional player in human cancer. *Endocr Relat Cancer* 2011; **18**: 91–102.
24 Assouline S, Culjkovic B, Cocolakis E, Rousseau C, Beslu N, Amri A *et al.* Molecular targeting of the oncogene eIF4E in AML: a proof-of principle clinical trial with ribavirin. *Blood* 2009; **114**: 257–260.
25 Wolpin BM, Hezel AF, Abrams T, Blaszkowsky LS, Meyerhardt JA, Chan JA *et al.* Oral mTOR inhibitor everolimus in patients with gemcitabine-refractory metastatic pancreatic cancer. *J Clin Oncol* 2008; **27**: 193–198.
26 Gonçalves V, Theisen P, Antunes O, Medeira A, Ramos JS, Jordan P *et al.* A missense mutation in the APC tumor suppressor gene disrupts an ASF/SF2 splicing enhancer motif and causes pathogenic skipping of exon 14. *Mutat Res* 2009; **662**: 33–36.
27 Sanz DJ, Acedo A, Infante M, Durán M, Pérez-Cabornero L, Esteban-Cardeñosa E *et al.* A high proportion of DNA variants of BRCA1 and BRCA2 is associated with aberrant splicing in breast/ovarian cancer patients. *Clin Cancer Res* 2010; **16**: 1957–1967.
28 Hayes GM, Carrigan PE, Miller LJ. Serine-arginine protein kinase 1 overexpression is associated with tumorigenic imbalance in mitogen-activated protein kinase pathways in breast, colonic, and pancreatic carcinomas. *Cancer Res* 2007; **67**: 2072–2080.
29 Hayes GM, Carrigan PE, Beck AM, Miller LJ. Targeting the RNA splicing machinery as a novel treatment strategy for pancreatic carcinoma. *Cancer Res* 2006; **66**: 3819–3827.
30 Busà R, Paronetto MP, Farini D, Pierantozzi E, Botti F, Angelini DF *et al.* The RNA-binding protein Sam68 contributes to proliferation and survival of human prostate cancer cells. *Oncogene* 2007; **26**: 4372–4382.
31 Pedrotti S, Bielli P, Paronetto MP, Ciccosanti F, Fimia GM, Stamm S *et al.* The splicing regulator Sam68 binds to a novel exonic splicing silencer and functions in SMN2 alternative splicing in spinal muscular atrophy. *EMBO J* 2010; **29**: 1235–1247.
32 O'Loghlen A, Gonzalez VM, Pineiro D, Pérez-Morgado MI, Salinas M, Martín ME. Identification and molecular characterization of Mnk1b, a splice variant of human MAP kinase-interacting kinase Mnk1. *Experimental Cell Res* 2004; **299**: 343–355.

Supplementary Information accompanies the paper on the Oncogene website (http://www.nature.com/onc)

CHAPTER IV

The RNA-binding protein Sam68

Sam68 (Src associated during mitosis) is an RNA binding protein of the STAR (Signal Transduction and Activation of RNA metabolism) family that links regulation of specific mRNAs with signal transduction pathways. The classic structure of the STAR proteins includes an RNA-binding domain, called GSG (GRP33/Sam68/GLD-1), containing a KH domain (hnRNP K homology) responsible for the RNA binding, flanked by an N-terminal (NK) and a C-terminal (CK) regions that allow dimerization of the protein and RNA binding specificity (Lukong and Richard, 2003; Vernet and Artzt 1997). In addition to the aforementioned domain, Sam68 contains six proline-rich sequences (P0-P5) extending from both sides of the GSG domain, which are responsible for the interaction with proteins containing Src homology 3 (SH3) and WW domains. The C-terminus of the protein is characterized by a region rich in tyrosine residues that are subject to phosphorylation, a modification that affects Sam68 ability to bind RNA (Lukong and Richard, 2003) (Fig 4).

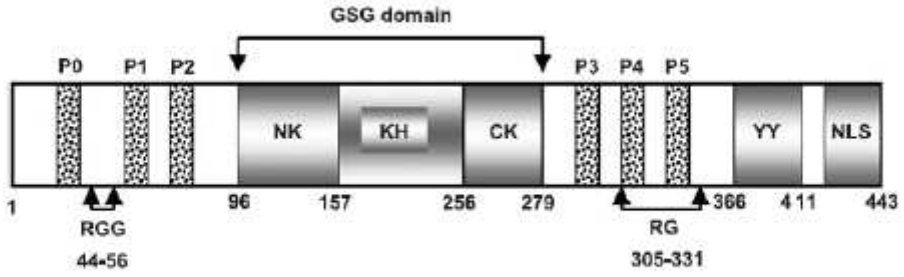

Figure 4: The structural and functional domains of Sam68
In the figure are indicated the GSG domain, containing the KH domain flanked by NK and CK sequences, the proline-rich sequences (P0-P5); arginine and glycine rich sequences ("RGG boxes"); tyrosine-rich domain (YY) and a nuclear localization signal (NLS). The relative aminoacids positions are indicated (Lukong and Richard, 2003).

The nuclear localization signal (NLS) of Sam68 targets this protein prevalently to the nucleus. Sam68 controls RNA metabolism at many levels that span from regulation of transcription (Hong W *et al*., 2002; Taylor SJ *et al*., 2004; Rajan P *et al*., 2008), to the modulation of splicing events (Chawla G *et al*., 2009; Paronetto MP *et al*., 2007, 2010; Matter N *et al*., 2002), to the

nuclear export of RNAs (Li J *et al*., 2002), and their translation (Grange J *et al*., 2009; Ben Fredj N*et al*., 2004; Paronetto MP *et al*., 2006, 2009). The activity of Sam68 is regulated by a large number of post-translational modifications that occur in response to various conditions and, in most cases, have an impact on its function by regulating its intracellular localization and its accessibility to RNA. (Lukong and Richard, 2003; Sette, 2010).

4.1 Sam68 and tumorigenesis

Sam68 was initially proposed as a tumor suppressor because its depletion was reported to cause neoplastic transformation of murine NIH3T3 fibroblasts (Liu K *et al*., 2000). Moreover, additional data established that overexpression of Sam68 promotes cell cycle arrest and apoptosis (Taylor SJ *et al*., 2004). However, subsequent studies clearly demonstrated that Sam68 plays positive roles in cancer cells and it is often overexpressed in human cancers (Busà R and Sette C, 2010; Bielli P *et al*., 2011). For instance, in breast cancer high levels of Sam68 correlates with short survival rates (Song L *et al*., 2010) and the attenuation of its expression delayed the onset of cancer in an animal model of mammary tumors (Richard S *et al*., 2008). Sam68 function is also required for proper cell proliferation and survival to drug treatment in prostate cancer (Busà *et al*., 2007, 2010). The key mechanism(s) regulated by Sam68 in cancer cells is not yet been identified, however it has been shown that this protein promotes tumorigenic features through the modulation of alternative splicing events (CD44, BCL-X, cyclin D1 and SRSF1; Matter N *et al*., 2002, Paronetto MP *et al*., 2007, 2010, Valacca C *et al*., 2010) (Fig 5). Thus, given the strong implication of aberrant regulation of alternative splciing in cancer (David & Manley, 2010), it is conceivable that the splicing activity of Sam68 contributes to neoplastic transformation in human cancer cells.

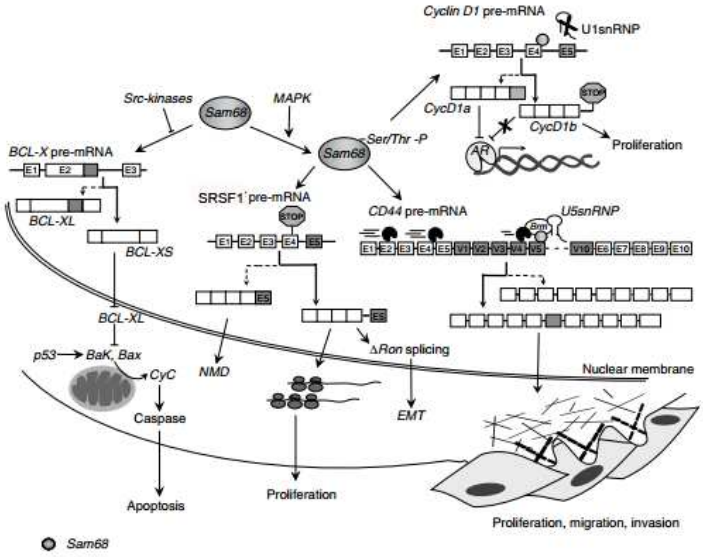

Figure 5: Cancer cell pathway regulated by Sam68
Tumorigenesis: Sam68 contributes to invasiveness by regulating the AS in the 3' UTR of SRSF1, which promotes the production of the oncogenic variant ΔRon that promotes EMT.
Proliferation: Sam68 modulates the production of Cyclin D1b isoform promoting androgen-dependent cancer cell proliferation.
Migration: Sam68 favors the inclusion of variable exons of CD44 mRNA, inducing the expression of isoforms that correlate with cancer progression and invasiveness
Apoptosis: Sam68 promotes the formation of the pro-apoptotic isoform Bcl-x(s), however tyrosine phosphorylation of Sam68 by Src family kinases, reverts this effect causing the expression of the anti-apoptotic variant, Bclx(L).
(adapted from Bielli *et al*, 2011).

References

Ben Fredj N, Grange J, Sadoul R, Richard S, Goldberg Y, Boyer V. Depolarization-induced translocation of the RNA-binding protein Sam68 to the dendrites of hippocampal neurons. *J Cell Sci.* 2004 Mar 1;117(Pt 7):1079-90.

Bielli P, Busà R, Paronetto MP, Sette C. The RNA-binding protein Sam68 is a multifunctional player in human cancer. *Endocr Relat Cancer.* 2011 Jul 1;18(4):R91-R102.

Busà R, Geremia R, Sette C. Genotoxic stress causes the accumulation of the splicing regulator Sam68 in nuclear foci of transcriptionally active chromatin. *Nucleic Acids Res.* 2010 May;38(9):3005-18.

Busà R, Paronetto MP, Farini D, Pierantozzi E, Botti F, Angelini DF, Attisani F, Vespasiani G, Sette C. The RNA-binding protein Sam68 contributes to proliferation and survival of human prostate cancer cells. *Oncogene.* 2007 Jun 28;26(30):4372-82

Busà R, Sette C. An emerging role for nuclear RNA-mediated responses to genotoxic stress. *RNA Biol*. 2010 Jul-Aug;7(4):390-6.

Chawla G, Lin CH, Han A, Shiue L, Ares M Jr, Black DL. Sam68 regulates a set of alternatively spliced exons during neurogenesis. *Mol Cell Biol.* 2009 Jan;29(1):201-13.

David CJ, Manley JL. Alternative pre-mRNA splicing regulation in cancer: pathways and programs unhinged. *Genes Dev*. 2010 Nov 1;24(21):2343-64.

Fumagalli S, NF Totty, JJ Hsuan, and SA Courtneidge (1994) A target for Src in mitosis. *Nature* 368:871-874

Grange J, Belly A, Dupas S, Trembleau A, Sadoul R, Goldberg Y. Specific interaction between Sam68 and neuronal mRNAs: implication for the activity-dependent biosynthesis of elongation factor eEF1A. *J Neurosci Res.* 2009 Jan;87(1):12-25.

Hong W, Resnick RJ, Rakowski C, Shalloway D, Taylor SJ, Blobel GA. Physical and functional interaction between the transcriptional cofactor CBP and the KH domain protein Sam68. *Mol Cancer Res*. 2002 Nov;1(1):48-55.

Li J, Liu Y, Kim BO, He JJ. Direct participation of Sam68, the 68-kilodalton Src-associated protein in mitosis, in the CRM1-mediated Rev nuclear export pathway. *J Virol*. 2002 Aug;76(16):8374-82.

Liu K, Li L, Nisson PE, Gruber C, Jessee J, Cohen SN Neoplastic transformation and tumorigenesis associated with sam68 protein deficiency in cultured murine fibroblasts. *J Biol Chem.*2000 275(51):40195-201.

Lukong KE and S. Richard (2003) Sam68, the KH domain-containing superSTAR. *Bioch. Biophys. Acta* 1653: 73-86.

Matter N, Herrlich P, König H. Signal-dependent regulation of splicing via phosphorylation of Sam68. *Nature*. 2002 Dec 12;420(6916):691-5.

Paronetto MP, Achsel T, Massiello A, Chalfant CE, Sette C. The RNA-binding protein Sam68 modulates the alternative splicing of Bcl-x. *J Cell Biol*. 2007 Mar 26;176(7):929-39.

Paronetto MP, Cappellari M, Busà R, Pedrotti S, Vitali R, Comstock C, Hyslop T, Knudsen KE, Sette C. Alternative splicing of the cyclin D1 proto-oncogene is regulated by the RNA-binding proteinSam68. *Cancer Res.* 2010 Jan 1;70(1):229-39.

Paronetto MP, Messina V, Bianchi E, Barchi M, Vogel G, Moretti C, Palombi F, Stefanini M, Geremia R, Richard S, Sette C. Sam68 regulates translation of target mRNAs in male germ cells, necessary for mouse spermatogenesis. *J Cell Biol.* 2009 Apr 20;185(2):235-49.

Paronetto MP, Zalfa F, Botti F, Geremia R, Bagni C, Sette C. The nuclear RNA-binding protein Sam68 translocates to the cytoplasm and associates with the polysomes in mouse spermatocytes. *Mol Biol Cell.* 2006 Jan;17(1):14-24.

Rajan P, Gaughan L, Dalgliesh C, El-Sherif A, Robson CN, Leung HY, Elliott DJ. The RNA-binding and adaptor protein Sam68 modulates signal-dependent splicing and transcriptional activity of the androgen receptor. *J Pathol.* 2008 May;215(1):67-77.

Richard S, Vogel G, Huot ME, Guo T, Muller WJ, Lukong KE Sam68 haploinsufficiency delays onset of mammary tumorigenesis and metastasis. Oncogene .*2008* 27(4):548-56.

Sette C. Post-translational regulation of star proteins and effects on their biological functions. *Adv Exp Med Biol*. 2010;693:54-66.

Song L, Wang L, Li Y, Xiong H, Wu J, Li J, Li M. Sam68 up regulation correlates with, and its down regulation inhibits, proliferation and tumourigenicity of breast cancer cells. *J Pathol*. 2010 222(3):227 37.

Taylor SJ and D Shalloway 1994 An RNA-binding protein associated with Src through its SH2 and SH3 domains in mitosis. *Nature* 1994 368: 867-871.

Taylor SJ, Resnick RJ, Shalloway D. Sam68 exerts separable effects on cell cycle progression and apoptosis. *BMC Cell Biol*. 2004 Jan 22;5:5.

Valacca C, Bonomi S, Buratti E, Pedrotti S, Baralle FE, Sette C, Ghigna C, Biamonti G.. Sam68 regulates EMT through alternative splicing-activated nonsense-mediated mRNA decay of the SF2/ASF protooncogene. *J Cell Biol.* 2010 191(1):87-99.

Vernet C, and K. Artzt STAR, a gene family involved in signal transduction and activation of RNA. *Trends Genet*. 1997 13: 479-484.

Zhang Z, Li J, Zheng H, Yu C, Chen J, Liu Z, Li M, Zeng M, Zhou F, Song L. Expression and cytoplasmic localization of SAM68 is a significant and independent prognostic marker for renal cell carcinoma. *Cancer Epidemiol Biomarkers Prev*. 2009 Oct;18(10):2685-93.

CHAPTER V

The RNA-binding protein PTB

PTB (polypyrimidine tract-binding protein, also called hnRNP I or PTBP1) is an abundant RNA-binding protein of the hnRNP (heterogeneous nuclear ribonucleoprotein) family involved in many different aspects of RNA metabolism. Structurally, PTB consists of four RRM (RNA recognition motif) domains all of which are capable of interacting with RNA, with three interdomain linkers and an N-terminal leader sequence containing nuclear localization and export signals (Fig 6).

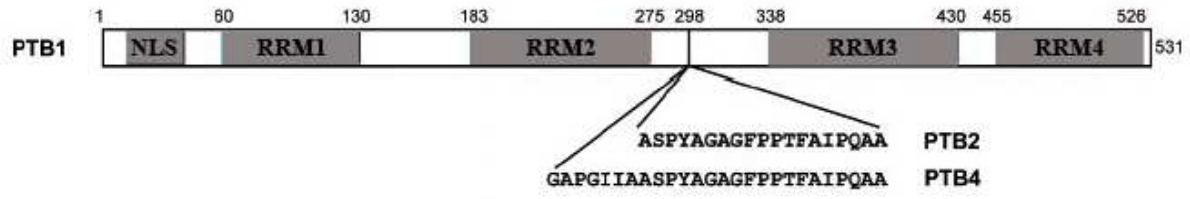

Figure 6: Structural and functional domains of PTB
PTB contains four RRMs and a nuclear localization signal (NLS). The amino acid sequences of the two other isoforms of PTB, PTB2 and PTB4 are shown. Relative aminoacids positions are indicated (adapted from Auweter and Allain, 2008)

PTB regulates numerous post-transcriptional steps of gene expression both in the nucleus and in the cytoplasm. PTB regulated processes include modulation of alternative splicing events (Mulligan GJ *et al*., 1992; Perez I *et al*., 1997), 3'-end processing (Lou H *et al*., 1999; Castelo-Branco P et al., 2004), mRNA stability (Wollerton MC *et al*., 2004), IRES (internal ribosome entry site) translation (Mitchell SA *et al*., 2005) and mRNA localization (Sawicka K *et al*., 2008).

PTB itself is subject to alternative splicing regulation, which gives rise to three isoforms: PTB1 that is the result of the skipping of exon 9, while the inclusion of exon 9 and usage of two competing 3' splice sites produces PTB2 and PTB4 isoforms that differ for the insertion of 19 or 26 amino acids respectively, between the second and third RNA recognition motif domains (Fig 5). These alternative splicing isoforms of PTB can vary in activity (Robinson and Smith, 2006; Wollerton MC *et al*., 2001), even though their specific cellular functions have not been described accurately.

Additional alternative splicing isoforms regulate PTB expression levels. Exon 11 skipping from the mature transcript produces a frameshift in the open reading frame, thus causing degradation of the mRNA by NMD (Wollerton MC *et al*., 2004). Notably, PTB autoregulates its own expression by modulating exon 11 skipping.

5.1 PTB and tumorigenesis

The role of PTB in cancer is still largely not understood. It has been shown that overexpression of PTB acts as inhibitor of cell growth in non small cell lung cancer cells (NSCLC) through the induction of the expression of $p19^{Ink4d}$, an inhibitor of cyclin-dependent kinase 4 (Lin S *et al*., 2013). Nevertheless, unlike other tumor suppressor genes, PTB is often increased in cancer cells and it has been shown that PTB depletion can reduce the growth of several types of cancer cells (Wang C *et al*., 2008). Depletion of PTB may also affect the invasive behavior of cancer cells causing either an inhibition or an increase of invasion in a cell type dependent manner (Wang C *et al*., 2008).

PTB was found overexpressed in ovarian cancer specimens *versus* normal controls and its depletion was shown to impair tumor cell proliferation, anchorage-independent growth and in vitro invasiveness of ovarian cancer cells (He X *et al*., 2007) strongly indicating a positive role for PTB in ovarian cancer. A similar role for PTB has also emerged in brain cancer, as PTB was found to be overexpressed in astrocytoma samples and glioblastoma multiforme samples *versus* normal brain tissues (David CJ *et al*., 2010). Moreover, it has been demonstrated that in this system PTB, in concert with hnRNPA1 and hnRNPA2, regulates the alternative splicing of the pyruvate kinase mRNA (PKM) promoting the induction of the embryonic pyruvate kinase isoform, PKM2, which promotes aerobic glycolysis whereas the adult isoform, PKM1, promotes oxidative phosphorylation (Fig 7). The glucose metabolism by aerobic glycolysis is an advantage for cancer cells since, despite it produces less energy, this metabolic route can facilitate the incorporation of more glycolytic metabolites into the biomass needed for rapid proliferation (Chen M *et al*., 2010). Similar results were also obtained in a cohort of different tumor cell lines (Clover CV *et al*., 2010), suggesting a more general PTB-mediated regulation of PKM splicing in cancer cells. All together, these observations strongly suggest that PTB acts as a positive regulator for tumorigenesis, at least in part by promoting alternative splicing events that are required for tumor cell proliferation.

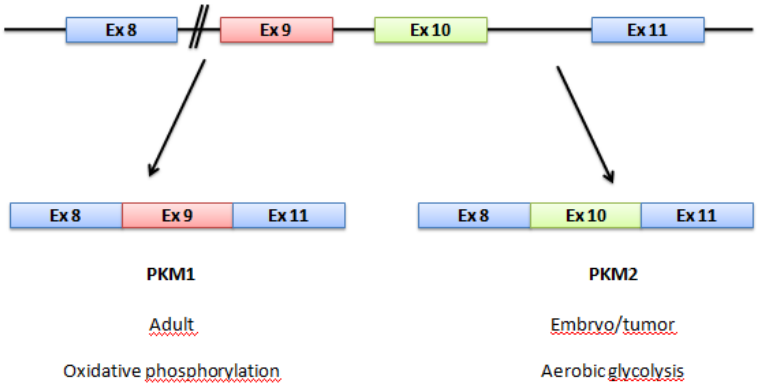

Figure 7: Pyruvate kinase alternative splicing isoforms
Alternative splicing generates two isoforms from the PKM mRNA: PKM1, resulting from the choice of two mutually exclusive exons: 9 (PKM2) and 10 (PKM1). The different isoforms possess different features: PKM1 in mainly expressed in adult cells and promote oxidative phosphorylation while PKM2 is express in embryonic cells and in cancer cells. This isoform switches the glucose metabolism to aerobic glicolyisis, favoring the proliferation of tumor cells. (Modified from David CJ *et al*., 2010)

References

Castelo-Branco P, Furger A, Wollerton M, Smith C, Moreira A, Proudfoot N. Polypyrimidine tract binding protein modulates efficiency of polyadenylation. Mol Cell Biol. 2004 May;24(10):4174-83.

Chen M, Zhang J, Manley JL. Turning on a fuel switch of cancer: hnRNP proteins regulate alternative splicing of pyruvate kinase mRNA. *Cancer Res*. 2010 Nov 15;70(22):8977-80.

Clower CV, Chatterjee D, Wang Z, Cantley LC, Vander Heiden MG, Krainer AR. The alternative splicing repressors hnRNP A1/A2 and PTB influence pyruvate kinase isoform expression and cell metabolism. *Proc Natl Acad Sci* U S A. 2010 Feb 2;107(5):1894-9.

David CJ, Chen M, Assanah M, Canoll P, Manley JL. HnRNP proteins controlled by c-Myc deregulate pyruvate kinase mRNA splicing in cancer. *Nature*. 2010 Jan 21;463(7279):364-8.

He X, Pool M, Darcy KM, Lim SB, Auersperg N, Coon JS, Beck WT. Knockdown of polypyrimidine tract-binding protein suppresses ovarian tumor cell growth and invasiveness in vitro. *Oncogene.* 2007 Jul 26;26(34):4961-8.

Lin S, Wang MJ, Tseng KY. Polypyrimidine tract-binding protein induces p19(Ink4d) expression and inhibits the proliferation of H1299 cells. *PLoS One.* 2013;8(3):e58227.

Lou H, Helfman DM, Gagel RF, Berget SM. Polypyrimidine tract-binding protein positively regulates inclusion of an alternative 3'-terminal exon. Mol Cell Biol. 1999 Jan;19(1):78-85.

Mitchell SA, Spriggs KA, Bushell M, Evans JR, Stoneley M, Le Quesne JP, Spriggs RV, Willis AE. Identification of a motif that mediates polypyrimidine tract-binding protein-dependent internal ribosome entry. Genes Dev. 2005 Jul 1;19(13):1556-71.

Mulligan GJ, Guo W, Wormsley S, Helfman DM. Polypyrimidine tract binding protein interacts with sequences involved in alternative splicing of beta-tropomyosin pre-mRNA. J Biol Chem. 1992 Dec 15;267(35):25480-7.

Perez, I., Lin, C.H., McAfee, J.G. and Patton, J.G. (1997) Mutation of PTB binding sites causes misregulation of alternative 3_ splice site selection *in vivo*. RNA 3, 764–778

Robinson F, Smith CW. A splicing repressor domain in polypyrimidine tract-binding protein. *J Biol Chem.* 2006 Jan 13;281(2):800-6.

S. D. Auweter and F. H.-T. Allain Structure-function relationships of the polypyrimidine tract binding protein *Cell. Mol. Life Sci*. 65 (2008) 516 – 527

Sawicka, K., Bushell, M., Spriggs, K.A. and Willis, A.E. (2008) Polypyrimidine-tract-binding protein: a multifunctional RNA-binding protein. *Biochem. Soc. Trans.* 36, 641–647

Wang C, Norton JT, Ghosh S, Kim J, Fushimi K, Wu JY, Stack MS, Huang S. Polypyrimidine tract-binding protein (PTB) differentially affects malignancy in a cell line-dependent manner. *J Biol Chem.* 2008 Jul 18;283(29):20277-87.

Wang MJ, Lin S (2009) A region within the 59-untranslated region of hypoxiainducible factor 1a mRNA mediates its turnover in lung adenocarcinoma cells. *J Biol Chem* 284: 36500–36510.

Wollerton MC, Gooding C, Robinson F, Brown EC, Jackson RJ, Smith CW. Differential alternative splicing activity of isoforms of polypyrimidine tract binding protein (PTB). *RNA*. 2001 Jun;7(6):819-32.

Wollerton MC, Gooding C, Wagner EJ, Garcia-Blanco MA, Smith CW. Autoregulation of polypyrimidine tract binding protein by alternative splicing leading to nonsense-mediated decay. Mol Cell. 2004 Jan 16;13(1):91-100.

Wollerton MC, Gooding C, Wagner EJ, Garcia-Blanco MA, Smith CW. Autoregulation of polypyrimidine tract binding protein by alternative splicing leading to nonsense-mediated decay. *Mol Cell*. 2004 Jan 16;13(1):91-100.

CHAPTER VI

RNA-binding proteins PTB and Sam68 contribute to the acquisition of the gemcitabine resistance in pancreatic cancer

The limited effect of conventional chemotherapy in pancreatic adenocarcinoma (PDAC) urges for novel therapies, targeting more directly the molecular aberrations of this disease. The molecular characterization of the drug resistant phenotype of PDAC cells remain unexplored, even though some evidence suggests a correlation with the expression of mesenchymal markers.
We found that the chronic exposure of PDAC cells to gemcitabine selected a subpopulation of cells that are more resistant to drug-induced cell death. This drug resistant subpopulation displays a more marked mesenchymal phenotype. Since we previously observed that gemcitabine treatment triggers a pro-survival mechanism that relies on upregulation of the oncogenic splicing factor SRSF1, we analyzed the expression of a cohort cancer related splicing factors in the drug resistant subpopulation. We found that PTB and Sam68 were markedly upregulated in drug resistant cells and, importantly, knockdown of PTB and Sam68 partially reverted the drug-resistant phenotype, with a more incisive effect for the PTB depletion.
Thus, our findings strongly indicate that the mechanism responsible for gemcitabine resistance in pancreatic cancer involves the upregulation of PTB and Sam68 and their consequent regulation of gene expression. Hence, PTB and Sam68 may represent novel suitable molecular targets for overcome drug resistance of PDAC.

RNA-binding proteins PTB and Sam68 contribute to the acquisition of the gemcitabine resistance in pancreatic cancer

Sara Calabretta [1,2], Ilaria Passacantilli [1,2], Chiara Naro [2,3], Gabriele Capurso [1], Raffaele Geremia [2], Gianfranco Delle Fave [1] and Claudio Sette [2,3]

[1]*Dept. of science medical/chirurgic and translational medicine, University of Rome La Sapienza, Italy*

[2]*Department of biomedicine and prevention, University of Rome Tor Vergata, Italy*

[3]*Laboratory of Neuroembriology, Fondazione Santa Lucia, Rome, Italy;*

Running title*:* PTB and Sam68 contributes to drug resistance

Keywords: PTB, Sam68, gemcitabine, drug resistance, pancreatic cancer, PDAC

Corresponding Authors:

Gianfranco Delle Fave
Dept. of science medical/chirurgic
and translational medicine
University of Rome "La Sapienza"
Via di Grottarossa, 1035
00189 Rome, Italy
Telephone: 3906 33775691
Email: gianfranco.dellefave@uniroma1.it

Claudio Sette
Dept. of Biomedicine and Prevention
University of Rome "Tor Vergata"
Via Montpellier, 1
00133 Rome, Italy
Telephone: 3906 72596260
Fax: 3906 72596268
Email: claudio.sette@uniroma2.it

INTRODUCTION

Pancreatic ductal adenocarcinoma (PDAC) is one of the most aggressive and malignant neoplastic diseases with a 5-years survival rate of less than 5% (Siegel R *et al.*, 2012; Kem SE *et al*., 2011). Indeed, despite the clinical use of the chemotherapeutic drug gemcitabine alone or in combination, PDAC remains extremely lethal in large part due to poor response to treatments (Hidalgo M, 2010). Thus, there is a strong need of further studies aiming at identifying novel molecular targets for the development of an innovative strategy to cure this disease. One promising strategy could be the identification of the escape pathways that cancer cells can use to survive to the genotoxic stress given by the drug treatment. In this regard, we have recently shown that PDAC cells are able to trigger a pro-survival mechanism in response to short-term treatment with gemcitabine (Adesso L *et al*., 2013). This escape pathway involves the upregulation of the SRSF1 splicing factor (SF), which consequently promotes the splicing of MNK2b, a constitutively active isoform of MNK2, thereby establishing a loop that stimulates phosphorylation of eIF4E during genotoxic stress and enhances PDAC cell survival. Remarkably, growing evidences suggest that the expression of splicing factors is often altered in cancer (Grosso AR *et al*., 2008). This alteration may be responsible for the differential balance of the alternative mRNA isoforms in neoplastic cells and tissues with respect to the non pathological conditions (Kim E *et al*.,2008). Emerging evidences report that aberrant expression of SFs (Zhou R *et al*., 2010) and SF regulators (Hayes GM *et al.*, 2006) also occurs in pancreatic cancer and the presence of differential splice isoforms has also emerged (Choudhury A *et al*., 2000; Hartel M *et al*., 2008; Wei D *et al*., 2010; Carrière C *et al*., 2011; Arafat H *et al*., 2011). Hence, all these observations suggest a central role for the alternative splicing regulation in the tumorigenesis of PDAC. SFs may play multiple roles in neoplastic cells. They may act as real proto-oncogenes, as SRSF1 that is over-expressed in many human carcinomas and its overexpression is sufficient to induce malignant transformation through the regulation of a cohort of alternative splicing events (Karni R *et al*., 2007). Sam68 (Src associated in mitosis) is another example of a splicing factor found to be involved in tumorigenesis in various human cancers (Bielli P *et al*., 2011), including prostate cancer where it was shown to contribute to proliferation and survival to genotoxic stress (Busà R *et al*., 2007; 2010). Among the RNA-binding proteins frequently up-regulated in cancer, there is also PTB (PTBP1, polypyrimidine-tract-binding protein), which is overexpressed in ovarian (He X *et al*., 2007) and brain cancers (David CJ *et al*., 2010). PTB depletion affects ovarian cancer cell proliferation and influence

brain cancer cell metabolism thought the promotion of the alternative splicing isoform PKM2 (embryonic variant 2) of the pyruvate-kinase (PK-M gene) mRNA. PKM2 promotes aerobic glycolisis instead the adult isoform, PKM1, promotes oxidative phosphorylation. Importantly, it has been recently shown that the depletion of PKM2 expression in glioblastoma cells caused an increase in cell death thereby suggesting an additional pro-survival role for this alternative splicing isoform in cancer (Wang Z *et al*., 2012).

Another fundamental cancer related pathway regulated by alternative splicing is the epithelial to mesenchymal transition (EMT) (Warzecha CC and Carstens RP, 2012), a process that supports cancer cell invasion of tissues and metastatic dissemination (Kalluri R *et al*; 2003). In particular, it has been demonstrated that in PDAC EMT is involved in cancer progression (Rhim AD *et al*., 2012) and drug resistance (Arumugam T *et al*., 2009). All these observations point to a positive role exerted by splicing factors in pancreatic cancer.

In the present work, we investigated the involvement of splicing factors to the long-term selection of a drug-resistant (DR) subpopulation of cancer cells. We observed that chronic gemcitabine treatment of PDAC cells caused the formation of DR subpopulations highly resistant to genotoxic stress. DR subpopulations displayed mesenchymal features with respect to the parental cells (PCL), a change that is accompanied by an increased expression of mesenchymal makers and enhanced cell migration. Importantly, we found that Sam68 and PTB were up-regulated in the DR-subpopulation and that their expression is required to promote survival of DR-cells to genotoxic stress. Hence, our results indicate a positive role for Sam68 and PTB in the acquisition of drug resistance and suggest that these splicing factors may represent novel promising potential therapeutic targets for PDAC.

RESULTS

Characterization of drug-resistant (DR)-PDAC cells

To isolate a drug-resistant sup-populations, we chronically treated Pt45P1 cell line, which displays higher sensitivity to the drug, and the more resistant PANC-1 cell line, with gemcitabine. Chronic treatment with gemcitabine caused massive cell death in both cell lines. However, 15 days after removal of the drug, few viable clones were visible in the plates of both cell lines. Selected clones were pooled and amplified (Figure 1A). Every week, a 24 hour-pulse of gemcitabine was performed to maintain drug selection of the DR populations. To evaluate if DR-cells were indeed more resistant to drug treatment than the original parental cell lines (PCL), a dosage of gemcitabine was performed. After 72 hours of gemcitabine treatment, cell death was evaluated by trypan blue cell count and immunofluorescence analysis of the cleaved/activated form of caspase-3. Drug treatment caused a much more dramatic induction of cell death in PCL cells than in DR-PDAC cells (Figure 1B and 1C), confirming that the selected DR-cells were more resistant to the gemcitabine-induced cell death than the corresponding parental cell lines from which they have originated. Clonogenic assay was perform to further confirm the acquired drug resistance of the DR-PDAC populations. PCL and DR cells were cultured for 24 hours with sub-optimal doses of gemcitabine and then allowed to growth in complete medium in order to form visible colonies in the plates. Treatment with gemcitabine reduced the number of colonies in a dose dependent-manner in PCL cells. However, DR cells were resistant to the lowest dose of drug used and the reduction in colony number was less pronounced even at higher doses (Figure 2A, 2B and C). Moreover, we measured the diameter of the colonies as an additional indicator of cell survival after treatment. Gemcitabine treatment affected the size of the colony in a more incisive manner in PCL than in DR cells even at the lower dosage, again highlighting the enhanced resistance to gemcitabine of the DR cells (Figure 2D). Collectively, all these results indicate that the DR-PDAC cell populations have acquired a drug-resistant phenotype.

DR-PDAC cells express mesenchymal markers

Previous observations correlated the acquisition of chemoresistance to gemcitabine with with an epithelial-to-mesenchymal transition (EMT) of PDAC cells (Shah AN *et al*., 2007; Wang Z *et*

al., 2009; Arumugam T *et al*., 2009). Thus, we performed an immunofluorescence with phalloidin in order whether DR-PDAC cells acquired differences a mesenchymal-like actin cytoskeleton morphology. We found that DR cells acquired a spindle shape while PCL cells appeared more cobblestone-like, suggesting that DR cells could possess mesenchymal features (Figure 3A). Next, we analyzed the expression of epithelial and mesenchymal markers and we found that DR cells overexpress markers of the mesenchymal phenotype like the transcription factors ZEB1, TWIST and SLUG, whereas the epithelial markers ESRP1/2 were repressed (Figure 3B). SNAIL and ZEB2 trascriptional factors were downregulated or unchanged in both DR-PDAC populations. This result could be explained by the observation that up-regulation of SNAIL and ZEB2 occurs in a preliminary stage of the EMT, while ZEB1, TWIST and SLUG are required for the maintenance of the stable mesenchymal phenotype (Thiery JP *et al*., 2009).

DR-PDAC cells displays enhanced migratory ability

EMT is associated with an enhancement of cancer cell ability to migrate and metastasize distal organs (Kalluri R *et al*; 2003). Thus, we investigated if the DR-populations showed increased cell migration. We performed a wound-healing assay in which cells are plated at very high density to minimize the effect of proliferation and then a scar is performed in the plate. Evaluation of the percentage of the closure of the scar after 6h clearly indicated that DR-cells were faster than PCL in filling the wound, thereby indicating their enhanced migratory capability (Figure 3C).

Sam68 and PTB are up-regulated in DR-PDAC cells

Up-regulation of the splicing factor SRSF1 was previously observed after short-term gemcitabine treatment in PDAC cells (Adesso L *et al*., 2013). Thus, we asked whether DR-cells may differ from PCL cells in the expression of specific splicing factors. Western blot analyses were performed to investigate whether a cohort of cancer-related splicing factors were differentially expressed in the DR populations. We found that Sam68 and PTB were markedly up-regulated in both DR-Pt45P1 and DR-PANC-1 cells (Figure 4A and 4B). Up-regulation of SRSF1 was detected in DR-Pt45P1 cells but not in DR-PANC-1 cells, possibly because PANC-1 cells are already more resistant to gemcitabine and express higher basal levels of SRSF1.

Downregulation of Sam68 and PTB sensitize DR-PDAC cells to gemcitabine-induced cell death

To investigate whether Sam68 and PTB played a role in DR-cell survival, we depleted their expression by si-RNA and then analyzed DR-cell survival after treatment with gemcitabine. Sam68 and PTB were silenced either alone or in combination, in order to observe if the depletion of both protein could exert an additive effect on cell survival (Figure 5A). Downregulation of either Sam68 or PTB alone rescued drug-induced cell death in DR cells, as determined by trypan blue cell count (Figure 5B) and immunofluorescence analysis of the cleaved/activated form of caspase-3 (Figure 5C). However, no additive effect was observed when both protein are depleted together (Figure 5B and 5C), possibly suggesting that the two splicing factors function in the same pathway of gene expression regulation. These results indicate that Sam68 and PTB are required for the drug-resistant phenotype of DR-PDAC cells.

Pyruvate-kinase (PKM) alternative splicing is modulated in DR-PDAC cells

A key alternative splicing event modulated by PTB is the alternative splicing of the pyruvate-kinase mRNA. PTB overexpression enhances the formation of the PKM isoform 2 (PKM2), a splicing variant express in embryo and re-expressed in cancer cells, responsible for the switch of cell metabolism from oxidative phosphorylation to aerobic glycolisis (David CJ *et al*., 2010; Clower CV *et al*., 2010). Importantly, depletion of PKM2 variant impairs glioblastoma cells survival indicating that this isoform could exert a protective role in cancer cells (Wang Z *et al*., 2012). To determine whether PKM alternative splicing was differentially regulated in DR-cells, we analyzed the expression of PKM1 and PKM2 variant as previously reported (David CJ *et al*., 2010) (Figure 6A). RT-PCR analysis showed that DR-cells express mainly PKM2 isoform while parental express comparable levels of PKM1 and PKM2 isoforms (Figure 6B). Importantly, depletion of PTB expression restored the ratio between PKM1 and PKM2 isoforms in a similar manner of the parental cells (Figure 6C). Thus, PTB expression is required for the up-regulation of PKM2 in DR-cells.

DISCUSSION

Since pancreatic cancer still remains an aggressive and non curable pathology (Siegel R *et al*., 2012; Kem SE *et al*., 2011), the characterization of the key modulators of escape pathways remains a crucial step for the development of novel therapeutic approaches. In the study presented here we found that chronic treatment with gemcitabine induced the selection of a drug resistant population of cells in two different PDAC cell lines. Importantly, we found that the drug-resistant phenotype relied on the upregulation of two cancer-related splicing factors: PTB and Sam68. It has been previously demonstrated that the regulation of alternative splicing mediated by splicing factors, is a critical response that cancer cells trigger in order to overcome hostile stimuli, including stresses caused by chemotherapeutic treatments (Dutertre M *et al*., 2011; Busà R and Sette C, 2010). Regulation of post-trascriptional gene expression through alternative splicing was found to be an essential step for cancer cell homeostasis, as mutations in core components of the spliceosome are a frequent feature of cancer cells and treatment with synthetic derivatives that target spliceosomal components result in antitumoral effects (Bonnal S *et al*., 2012). Thus, we investigated whether there were alterations in the expression of a cohort of selected splicing factors in DR-PDAC cells, chosen because it was demonstrated that these RNA binding proteins are often overexpressed in cancer (Grosso AR *et al*., 2008). Importantly, we found that Sam68 and PTB were markedly up-regulated in DR-PDAC cells with respect to the parental cells from which they have originated. A positive role for Sam68 in cancer has already been extensively described. Sam68 is highly express in cancer and its depletion affects prostate and breast cancer cell proliferation (Busà R *et al*., 2007; Song L *et al*., 2010). Moreover, higher levels of Sam68 correlate with shorter survival rates of breast cancer patients (Song L *et al*., 2010) while haploinsufficiency of Sam68 can delay the onset of mammary tumors and can decrease metastasis in an animal model of breast cancer (Richard S *et al*., 2008). Thus, higher expression of Sam68 in cancer seems to be responsible for a more aggressive tumor behavior. Several studies also demonstrated that PTB is up-regulated in cancer, particularly in ovarian cancer where PTB depletion affects cancer cell proliferation and invasiveness (He X *et al*., 2007). Thus, to investigate if Sam68 and PTB exert a protective role in DR-PDAC cells, we depleted their expression and we evaluated DR-PDAC cell survival after gemcitabine treatment. We found that knockdown of Sam68 or PTB rescues sensitivity to drug treatment of the DR sub-populations, indicating that their overexpression is required for the acquired resistance to gemcitabine. We were not able to observe an additive effect when both proteins are depleted simultaneously in DR-PDAC cells. One explanation of this phenomenon could be that Sam68

and PTB are both required on the same molecular pathway thus, the depletion of one of them is sufficient to impair this function.

Genotoxic stress modulates the intra-nuclear localization and the function of Sam68 in prostate cancer cells and its depletion affects cancer cell survival to drug treatment (Busà R *et al*., 2007, 2010), clearly indicating that Sam68 expression promotes the survival to DNA damage. Similar studies have not been performed for PTB. However, up-regulation of PTB was also been observed in brain tumors and other carcinomas (David CJ *et al*., 2010; Clower CV *et al*., 2010). In these systems, PTB, together with hnRNP A1 and A2, controls cancer cell metabolism through the regulation of the alternative splicing of the pyruvate-kinase mRNA (PKM gene). PTB promotes the PKM2 variant which is physiologically expressed in embryo and it has been found re-expressed in cancer. PKM2 variant switch the glucose metabolism from oxidative phosphorylation to aerobic glycolysis, a change that promotes cancer cell proliferation (Chen M *et al*., 2010). Hence, PTB overexpression seems to favour tumor cell establishment. Recent evidence has also demonstrated that the depletion of PTB-induced PKM2 variant in glioblastoma cell line caused apoptosis (Wang Z *et al*., 2012), indicating the involvement of PTB in the protection of cell death thought the modulation of PKM splicing. Importantly, we found that in DR-PDAC cells the ratio between PKM1 and the PKM2 variant favours the PKM2 variant with respect to PCL which express similar levels of PKM1 and PKM2. Strikingly, depletion of PTB in DR-PDAC cells re-established the ratio in PKM variants observed in PCL cells, suggesting that modulation of this splicing event is part of the mechanism by which PTB promotes drug resistance in PDAC cells.

A key step involved in gemcitabine resistance in PDAC is the epithelial to mesenchymal transition (EMT), a process strongly regulated by alternative splicing (Warzecha CC and Carstens RP, 2012; Biamonti G *et al*., 2012). The expression of mesenchymal markers was found to be correlated and to be responsible for high resistance to gemcitabine in PDAC (Arumugam T *et al*., 2009). Analysis of cell morphology and EMT markers demonstrated that DR-PDAC cells shows a mesenchymal phenotype that results in enhanced cell migration. Importantly, both Sam68 and PTB were previously proposed to be involved in the promotion of the mesenchymal status. Sam68 regulates the expression of SRSF1 through modulation of an alternative splicing event in the SRSF1 3'UTR; higher levels of SRSF1 in turn favour splicing of the ΔRon variant that promotes EMT and enhances cell migration (Valacca C *et al*., 2010). PTB promotes the formation of the mesenchymal-related alternative splicing isoform of the FGFR2 receptor (Carstens RP *et al*., 2000), a splicing variant found to be expressed in poorly differentiated tumors (Grosso AR *et al*., 2008). Thus, it could be possible that the overexpression

of Sam68 and PTB in DR-PDAC cells is also required to maintain the mesenchymal phenotype that characterizes this populations.

In conclusion, our studies identify that chronic treatment with gemcitabine selects drug resistant PDAC cells that are capable to survive more efficiently to drug treatment. This phenotype relies on the up-regulation of Sam68 and PTB and their mediated protective role in response to drug treatment. Thus, our results suggest that Sam68 and PTB could represent novel molecular targets for therapeutic approaches aimed at enhancing the response of PDAC cells to chemotherapeutic drugs.

MATERIALS AND METHODS

Cell Culture and treatments

Pt45P1 and PANC-1 parental cells and DR cells were cultured in RPMI 1640 medium (Lonza), supplemented with 10% fetal bovine serum (Lonza), penicillin and streptomycin and grown in a 37°C humidified atmosphere of 5% CO2. Gemcitabine (Eli Lilly & Company, Indianapolis, IN, USA) was dissolved in water and stored at -20 °C.

Cell transfections

For RNA interference, cells at ~50-60% confluence were transfected with siRNAs (Sigma-Aldrich) using Lipofectamine RNAiMAX (Invitrogen) and OptiMEM medium (Invitrogen), according to the manufacturer's instructions. Sequences and conditions for SAM68 siRNA were previously described (Busà R *et al*., 2007). PTB silencing was obtained using the Smart pool reagent mix from Dharmacon, cells at ~50/60% confluency were transfected for 2 consecutive days with 30 nM of siRNAs.

RT-PCR analysis

Total RNA was extracted from cells using Trizol reagent (Invitrogen) according to the manufacturer's instructions. After digestion with RNase free DNase (Ambion), RNA was resuspended in RNase free water (Sigma Aldrich); 1µg of total RNA was used for RT-PCR using M-MLV reverse transcriptase (Promega). Five percent of the RT reaction was used as template for PCR analysis (GoTaq, Promega). Primers used to amplify SLUG, SNAIL and ZEB2 were described elsewhere (Valacca C *et al*., 2010; Evdokimova V *et al*., 2009; Beltran M *et al*., 2008). Primers and conditions used for the analysis of the pyruvate-kinase isoforms were described elsewhere (David CJ *et al*., 2010). The sequences of all additional primers used are listed in Table1.

Protein extraction and Western blot analysis

For protein extraction, cells were resuspended in lysis buffer (150 mM sodium chloride, 1.0% NP-40, 0.5% sodium deoxycholate, 0.1% sodium dodecyl sulphate, 50 mM Tris pH 8.0). After 10 min of incubation in ice, the extracts were centrifuged for 10 min at 12,000 rpm at 4°C and the supernatants were collected for further analysis. Western blot analysis was performed as previously described (Paronetto MP *et al.*, 2007). Following primary antibodies (overnight at 4°C) were used: rabbit anti-Sam68 (1:1000, Santa Cruz Biotechnology), goat anti-PTB (1:500,

Santa Cruz Biotechnology), mouse anti-SRSF1 (1:1000, Santa Cruz Biotechnology), mouse anti-hnRNPA1 (1:1000, Sigma-Aldrich) mouse anti-hnRNPA2/B1 (1:1000, Sigma-Aldrich), mouse anti-hnRNRP F/H (1:1000, Abcam) Secondary anti-mouse, anti-rabbit or anti-goat IgGs conjugated to horseradish peroxidase (Amersham) were incubated for 1 h at RT (1:10000). Immunostained bands were detected by chemiluminescence method (Santa Cruz Biotechnology).

Coomassie staining

After separation on 10% SDS-PAGE, protein bands were visualized by placing gels in a solution of 40% distilled water, 10% acetic acid, and 50% methanol with the addition of 0.25% by weight Coomassie Brilliant Blue R-250 (Sigma-Aldrich). Gels were incubated 2 hours at room temperature and then transferred in a mixture of 40% distilled water, 10% acetic acid, and 50% methanol, placed on shaker for washing. The washing mixture was replaced with fresh rinse mixture until the excess dye has been removed.

Colony formation assay

Single-cell suspensions were plated in 35mm plates (500 cells/plate for Pt45P1 PCL and DR; 750 cells/plate for PANC-1 PCL and DR). After 1 day, cells were treated for 24 h with gemcitabine. At the end of the incubation, the medium was replaced every 48 h. After 10 days for Pt45P1 and 12 days for PANC-1, cells were fixed in methanol for 10 min, stained overnight with 5% Giemsa, washed twice in PBS and dried. Pictures were taken using a digital camera to count and measure the colonies.

Trypan blue cell count

PCL and DR cells were seeded at ~70% confluence in 24-well plate and treated as described in the text for 72 h, washed in PBS and trypsinized. Cellular suspension was incubated with of 0.4% Trypan Blue Stain (Sigma-Aldrich) and cells were counted using the Thoma's chamber.

Immunofluorescence analysis

For phalloidin analysis, PCL and DR cells were fixed in 4% paraformaldehyde and washed three times with PBS. Cells were permeabilized with 0.1% Triton X-100 for 10 min and incubated for 1 h in 3% BSA. Cells were washed three times with PBS and incubated for 2 h at room temperature with antibodies (anti-phalloidin 1:400, Sigma-Aldrich). For apoptotic markers, immunofluorescence was performed as described above and cell were stained with anti-cleaved caspase-3 antibody (1:400; Sigma-Aldrich), followed by 1 h of incubation with secondary

antibodies,cy3-conjugated donkey anti-rabbit (1:500; Jackson Immunoresearch, Bar Harbor, ME, USA). Hoechst dye (0.1mg/ml; Sigma–Aldrich) was added for the last 45 min. Slides were mounted in Mowiol 4–88 (Calbiochem, Darmstadt, Germany). Results represent the mean ± S.D of three experiments. At least 1000 cells for PCL or DR in each experiment were counted.

Scratch wound-healing motility assay

PCL and DR cells were plated at 60% of confluence and incubated at 37 °C until the plate was confluent. A wound by scratching with a sterile pipette tip was created. The plate was photographed immediately and 6h after scratching.

Table1- Sequences of primers used for PCR analysis.

TWIST1 Fw	5’-CATGTCCGCGTCCCACTAG-3’
TWIST1 Rev	5’-TGTCCATTTTCTCCTTCTCTGG-3’
ESRP1 Ex1 Fw	5’-GGCTCGGATGAGAAGGAGTTGAT-3’
ESRP1 Ex3 Rev	5’-GAAGGAAGTCCCTACTCCAAT-3’
ESRP2 Ex2 Fw	5’-ACGCTGCACAAATCGCTGGTT-3’
ESRP2 Ex3 Rev	5’-GTGCAGGACCTGTCGCAAT-3’
ZEB1D Fw	5’-CATTGCTGACCAGAACAGTGTTCC-3’
ZEB1E Rev	5’-TGGGCGGTGTAGAATCAGAGTCAT-3’
HPRT Fw	5’-TGACCAGTCAACAGGGGACA-3’
HPRT Rev	5’-TTCGTGGGGTCCTTTTCACC-3’

References

Adesso L, Calabretta S, Barbagallo F, Capurso G, Pilozzi E, Geremia R, Delle Fave G, Sette C. Gemcitabine triggers a pro-survival response in pancreatic cancer cells through activation of the MNK2/eIF4E pathway. *Oncogene.* 2013 Jun 6;32(23):2848-57.

Arafat H, Lazar M, Salem K, Chipitsyna G, Gong Q, Pan TC, Zhang RZ, Yeo CJ, Chu ML. Tumor-specific expression and alternative splicing of the COL6A3 gene in pancreatic cancer. *Surgery*. 2011 Aug;150(2):306-15.

Arumugam T, Ramachandran V, Fournier KF, Wang H, Marquis L, Abbruzzese JL, Gallick GE, Logsdon CD, McConkey DJ, Choi W. Epithelial to mesenchymal transition contributes to drug resistance in pancreatic cancer. *Cancer Res.* 2009 Jul 15;69(14):5820-8.

Beltran M, Puig I, Peña C, García JM, Alvarez AB, Peña R, Bonilla F, de Herreros AG. A natural antisense transcript regulates Zeb2/Sip1 gene expression during Snail1-induced epithelial-mesenchymal transition. *Genes Dev*. 2008 Mar 15;22(6):756-69.

Biamonti G, Bonomi S, Gallo S, Ghigna C. Making alternative splicing decisions during epithelial-to-mesenchymal transition (EMT). *Cell Mol Life Sci*. 2012 Aug;69(15):2515-26.

Bielli P, Busà R, Paronetto MP, Sette C. The RNA-binding protein Sam68 is a multifunctional player in human cancer. *Endocr Relat Cancer*. 2011 Jul 1;18(4):R91-R102.

Bonnal S, Vigevani L, Valcárcel J. The spliceosome as a target of novel antitumour drugs. Nat Rev Drug Discov. 2012 Nov;11(11):847-59

Busà R, Geremia R, Sette C. Genotoxic stress causes the accumulation of the splicing regulator Sam68 in nuclear foci of transcriptionally active chromatin. *Nucleic Acids Res.* 2010 May;38(9):3005-18.

Busà R, Paronetto MP, Farini D, Pierantozzi E, Botti F, Angelini DF, Attisani F, Vespasiani G, Sette C. The RNA-binding protein Sam68 contributes to proliferation and survival of human prostate cancer cells. *Oncogene.* 2007 Jun 28;26(30):4372-82

Busà R, Sette C. An emerging role for nuclear RNA-mediated responses to genotoxic stress. *RNA Biol*. 2010 Jul-Aug;7(4):390-6.

Carrière C, Mirocha S, Deharvengt S, Gunn JR, Korc M. Aberrant expressions of AP-2α splice variants in pancreatic cancer. Pancreas. 2011 Jul;40(5):695-700.

Carstens RP, Wagner EJ, Garcia-Blanco MA An intronic splicing silencer causes skipping of the IIIb exon of fibroblast growth factor receptor 2 through involvement of polypyrimidine tract binding protein. Mol Cell Biol. 2000 Oct;20(19):7388-400.

Chen M, Zhang J, Manley JL. Turning on a fuel switch of cancer: hnRNP proteins regulate alternative splicing of pyruvate kinase mRNA. Cancer Res. 2010 Nov 15;70(22):8977-80

Choudhury A, Moniaux N, Winpenny JP, Hollingsworth MA, Aubert JP, Batra SK. Human MUC4 mucin cDNA and its variants in pancreatic carcinoma. *J Biochem*. 2000 Aug;128(2):233-43.

Clower CV, Chatterjee D, Wang Z, Cantley LC, Vander Heiden MG, Krainer AR. The alternative splicing repressors hnRNP A1/A2 and PTB influence pyruvate kinase isoform expression and cell metabolism. *Proc Natl Acad Sci U S A*. 2010 Feb 2;107(5):1894-9

David CJ, Chen M, Assanah M, Canoll P, Manley JL. HnRNP proteins controlled by c-Myc deregulate pyruvate kinase mRNA splicing in cancer. *Nature*. 2010 Jan 21;463(7279):364-8.

David CJ, Manley JL.Alternative pre-mRNA splicing regulation in cancer: pathways and programs unhinged. *Genes Dev*. 2010 Nov 1;24(21):2343-64.

Dutertre M, Sanchez G, Barbier J, Corcos L, Auboeuf D. The emerging role of pre-messenger RNA splicing in stress responses: sending alternative messages and silent messengers. *RNA Biol*. 2011 Sep-Oct;8(5):740-7.

Evdokimova V, Tognon C, Ng T, Ruzanov P, Melnyk N, Fink D, Sorokin A, Ovchinnikov LP, Davicioni E, Triche TJ, Sorensen PH. Translational activation of snail1 and other developmentally regulated transcription factors by YB-1 promotes an epithelial-mesenchymal transition. *Cancer Cell.* 2009 May 5;15(5):402-15

Grosso AR, Martins S, Carmo-Fonseca M. The emerging role of splicing factors in cancer. EMBO Rep. 2008 Nov;9(11):1087-93.

Hartel M, Narla G, Wente MN, Giese NA, Martignoni ME, Martignetti JA, Friess H, Friedman SL. Increased alternative splicing of the KLF6 tumour suppressor gene correlates with prognosis and tumour grade in patients with pancreatic cancer. *Eur J Cancer*. 2008 Sep;44(13):1895-903.

Hayes GM, Carrigan PE, Beck AM, Miller LJ. Targeting the RNA splicing machinery as a novel treatment strategy for pancreatic carcinoma. *Cancer Res.* 2006 Apr 1;66(7):3819-27.

He X, Pool M, Darcy KM, Lim SB, Auersperg N, Coon JS, Beck WT. Knockdown of polypyrimidine tract-binding protein suppresses ovarian tumor cell growth and invasiveness in vitro. *Oncogene.* 2007 Jul 26;26(34):4961-8.

Hidalgo M. Pancreatic cancer. *N Engl J Med*. 2010 Apr 29;362(17):1605-17.

Kalluri R, Neilson EG. Epithelial-mesenchymal transition and its implications for fibrosis. *J Clin Invest*. 2003 Dec;112(12):1776-84.

Karni R, de Stanchina E, Lowe SW, Sinha R, Mu D, Krainer AR. The gene encoding the splicing factor SF2/ASF is a proto-oncogene. *Nat Struct Mol Biol*. 2007 Mar;14(3):185-93.

Kern SE, Shi C, Hruban RH. The complexity of pancreatic ductal cancers and multidimensional strategies for therapeutic targeting. *J Pathol* 2011; 223: 295–306

Kim E, Goren A, Ast G. Insights into the connection between cancer and alternative splicing. *Trends Genet*. 2008 Jan;24(1):7-10.

Paronetto MP, Achsel T, Massiello A, Chalfant CE, Sette C. The RNA-binding protein Sam68 modulates the alternative splicing of Bcl-x. *J Cell Biol*. 2007 Mar 26;176(7):929-39.

Rhim AD, Mirek ET, Aiello NM, Maitra A, Bailey JM, McAllister F, Reichert M, Beatty GL, Rustgi AK, Vonderheide RH, Leach SD, Stanger BZ. EMT and dissemination precede pancreatic tumor formation. *Cell*. 2012 Jan 20;148(1-2):349-61.

Richard S, Vogel G, Huot ME, Guo T, Muller WJ, Lukong KE Sam68 haploinsufficiency delays onset of mammary tumorigenesis and metastasis. Oncogene .*2008* 27(4):548-56.

Shah AN, Summy JM, Zhang J, Park SI, Parikh NU, Gallick GE. Development and characterization of gemcitabine-resistant pancreatic tumor cells. *Ann Surg Oncol*. 2007 Dec;14(12):3629-37

Siegel R, Naishadham D, Jemal A. Cancer statistics, 2012. *CA Cancer J Clin*. 2012 Jan-Feb;62(1):10-29.

Song L, Wang L, Li Y, Xiong H, Wu J, Li J, Li M. Sam68 up-regulation correlates with, and its down-regulation inhibits, proliferation and tumourigenicity of breast cancer cells. *J Pathol*. 2010 222(3):227-37.

Thiery JP, Acloque H, Huang RY, Nieto MA. Epithelial-mesenchymal transitions in development and disease. Cell. 2009 Nov 25;139(5):871-90.

Valacca C, Bonomi S, Buratti E, Pedrotti S, Baralle FE, Sette C, Ghigna C, Biamonti G. Sam68 regulates EMT through alternative splicing-activated nonsense-mediated mRNA decay of the SF2/ASF proto-oncogene. *J Cell Biol.* 2010 Oct 4;191(1):87-99.

Wang Z, Jeon HY, Rigo F, Bennett CF, Krainer AR. Manipulation of PK-M mutually exclusive alternative splicing by antisense oligonucleotides. *Open Biol*. 2012 Oct;2(10):120133.

Wang Z, Li Y, Kong D, Banerjee S, Ahmad A, Azmi AS, Ali S, Abbruzzese JL, Gallick GE, Sarkar FH.Acquisition of epithelial-mesenchymal transition phenotype of gemcitabine-resistant pancreatic cancer cells is linked with activation of the notch signaling pathway. *Cancer Res*. 2009 Mar 15;69(6):2400-7.

Warzecha CC, Carstens RP. Complex changes in alternative pre-mRNA splicing play a central role in the epithelial-to-mesenchymal transition (EMT). *Semin Cancer Biol*. 2012 Oct;22(5-6):417-27.

Wei D, Wang L, Kanai M, Jia Z, Le X, Li Q, Wang H, Xie K. KLF4α up-regulation promotes cell cycle progression and reduces survival time of patients Gastroenterology. 2010 Dec;139(6):2135-45

Zhou R, Shanas R, Nelson MA, Bhattacharyya A, Shi J. Increased expression of the heterogeneous nuclear ribonucleoprotein K in pancreatic cancer and its association with the mutant p53. *Int J Cancer*. 2010 Jan 15;126(2):395-404.

Figure legends

Figure 1: Chronic gemcitabine treatment selects DR-PDAC cells

(A) Schematic illustration of the experimental plan adopted to select drug resistant DR-PDAC cells. (B) Trypan blue cell count was performed to analyze cell survival after gemcitabine treatment. Bar graph represents the mean + SD of 3 experiments, each performed in triplicate, in which PCL and DR were compared. *P < 0.05 in paired t-test, **P < 0.01 in paired t-test . (C) Analysis of apoptosis in PCL and DR treated as indicated through the staining with anti-cleaved caspase 3. Bar graph represents the mean +SD of 3 experiments, each performed in duplicate. *P < 0.05 in paired t-test, **P < 0.01 in paired t-test.

Figure 2: Clonogenic assay confirm the higher resistance of DR-PDAC cells

(A) Representative images of colonies of Pt45P1 PCL (upper panels) and DR (lower panels). (B) Representative images of colonies of PANC-1 PCL (upper panels) and DR (lower panels). (C) Histograms shows % of cell survival calculated as the ratio of % of colony numbers in treated plates *vs* control. Data represents three experiments (mean + S.D.). *P < 0.05 in paired t-test, **P < 0.01 in paired t-test. (D) Analysis of colony size, bar graph represents the mean + S.D. of 3 experiments. *P < 0.05 in paired t-test, **P < 0.01 in paired t-test.

Figure 3: DR-population express mesenchymal markers and increased cell migration

(A) Representative images (40x magnification) of PCL and DR cells stained for phalloidin. White bars = 50 μm. (B) RT-PCR analysis of mesenchymal and epithelial markers in PCL and DR cells. HPRT was used as loading control. (C) Wound healing assay of PCL and DR cells. The % of wound closure was calculated as a % of reduction of the scar length compared with the initial scar length. Data represents three experiments (mean + S.D.). **P < 0.01 in paired t-test.

Figure 4: Sam68 and PTB are upregulated in DR-PDAC cells

Western blot analysis of cancer-related splicing factors in Pt45P1 (A) and PANC-1 (B) parental PCL and DR. Gels were also stained with Coomassie (right panels) as loading control.

Figure 5: Downregulation of Sam68 and PTB sensitizes DR-PDAC cells to gemcitabine-induced cell death

(A) Western blot analysis of Sam68 and PTB expression after two cycles of transfection with indicated si-RNA in Pt45P1 and PANC-1. Coomassie staining was used as loading control. (B) Trypan blue cell count was performed in PCL, DR-DPAC cells scr and DR-PDAC cells depleted for Sam68 and/or PTB to analyze cell survival after gemcitabine treatment. Bar graph represents the mean + S.D. of 3 experiments, each performed in triplicate. **P < 0.01 in paired t-test. (C) Analysis of apoptosis through the staining with anti-cleaved caspase 3 in PCL and DR-DPAC cells scr and DR-DPAC cells depleted for Sam68 and/or PTB treated as indicated. Bar graph represents the mean + S.D. of 3 experiments, each performed in duplicate. Statistical analysis was performed comparing values of PCL cells and DR-PDAC scr cells and comparing DR-PDAC cells silenced for Sam68 and/or PTB with DR cells transfected with the scramble siRNA. **P < 0.01 in paired t-test.

Figure 6: Modulation of PKM alternative splicing isoforms in DR-PDAC cells

(A) Schematic representation of the PKM alternative splice-variants. Black arrows indicates primers used for PCR analysis, which was followed by PstI digestion, in order to distinguish between PKM1 and PKM2 products. (B) RT–PCR analysis of PKM isoforms. Panels show expression of the PKM1 and PKM2 isoforms in PCL and DR-PDAC cells. (C) RT–PCR analysis of PKM isoforms after PTB depletion. Panels show expression of the PKM1 and PKM2 isoforms in PCL and DR-PDAC cells depleted or not for PTB expression.

A


Pt45P1 and PANC-1 cells
+ gemcitabine (7 days)
Release in growth medium
(15 days)
isolation and propagation
of the drug resistant cells

B

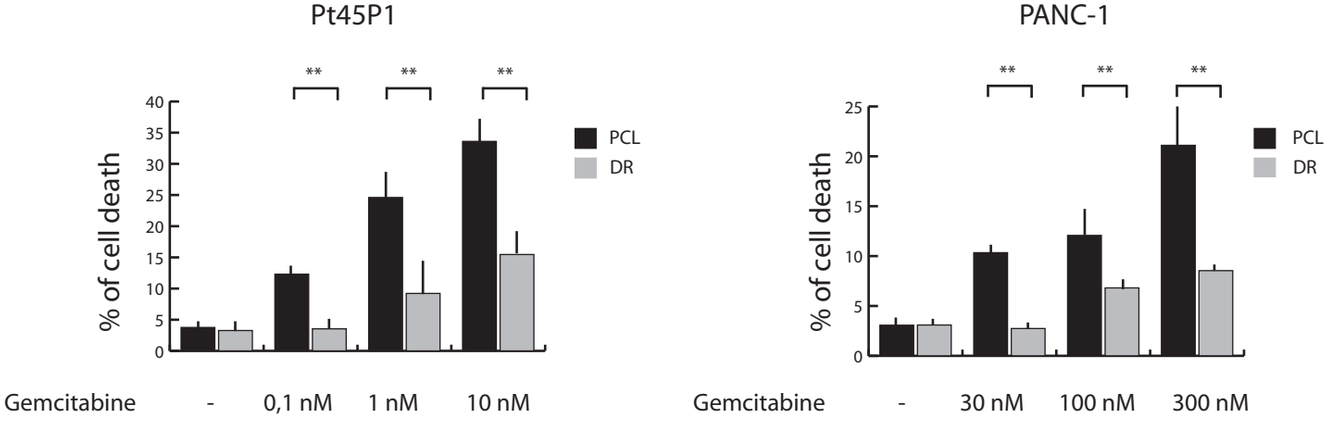
Pt45P1
PANC-1
% of cell death
PCL
DR
**
Gemcitabine
-
0,1 nM
1 nM
10 nM
30 nM
100 nM
300 nM

C

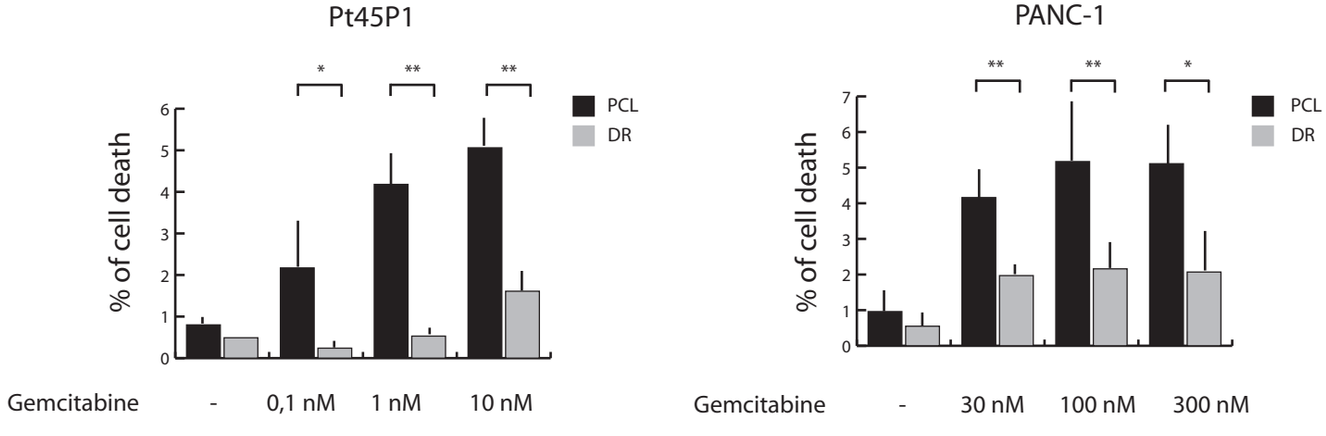
Pt45P1
PANC-1
% of cell death
PCL
DR
*
**
Gemcitabine
-
0,1 nM
1 nM
10 nM
30 nM
100 nM
300 nM

Figure 1

A

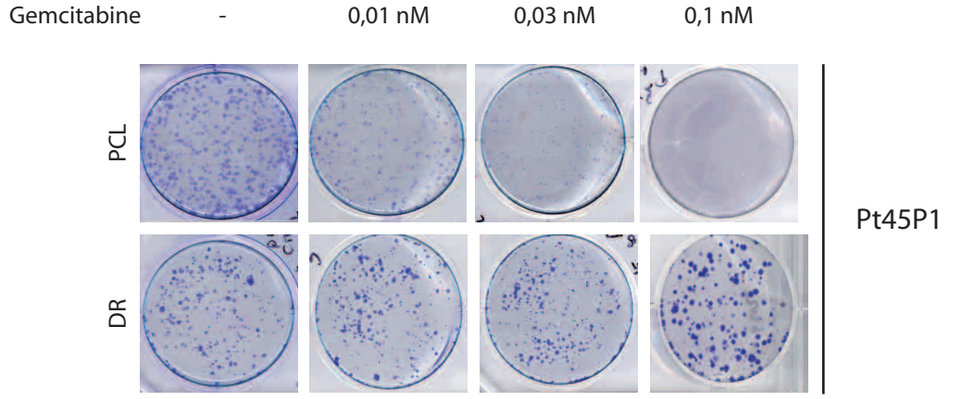

B

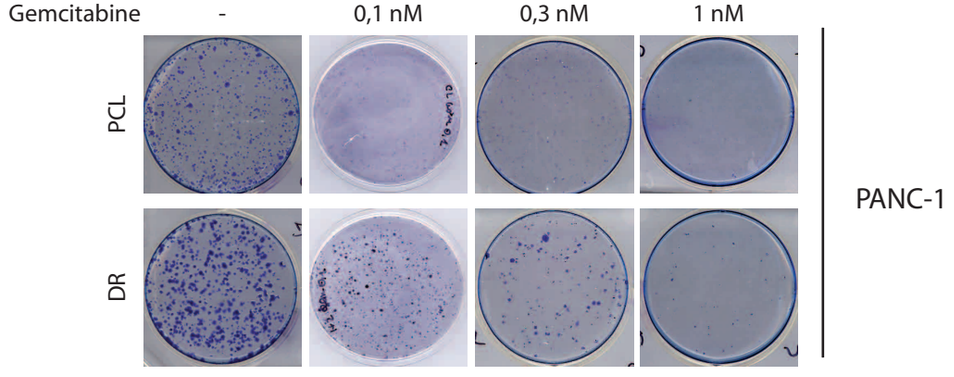

C

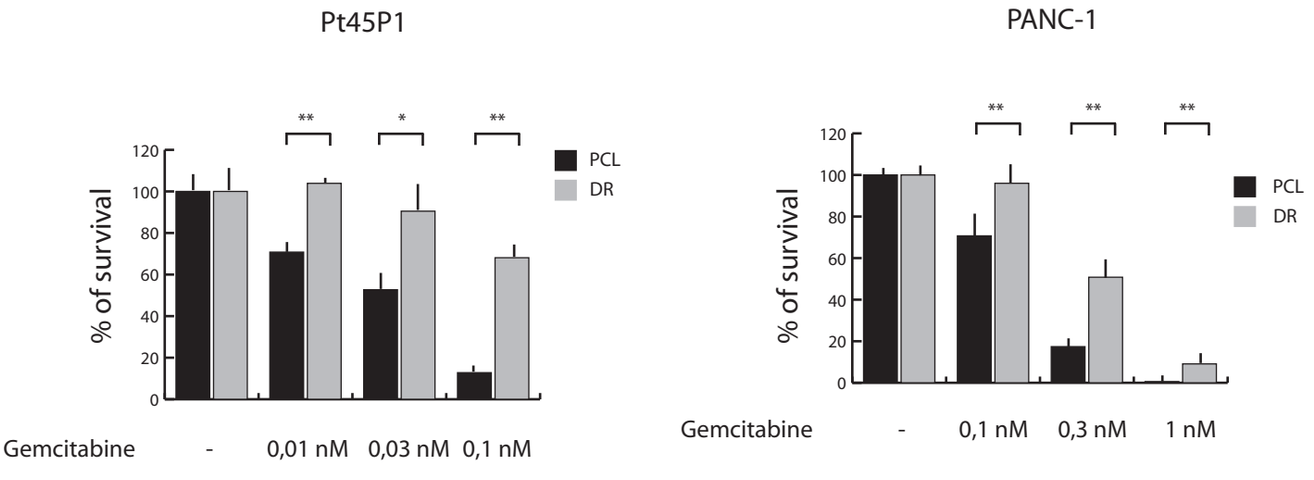

D

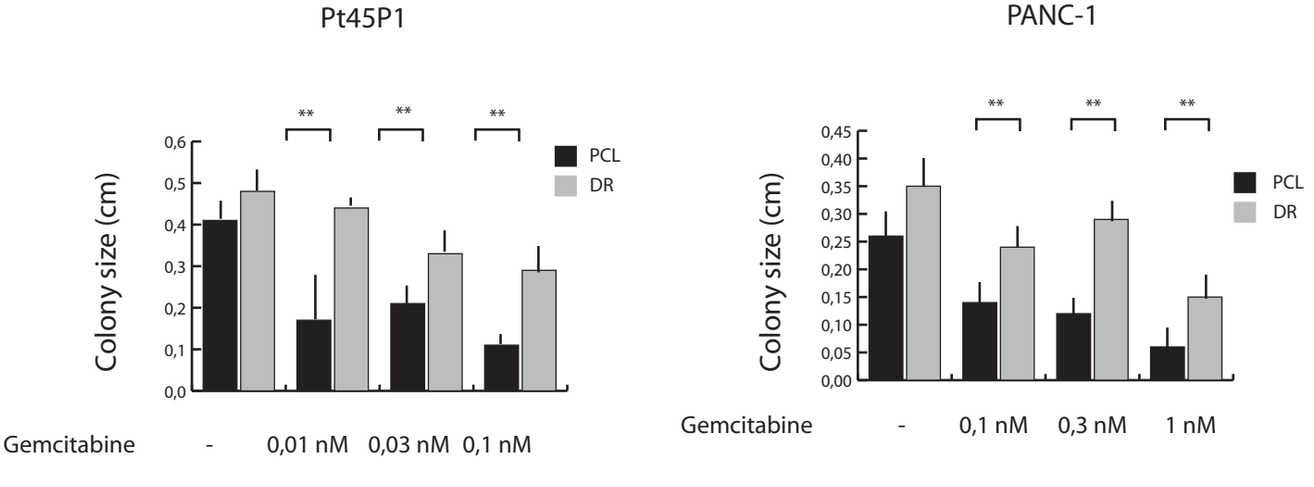

Figure 2

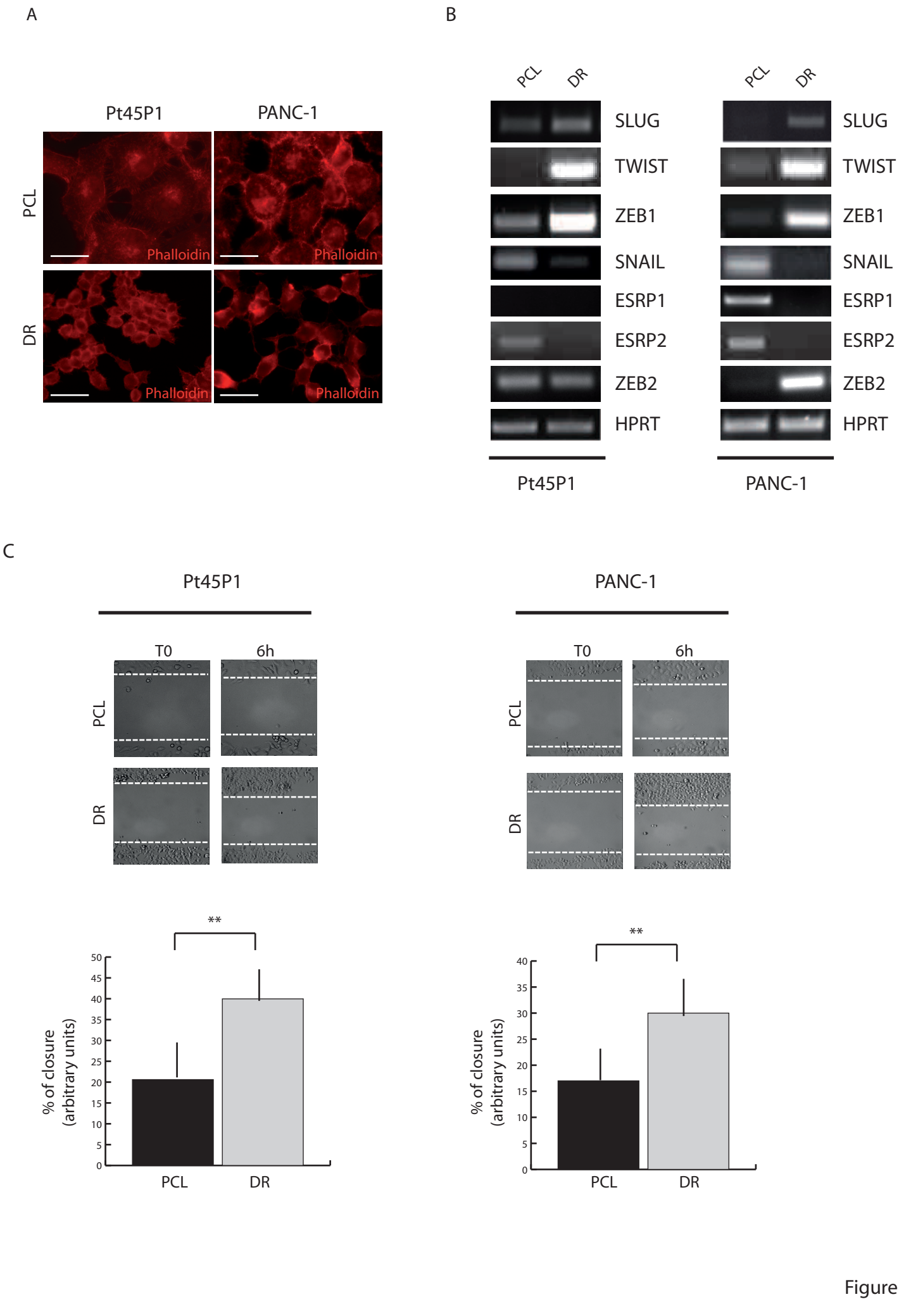
A
Pt45P1
PANC-1
PCL
DR
Phalloidin
B
PCL
DR
SLUG
TWIST
ZEB1
SNAIL
ESRP1
ESRP2
ZEB2
HPRT
Pt45P1
PANC-1
C
Pt45P1
PANC-1
T0
6h
PCL
DR
**
% of closure
(arbitrary units)
0
5
10
15
20
25
30
35
40
45
50
PCL
DR

Figure 3

A

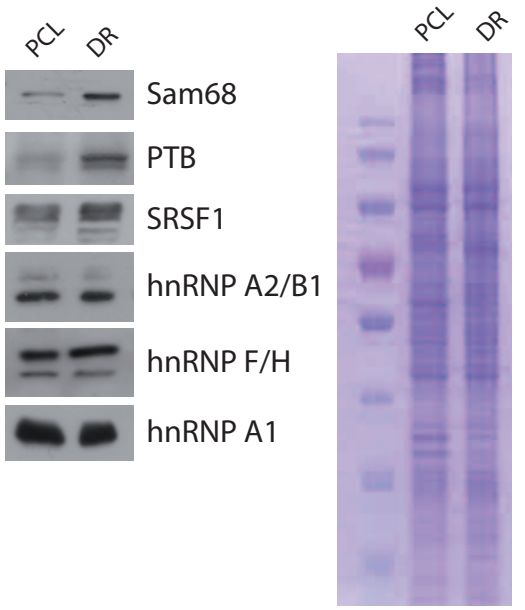

PT45P1

B

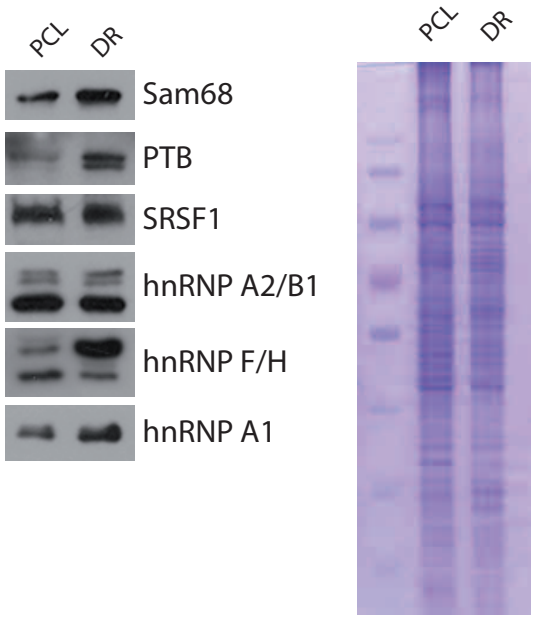

PANC-1

Figure 4

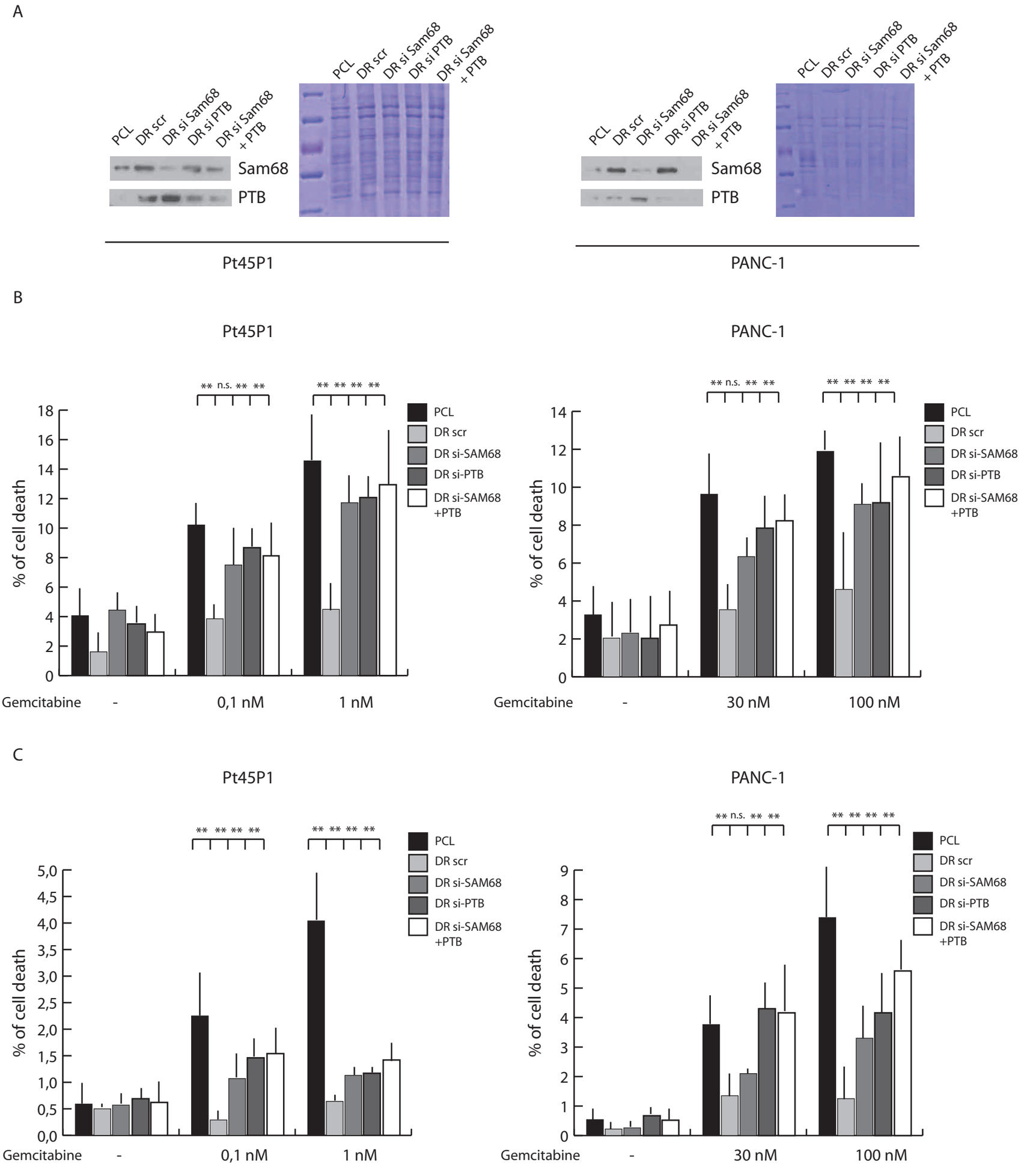
A
PCL
DR scr
DR si Sam68
DR si PTB
DR si Sam68 + PTB
Sam68
PTB
Pt45P1
PANC-1
B
Pt45P1
PANC-1
** n.s. ** **
** ** ** **
PCL
DR scr
DR si-SAM68
DR si-PTB
DR si-SAM68 +PTB
% of cell death
Gemcitabine
-
0,1 nM
1 nM
30 nM
100 nM
C
Pt45P1
PANC-1

Figure 5

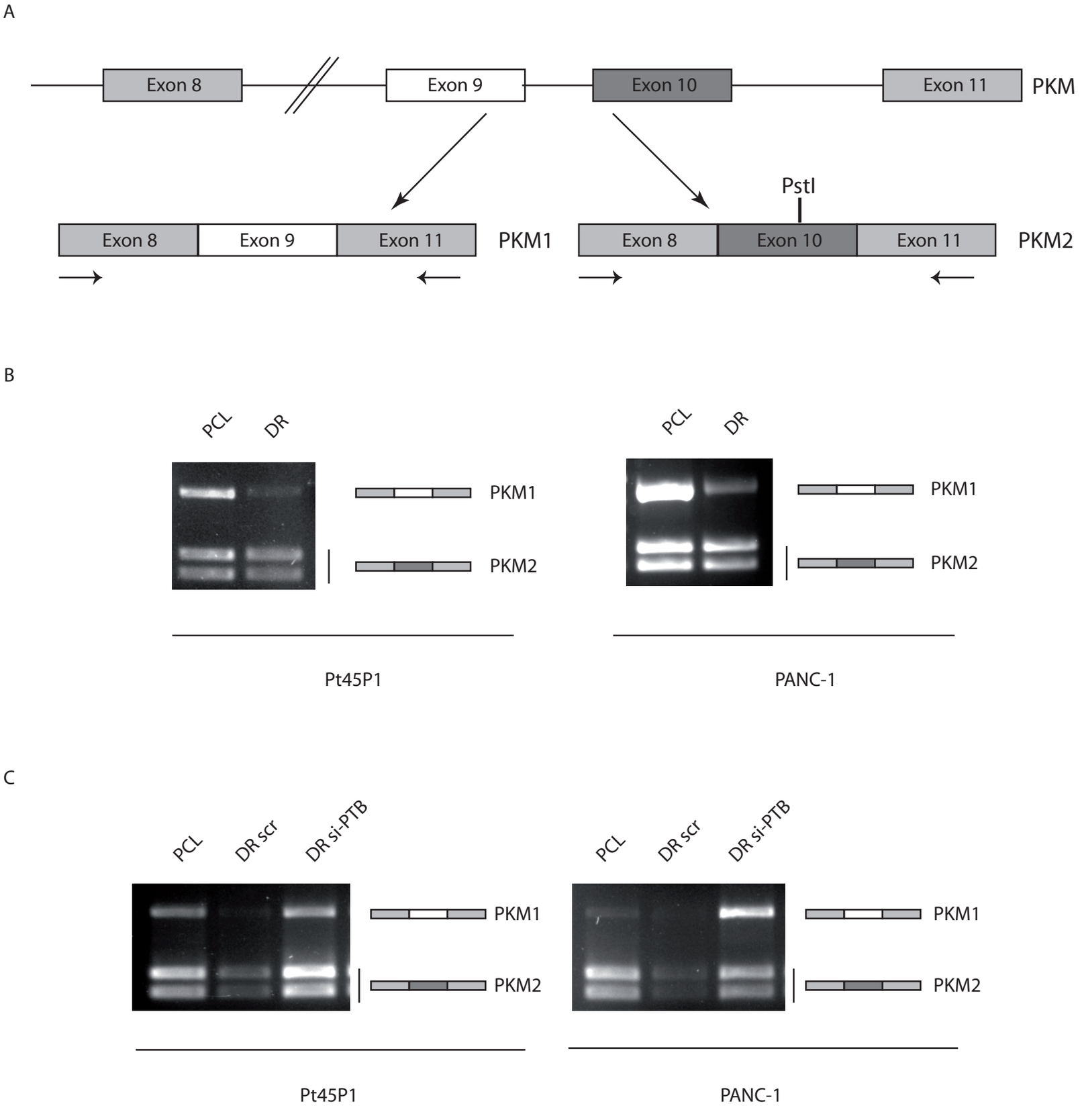
A
Exon 8
Exon 9
Exon 10
Exon 11
PKM
PstI
Exon 8
Exon 9
Exon 11
PKM1
Exon 8
Exon 10
Exon 11
PKM2
B
PCL
DR
PKM1
PKM2
Pt45P1
PCL
DR
PKM1
PKM2
PANC-1
C
PCL
DR scr
DR si-PTB
PKM1
PKM2
Pt45P1
PCL
DR scr
DR si-PTB
PKM1
PKM2
PANC-1

Figure 6

APPENDIX

The RNA binding protein SAM68 transiently localizes in the chromatoid body of male germ cells and influences expression of select microRNAs

SAM68 is important for proper mouse spermatogenesis and male fertility, a regulation exerted by its role in the nodulation of alternative splicing and transaltion of specific mRNAs. We identify an additional level of SAM68-mediated regulation in male germ cells. In the present study we observe a transient localization of SAM68 in the chromatoid body (CB) during the meiotic divisions of mouse spermatocytes. The chromatoid body (CB) is a specific male germ cells structure in which a cohort of proteins that regulates RNA metabolism were identified. Importantly, several regulators of microRNA biogenesis were also identified in the CB. The presence of SAM68 in the CB is not required for its assembling, neither for the localization of MVH in the CB, one of its major components. However, SAM68 ablation impairs the maturation of a cohort of microRNA. We also demonstrate that SAM68 interacts with DROSHA and DICER in secondary spermatocytes and early round spermatids. These results suggest a novel role for SAM68 in the regulation of miRNA pathway during spermatogenesis.

OPEN ACCESS Freely available online

PLoS one

The RNA Binding Protein SAM68 Transiently Localizes in the Chromatoid Body of Male Germ Cells and Influences Expression of Select MicroRNAs

Valeria Messina[1,2], Oliver Meikar[3], Maria Paola Paronetto[2,4], Sara Calabretta[1,5], Raffaele Geremia[1], Noora Kotaja[3], Claudio Sette[1,2]*

1 Section of Anatomy, Department of Public Health and Cell Biology, University of Rome "Tor Vergata", Rome, Italy, **2** Laboratory of Neuroembryology, Fondazione Santa Lucia IRCCS, Rome, Italy, **3** Department of Physiology, Institute of Biomedicine, University of Turku, Turku, Finland, **4** Department of Health Sciences, University of Rome "Foro Italico", Rome, Italy, **5** Digestive and Liver Disease Unit, II Medical School, University of Rome "La Sapienza", S. Andrea Hospital, Rome, Italy

Abstract

The chromatoid body (CB) is a unique structure of male germ cells composed of thin filaments that condense into a perinuclear organelle after meiosis. Due to the presence of proteins involved in different steps of RNA metabolism and of different classes of RNAs, including microRNAs (miRNAs), the CB has been recently suggested to function as an RNA processing centre. Herein, we show that the RNA binding protein SAM68 transiently localizes in the CB, in concomitance with the meiotic divisions of mouse spermatocytes. Precise staging of the seminiferous tubules and co-localization studies with MVH and MILI, two well recognized CB markers, documented that SAM68 transiently associates with the CB in secondary spermatocytes and early round spermatids. Furthermore, although SAM68 co-immunoprecipitated with MVH in secondary spermatocytes, its ablation did not affect the proper localization of MVH in the CB. On the other hand, ablation of the CB constitutive component MIWI did not impair association of SAM68 with the CB. Isolation of CBs from *Sam68* wild type and knockout mouse testes and comparison of their protein content by mass spectrometry indicated that *Sam68* ablation did not cause overall alterations in the CB proteome. Lastly, we found that SAM68 interacts with DROSHA and DICER in secondary spermatocytes and early round spermatids and that a subset of miRNAs were altered in *Sam68*$^{-/-}$ germ cells. These results suggest a novel role for SAM68 in the miRNA pathway during spermatogenesis.

Citation: Messina V, Meikar O, Paronetto MP, Calabretta S, Geremia R, et al. (2012) The RNA Binding Protein SAM68 Transiently Localizes in the Chromatoid Body of Male Germ Cells and Influences Expression of Select MicroRNAs. PLoS ONE 7(6): e39729. doi:10.1371/journal.pone.0039729

Editor: Emanuele Buratti, International Centre for Genetic Engineering and Biotechnology, Italy

Received April 2, 2012; **Accepted** May 25, 2012; **Published** June 22, 2012

Funding: This work was supported by Grants from Telethon to C.S. (GGP09154), The Associazione Italiana Ricerca sul Cancro (AIRC) to C.S. (IG 10348) and to M.P.P. (MFAG 11658) and the Italian Ministry of Education (PRIN 2008) to R.G. The funders had no role in study design, data collection and analysis, decision to publish, or preparation of the manuscript.

Competing Interests: The authors have declared that no competing interests exist.

* E-mail: claudio.sette@uniroma2.it

Introduction

Spermatogenesis is characterized by a complex regulation of gene expression. Male germ cells have to face an extended period of silencing of the genome, which occurs during meiotic homologous recombination and during morphological differentiation of haploid spermatids into spermatozoa [1]. As a consequence, a large amount of RNAs is synthesized and stored in male germ cells within ribonucleoprotein particles and granules. The most peculiar example is provided by the chromatoid body (CB), a perinuclear, non-membranous, cloud-like structure that closely resembles the fibrous and dense material named "germ plasm" in lower organisms [2]. In mouse germ cells, few particles resembling the CB first appear in the cytoplasm of late pachytene spermatocytes. After meiosis, the CB condenses to form a single granule in round spermatids, which can be detected until the nucleus of the differentiating spermatids begins to elongate [2]. Due to its large size (~0.5 μm), the CB can be easily observed by phase contrast microscopy and was first described more than 130 years ago in the cytoplasm of rat spermatids [3]. Nevertheless, its molecular composition and biological function(s) have remained largely unknown for over a century [2,4,5]. The recent purification of the CB from mouse germ cells has allowed a more detailed description of its composition [6]. Analysis of the protein content by mass spectrometry revealed that the bulk of the CB mass is composed of six proteins that are involved in different aspects of RNA processing. They include the RNA helicase DDX4/MVH (Mouse VASA Homologue), the PIWI protein named PIWIL1/MIWI, the Tudor domain containing proteins TDRD6 and 7, the gonadotropin regulated testicular helicase DDX25/GRTH and the polyA binding protein PABPC3 [6]. Genetic studies revealed that ablation of *Mvh*, *Miwi*, *Grth*, *Tdrd6* and *Tdrd7* in mice impairs spermatogenesis and male fertility [7–11]. Moreover, the CB of round spermatids in *Miwi*, *Grth*, *Tdrd6* and *Tdrd7* knockout germ cells exhibits morphological abnormalities [8–12]. Although the early meiotic arrest of spermatogenesis in *Mvh* knockout mice prevented this analysis [7], it is likely that MVH also plays a key role in CB assembly and function. Thus, the CB seems to function as an RNA-processing centre in male germ cells, as previously demonstrated for the germ plasm of lower organisms [2].

Pioneer studies using cell labelling and histochemistry had already suggested the presence of RNA and ribonucleoproteins in the CB few decades ago [13,14]. More recent observations have

confirmed that the CB is a site of accumulation of several classes of RNAs, such as microRNAs (miRNAs) [15], PIWI-interacting RNAs (piRNAs) and mRNAs [6]. The finding that polyadenylated mRNAs accumulate in the CB of spermatids [15] together with miRNAs and proteins that are essential for mRNA silencing, further suggests that the CB participates in translational regulation of specific mRNAs. Interestingly, the CB displays a very dynamic nature in germ cells [4,16], suggesting that it may collect RNAs and proteins from the nucleus and function as a control station where the fate of a given RNA is decided [2]. However, in spite of its highly dynamic nature, very few proteins have been shown to transiently localize in the CB at specific stages of spermatogenesis. One example is provided by the RNA binding protein (RBP) HuR, which accumulates in the CB of early round spermatids [17]. In this work, we report that SAM68 transiently localizes in the CB during the meiotic divisions and in early post-meiotic cells. SAM68 is a KH-type RBP involved in several steps of RNA processing in male germ cells, whose function is essential for male fertility [18]. We previously described that SAM68 regulates the alternative splicing and translation of specific mRNAs in meiotic and post-meiotic germ cells [18–20], and that these functions are necessary for the formation of a functional gamete [18]. We now found that, although the major protein components of the CB are correctly recruited in the absence of SAM68, expression of selected miRNAs is altered in *Sam68*$^{-/-}$ male germ cells. Together with the observation that SAM68 interacts with DROSHA and DICER, these results suggest a novel role for SAM68 in CB-linked RNA processing events and in the miRNA pathway during spermatogenesis.

Results

SAM68 localizes in perinuclear granules in secondary spermatocytes and early round spermatids

SAM68 shuttles between nucleus and cytoplasm in differentiating germ cells [18,20]. To investigate in more detail the dynamic nature of its localization, we performed immunofluorescence analysis of purified male germ cells. As previously reported [20], SAM68 is localized in the nucleus of pachytene spermatocytes, it translocates into the cytoplasm of secondary spermatocytes and it localizes again in the nucleus of round spermatids (Figure 1A). However, we also observed that SAM68 accumulates in perinuclear, dense granules resembling the CB in secondary spermatocytes and early round spermatids (Figure 1A).

SAM68 was reported to accumulate in cytoplasmic stress granules upon several cellular stresses [21–23]. To rule out the possibility that the accumulation of SAM68 in perinuclear granules is caused by stress occurring during the purification procedure, we analysed its localization in germ cells squashed out directly from the seminiferous tubules. This technique allows precise description of the stage of the seminiferous tubule by phase contrast microscopy before fixation [24]. We found that SAM68 localized in the cytoplasm and was enriched in perinuclear granules in meiotic spermatocytes from stage XII tubules and in early round spermatids from stages XII and I (Figure 1B). By contrast, starting from late stage I spermatids, SAM68 was predominantly nuclear and this localization was maintained from stage II through VIII (Figure 1B).

These results indicate that SAM68 transiently accumulates in perinuclear granules during the meiotic divisions and the early phases of spermiogenesis.

SAM68 co-localizes with MVH and MILI in the chromatoid body of secondary spermatocytes

To test whether the SAM68-containing granule is the CB, we co-stained purified male germ cells with anti-SAM68 and anti-MVH antibodies or anti-MILI antibodies. SAM68 and MVH localize to different compartments in primary spermatocytes and round spermatids. Namely, SAM68 was found exclusively in the nucleus of meiotic and post-meiotic cells, whereas MVH accumulated in perinuclear structures of primary spermatocytes and in the CB of round spermatids (Figure 2A). However, in secondary spermatocytes a fraction of SAM68 accumulated in the CB-like granules together with MVH (Figure 2A). Similar results were obtained by comparing the localization of SAM68 with that of MILI [25]. As shown in Figure 2B, MILI localized to fibrous, perinuclear structures in primary spermatocytes and in CB-like perinuclear granules that also contained SAM68 in secondary spermatocytes. By contrast, MILI was absent in the majority of round spermatids whereas SAM68 was localized in the nucleus. These results strongly suggest that SAM68 transiently accumulates in the granules that will form the CB during the second meiotic division and in early round spermatids.

To corroborate the association of SAM68 with CB components, we performed immunoprecipitation experiments from purified germ cells. Extracts obtained from a germ cell fraction enriched in secondary spermatocytes [20] were immunoprecipitated with anti-SAM68 or control antibodies. Western blot analysis revealed that MVH was co-immunoprecipitated with the anti-SAM68, but not with control IgGs (Figure 3A). Importantly, co-immunoprecipitation was due to a specific interaction in the dividing meiotic germ cells, as it was not detected in primary spermatocytes and round spermatids (Figure 3B), in which the two proteins localize in different cellular compartments (Figure 2A).

Structural proteins of the chromatoid body are not affected by the ablation of *Sam68*

To further investigate the role of SAM68 in the CB, we subjected sections of *Sam68* wild-type and knockout testes to high-resolution morphological analysis by transmission electron microscopy (EM). We found that the CBs in *Sam68*$^{-/-}$ late round spermatids (steps 6–8) were often smaller and/or appeared incorrectly assembled (Figure 4E, F) as compared to those of wild type germ cells, which are characterized by large and dense masses with many clear islands (Figure 4B). However, in some *Sam68*$^{-/-}$ late round spermatids the CB appeared normal (Figure 4D). Furthermore, in early round spermatids (steps 1–3), the CBs appeared mostly unaffected (Figure 4A, C).

Since the *Sam68* knockout testis is characterized by abnormal differentiation and extensive loss of haploid germ cells [18], the impaired morphology of the CB could be a secondary, indirect effect. To test this hypothesis, we checked whether any CB structural component was lacking in the *Sam68* knockout spermatids. First, we determined the localization of MVH by immunofluorescence analysis of wild type and knockout secondary spermatocytes and early round spermatids. As shown in Figure 5A, the absence of SAM68 did not impair MVH localization in the CB. In addition, we also found that ablation of MIWI, a constitutive component of the CB [6], did not impair the localization of SAM68 in the CB (Figure 5B).

Next, to obtain a comprehensive picture of the CB in *Sam68*$^{-/-}$ germ cells, we used a recently developed method to isolate the CB by immunoprecipitation of MVH after crosslinking and lysis of testicular germ cells [6]. The CB isolation protocol is schematically represented in Figure 6A. All the steps of the immunoprecipitation

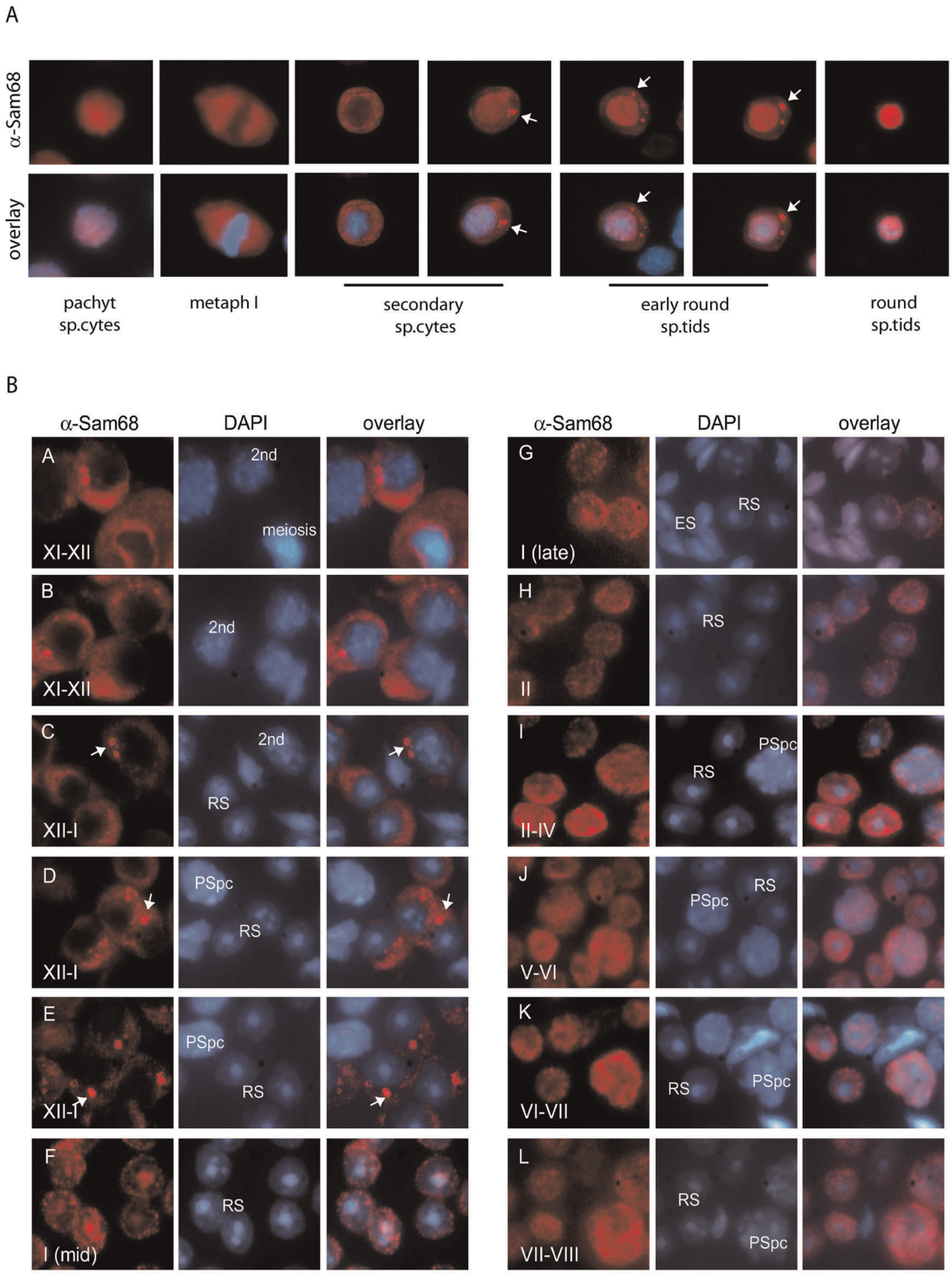

Figure 1. SAM68 accumulates in a perinuclear organelle in secondary spermatocytes and early round spermatids. (**A**) Purified male germ cells were stained with an anti-SAM68 antibody (red) and co-stained with Hoechst (blue) to detect nuclei and to identify cell stages by nuclear morphology. In secondary spermatocytes and early round spermatids SAM68 accumulates into a granule (white arrows) resembling the chromatoid body. (**B**) Stage specific localization of SAM68 during spermatogenesis. Squashes of male germ cells from seminiferous tubules at different stages of spermatogenesis show that SAM68 (red) localizes in the cytoplasm and was enriched in perinuclear granules (arrows) in meiotic spermatocytes from stage XII tubules and in early round spermatids from stages XII and I (A–E). In late stage I spermatids and from stage II through VIII, SAM68 was predominantly nuclear (F–L). Cells were co-stained with DAPI to detect nuclei. 2nd = secondary spermatocytes; RS = round spermatid; PSpc = pachytene spermatocyte; ES = elongated spermatid.
doi:10.1371/journal.pone.0039729.g001

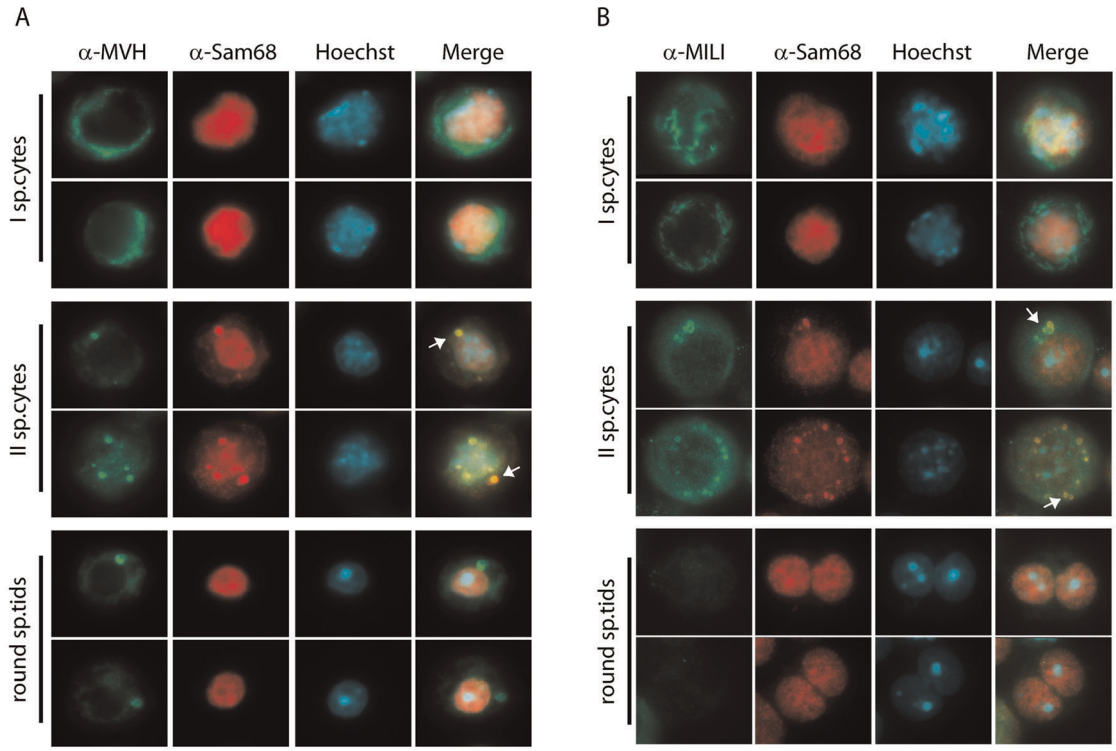

Figure 2. Co-localization of SAM68 with MVH and MILI in male germ cells. (**A**) Isolated male germ cells were co-stained with an anti-SAM68 antibody (red), an anti-MVH antibody (green) and with Hoechst (blue) to detect nuclei. SAM68 and MVH partially co-localize in the CB of secondary spermatocytes (arrows), while in primary spermatocytes SAM68 is nuclear and MVH is cytoplasmic, and in round spermatids SAM68 is nuclear and MVH is predominantly localized in the CB. (**B**) Isolated germ cells were analysed by immunofluorescence using the anti-SAM68 antibody (red) and the anti-MILI antibody (green). Nuclei were stained with Hoechst (blue) to identify cell stages by nuclear morphology. In primary spermatocytes SAM68 localizes in the nucleus, while MILI is cytoplasmic; in round spermatids SAM68 is nuclear and MILI is absent. The localization of the two proteins partially overlaps only in the CB of secondary spermatocytes.
doi:10.1371/journal.pone.0039729.g002

were monitored by immunofluorescence analysis with the CB-specific anti-MVH antibody, which detected a CB-associated granular signal in the pellet fractions (PEL and P2F) (Figure 6B), but not in the supernatant fractions (data not shown). As previously reported [18], the number of round spermatids in the knockout testes was lower than in the wild type testes, thus the isolation yielded less CBs. This is evident from the much weaker MVH signal observed by Western blot analysis in the CB extracts of the knockout samples (Figure 6C). Poly(A)-containing RNAs and small regulatory RNAs such as piRNAs are known to accumulate in the CB [6]. To visualize the small RNA species present in the CBs, total RNA extracted from the control and knockout fractions were 5'-labeled with [γ-32P]ATP and separated on a 15% denaturing polyacrylamide gel. This analysis showed that the *Sam68*$^{-/-}$ CBs contained the characteristic ~30 nucleotide (nt) piRNA band (Figure 6D), although in lower quantities probably due to the lower yield of CBs obtained from the knockout sample.

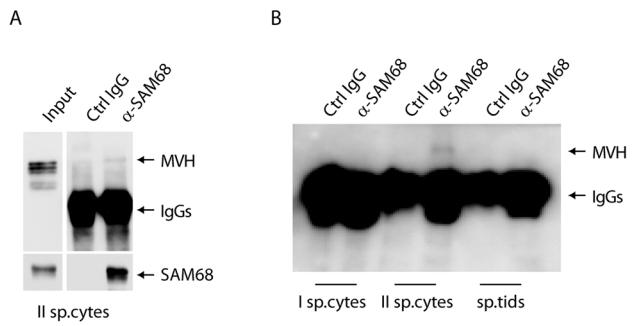

Figure 3. SAM68 co-immunoprecipitates with MVH in secondary spermatocytes. (**A**) Total extract from secondary spermatocytes were immunoprecipitated with an anti-SAM68 antibody and analysed in Westeern blot with anti-MVH and anti-Sam68 antibodies. (**B**) Cellular extracts from spermatocytes (I sp.cytes), secondary spermatocytes (II sp.cytes) and round spermatids (sp.tids) were immunoprecipitated with an anti-SAM68 antibody and detected with anti-MVH antibody. Western blot analysis shows a specific interaction of the two proteins in secondary spermatocytes, while no signal is detected in other germ cell populations.
doi:10.1371/journal.pone.0039729.g003

The purified CBs from wild type and knockout germ cells were then subjected to analysis by mass spectrometry. The main constituents of the CB are MVH, MIWI, TDRD6, TDRD7, GRTH and PABPC3 [6]. In particular, four of these proteins (MIWI, GRTH, TDRD6 and TDRD7) are essential in the maintenance of the normal architecture of the CB [2]. All the main components including the Tudor-domain containing proteins (TDRD1, TDRD6, TDRD7), DEAD box helicases (DDX25 and MVH), poly(A)-containing proteins (PABPC1), PIWI proteins (MIWI and MILI) and other proteins associated with piRNA pathways (MAEL) were present in the knockout CBs (Figure 6E). In agreement with the immunofluorescence results, SAM68 was found in the control CBs but not in the knockout CBs. Some less abundant CB proteins present in the control samples were missing from the *Sam68*$^{-/-}$ CBs (data not shown). However, since the

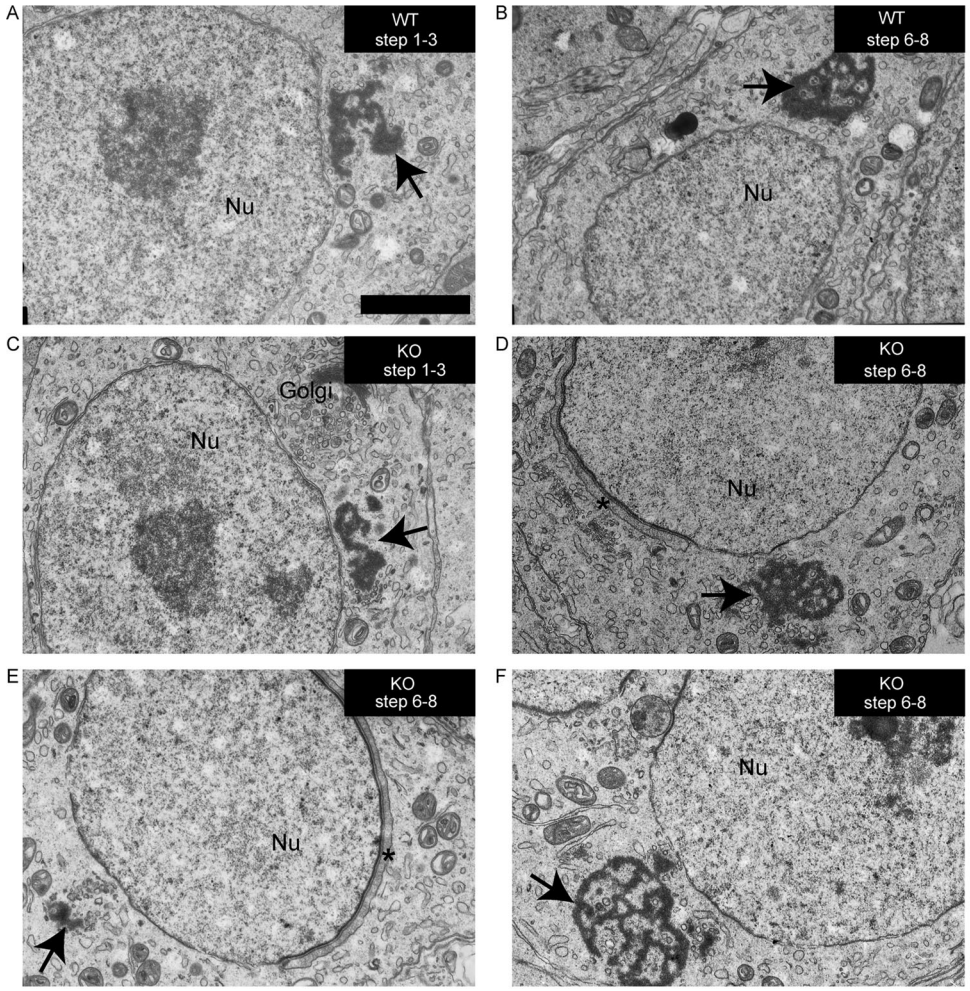

Figure 4. Morphology of the chromatoid body in *Sam68*$^{-/-}$ germ cells. (**A, B**) Round spermatids were analyzed by electron microscopy to study the possible changes in the morphology of the CB caused by the deletion of *Sam68* gene. No differences were found between the early chromatoid bodies (steps 1–3 of round spermatid differentiation) in the control (**A**) and knockout (**C**) testes. The knockout CBs appeared condensed and morphologically normal. In late round spermatids (steps 6–8), the knockout CBs appeared mostly normal (**D**) as compared to the control CBs (**B**). Abnormalities in the CB morphology were also commonly observed in *Sam68*$^{-/-}$ late round spermatids, such as decreased amount of the chromatoid material (**E**) or excess space between the CB lobes (**F**). Arrows point to the CB. Acrosome is indicated by an asterisk. The genotypes and the steps of spermatid differentiation are shown in the upper right corner of each image. WT, *Sam68*$^{+/+}$; KO, *Sam68*$^{-/-}$; Nu, nucleus. Scale bar is 2 µm.
doi:10.1371/journal.pone.0039729.g004

Sam68$^{-/-}$ CB samples were less concentrated, it is likely that less abundant CB components could not be identified reliably.

These results suggest that SAM68 expression is not essential for the CB structure.

SAM68 ablation affects the expression of a subset of microRNAs in male germ cells

In addition to PIWI proteins and piRNAs, the CB was also shown to contain miRNAs and proteins involved in the miRNA maturation pathway [15]. Notably, recent studies have documented a role of splicing factors in the biogenesis of selected miRNAs [26–29]. To investigate the possible involvement of SAM68, a well known splicing regulator [30], in miRNA biogenesis, we first tested its association with key proteins in the pathway. All miRNAs are initially transcribed as primary transcripts that are successively cleaved by two RNase III enzymes, DROSHA in the nucleus and DICER in the cytoplasm, to produce ~70 nt long precursor miRNAs and 22 nt long mature miRNAs, respectively [31]. Co-immunoprecipitation experiments indicated that SAM68 interacts with both DICER (Figure 7A) and DROSHA (Figure 7B) in male germ cells. These interaction were not disrupted by treatment with RNase, indicating that they were not mediated by a bridging RNA (Fig. 7C). These results suggest that SAM68 may participate to miRNA biogenesis. To test this hypothesis, we performed a microarray analysis of miRNAs purified from wild type and knockout primary spermatocytes, secondary spermatocytes and round spermatids (Figure 7D). Hybridization of the purified RNAs to the miRCURY LNA microarray revealed that *Sam68* ablation selectively affected 12 miRNAs, the majority of which (9 out of 12) were upregulated in knockout germ cells (Figure 7D). Interestingly, with the exception of miR-138, all these miRNAs were differentially expressed at stages that are concomitant (secondary spermatocytes) or subsequent (round spermatids) to the association of SAM68 with the CB (Figure 7D). To validate the results of the array, we analyzed the expression of three of these miRNAs (miR-720, miR-142-3p and miR-29b) by quantitative real time PCR. As shown in Figure 7E, all of them were upregulated in *Sam68*$^{-/-}$ germ cells with respect to the corresponding wild type cells.

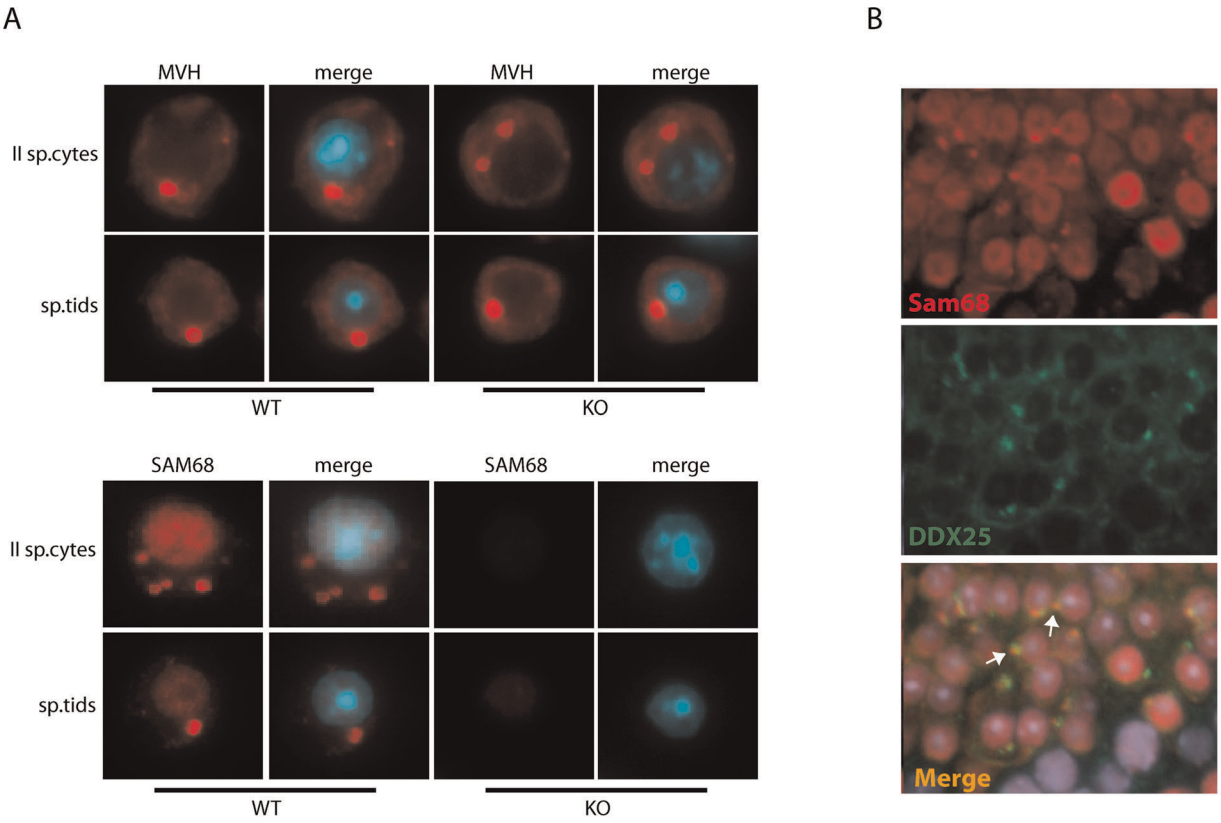

Figure 5. Localization of MVH and SAM68 in the chromatoid body of Sam68 and Miwi knockout germ cells. (**A**) Immunofluorescence analysis with anti-MVH (upper panels) or anti-SAM68 (bottom panels) antibodies of *Sam68* wild type (left panels) and knockout (right panels) male germ cells. Nuclei were detected with Hoechst (blue). (**B**) Immunofluorescence analysis with anti-SAM68 (red) and anti-DDX25 (green) antibodies of *Miwi* knockout (right panels) male germ cells. Nuclei were detected with Hoechst (blue).
doi:10.1371/journal.pone.0039729.g005

These results suggest that SAM68 is involved in the miRNA pathway of male germ cells.

Discussion

The molecular nature and the function of the CB in germ cells have remained elusive and debated for years [2,4,5,32]. Recently, the demonstration that many RBPs and RNA species associate with this structure, has lead to the general consensus that the CB functions as an RNA-processing centre [2,5]. The CB material appears in late pachytene spermatocytes and it fuses together to mould into a single structure in each round spermatid after meiosis [2–4,32,33]. During spermiogenesis, the CB increases in size until step 6, then it moves caudally to the neck region and gradually decreases in size until it disappears in elongating spermatids [5,14,33,34]. Furthermore, the CB dynamically moves within the cytoplasm and exhibits continuous changes in shape and size [4,14]. Nevertheless, very few examples of proteins that transiently associate with the CB have been reported [2,16]. In the present study we demonstrate that SAM68 is one of such proteins, which transiently associates with the CB of secondary spermatocytes and early round spermatids.

SAM68 is a ubiquitously expressed KH-type RBP, whose expression levels and localization vary during cell differentiation in several tissues [35]. In particular, in male germ cells SAM68 is mainly nuclear, but it translocates into the cytoplasm of secondary spermatocytes, where it regulates the translation of specific mRNA targets [18,20]. This function of the protein is essential for the production of a functional gamete, as $Sam68^{-/-}$ haploid germ cells express lower levels of a subset of proteins involved in cell differentiation, display abnormal morphology and undergo massive cell death through apoptotic pathways [18]. We have now observed that during its translocation in the cytoplasm, SAM68 accumulates in perinuclear structures. Co-staining analysis with both anti-MVH and anti-MILI antibodies confirmed that these granules correspond to the forming CB in meiotic and post-meiotic male germ cells. However, SAM68 expression does not seem to be required for CB assembly and structure. Our EM analysis showed that the CB of $Sam68^{-/-}$ early round spermatids (step-2–3) is normal. In late round spermatids (steps 6–8) from knockout testes we often observed smaller and/or incorrectly assembled CBs as compared to those of wild type germ cells. Nevertheless, it is likely that these abnormalities are indirect consequences of the morphological and molecular defects occurring in $Sam68^{-/-}$ haploid germ cells, which ultimately lead to apoptosis (18). This interpretation is also supported by our mass spectrometry analysis of purified CBs. We found that, although less material was obtained from $Sam68^{-/-}$ testes, the main CB protein constituents were all correctly recruited in the absence of SAM68. This unbiased analysis also confirmed that SAM68 was present in the CB purified from wild type germ cells, thus corroborating the immunofluorescence results. Our study also showed that some of the less abundant CB proteins were absent in the CBs of knockout samples, whereas piRNAs were present in lower amounts. However, since a general lower yield in CB material was obtained from the knockout germ cells, we suggest

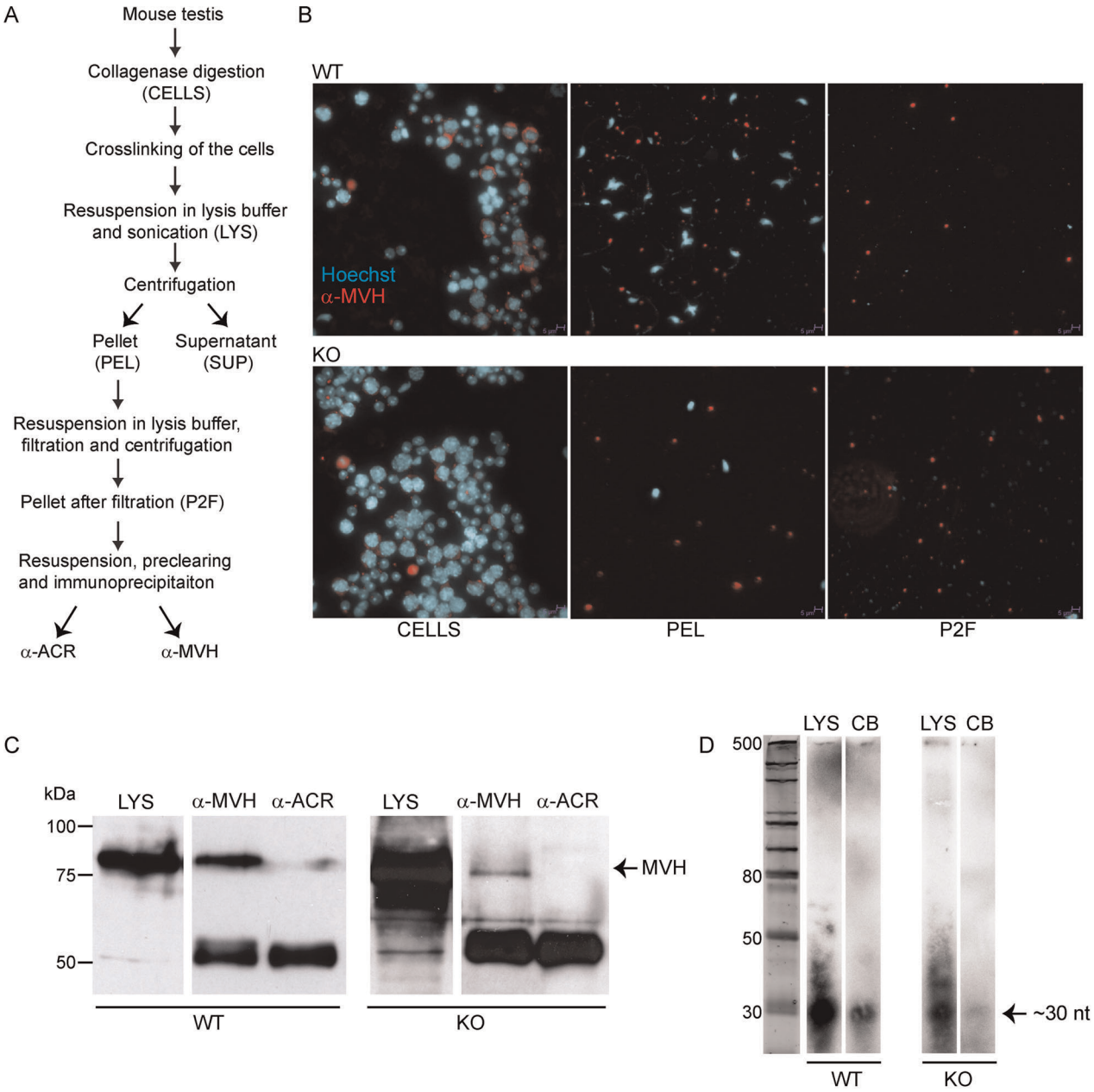

E

Wild Type CB proteins:			
Uniprot Entry Name	Mascot Score	Mass	emPAI
TDRD6_MOUSE	36335	241241	20,6
PIWL1_MOUSE	28098	99424	54,4
DDX4_MOUSE	26269	77278	68,7
TDRD7_MOUSE	21073	123636	17,8
TDRD1_MOUSE	9250	132064	7,5
PIWL2_MOUSE	8247	110615	9,9
RNF17_MOUSE	7204	188616	3,6
DDX25_MOUSE	5453	55354	8,6
PABP1_MOUSE	4587	70854	6,6
TDRD9_MOUSE	2753	157364	1,5
TDRD5_MOUSE	1706	117026	1,3
HS90A_MOUSE	1666	85134	1,6
MAEL_MOUSE	1412	50081	3,6
KHDR1_MOUSE	99	48511	0,2

Sam68-/- CB proteins:			
Uniprot Entry Name	Mascot Score	Mass	emPAI
TDRD6_MOUSE	10402	241241	2,04
DDX4_MOUSE	8145	77278	5,2
PIWL1_MOUSE	6876	99424	3,14
TDRD7_MOUSE	4111	123636	2,22
PIWL2_MOUSE	2370	110615	1,06
RNF17_MOUSE	2350	188616	0,63
TDRD1_MOUSE	1800	132064	0,67
PABP1_MOUSE	1156	70854	1,09
DDX25_MOUSE	1084	55354	0,55
MAEL_MOUSE	674	50081	0,53
TDRD9_MOUSE	348	157364	0,1
HS90A_MOUSE	129	85134	0,11
TDRD5_MOUSE	129	117026	0,08
KHDR1_MOUSE	-	-	-

Figure 6. Isolation and analysis of chromatoid bodies from male germ cells. (**A**) Schematic representation of the CB isolation protocol. (**B**) Immunofluorescence analysis of different steps of CB immunoprecipitation experiment, comparing *Sam68* wild type (WT) and knockout (KO) extracts. Cells were stained with an anti-MVH antibody (red) and with Hoechst to detect nuclei. CELLS = cells before lysis; LYS = lysate; PEL = pellet fraction; P2F = pellet fraction after filtration. (**C**) Immunoblotting of the CB extracts with anti-MVH antibody to validate the success of the purification. The less intensive signal in the knockout CB fraction indicates the lower number of CBs isolated from the knockout testes compared to the control. anti-ACR, negative control IP; anti-MVH, CB IP. (**D**) RNA gel to demonstrate the presence of piRNAs. Total RNA was extracted from the the lysate (LYS) and CB IPs (CB), radiolabelled and run into a polyacrylamide gel in. (**E**) Mascot analysis of the main CB components. All major CB proteins were present in the knockout CBs. The uniprot entry name KDHR_MOUSE equals to SAM68.
doi:10.1371/journal.pone.0039729.g006

that these differences are mainly attributable to the lower concentration of these proteins than to their selective differential recruitment.

Several reports have recently linked the CB to components of the miRNA pathway [2]. First, it was shown that DICER, AGO2, AGO3 and some miRNAs were enriched in the CB of round spermatids [15]. Furthermore, ablation of expression of TDRD6, a CB architectural protein, affected the expression of several miRNAs in the testis, suggesting that TDRD6 is involved in the miRNA pathway [10]. More recently, the RNA DEAD-box helicase GEMIN3 (DDX20), a microRNA biogenesis factor, was shown to accumulate in the CB of human and mouse germ cells [36]. On the other hand, many RBPs that play key role in pre-mRNA splicing, like SAM68, have been recently reported to participate to various steps in the processing of miRNAs [26–29]. Thus, we directly investigated whether SAM68 is involved in miRNA biogenesis in male germ cells. Indeed, we found that SAM68 interacts with DROSHA and DICER, the two RNase III enzymes involved in the nuclear and cytoplasmic processing of the miRNA precursors [31]. The contribution of Sam68 in the processing of miRNAs was also supported by the changes in selected miRNAs observed in *Sam68*$^{-/-}$ male germ cells. Twelve miRNAs were differentially expressed between wild-type and knockout germ cells. The majority of them were up-regulated,

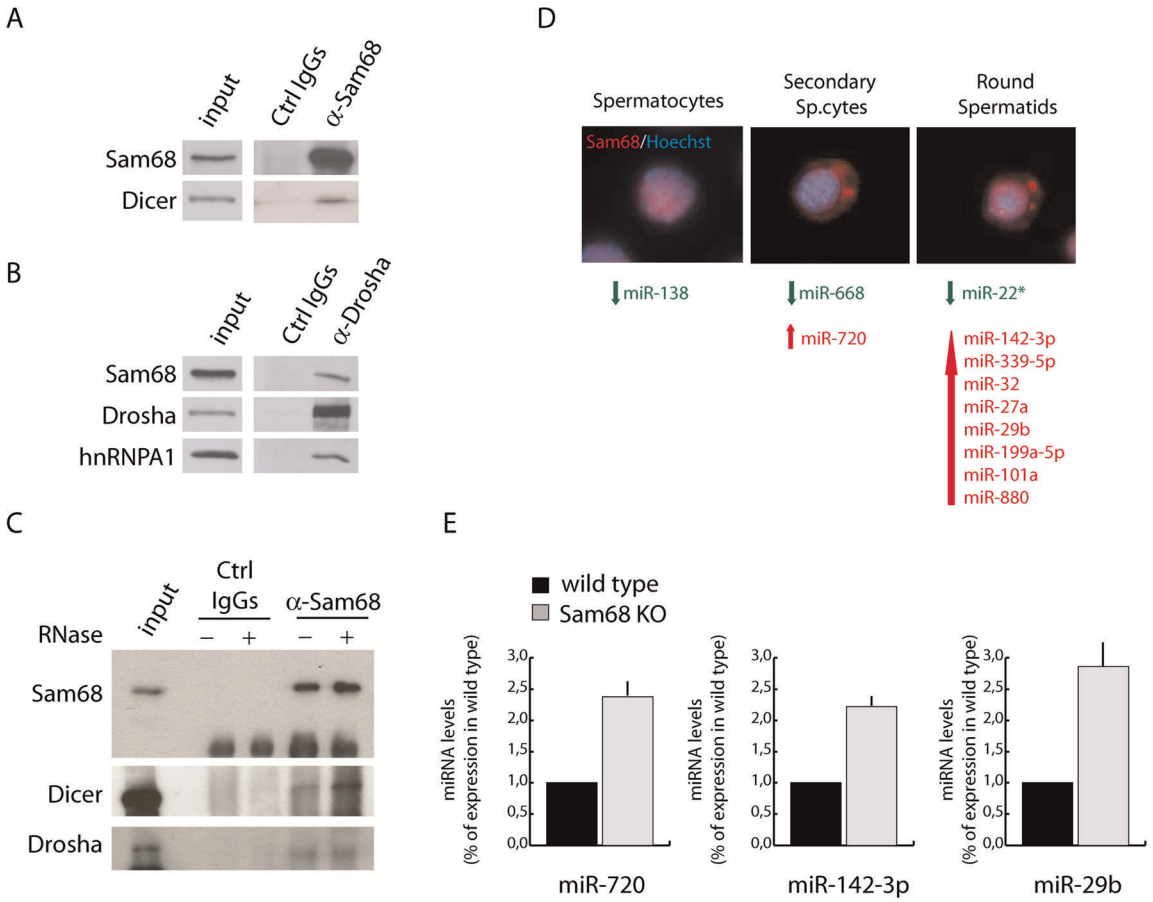

Figure 7. SAM68 is involved in the miRNA pathway in male germ cells. (**A**) Total extract from secondary spermatocytes were immunoprecipitated with an anti-SAM68 antibody and analysed in Western blot with anti-DICER and anti-Sam68 antibodies. (**B**) Cellular extracts from secondary spermatocytes (II sp.cytes) were immunoprecipitated with an anti-DROSHA antibody and detected with anti-DROSHA, anti-SAM68 and anti-hnRNP A1 antibodies. (**C**) Western blot analysis of co-immunoprecipitation performed in the presence of RNase in the cell extract. (**D**) Schematic representation of the microRNAs differentially expressed in the indicated *Sam68* knockout germ cells. In green are indicated the down-regulated microRNAs, in red the up-regulated ones. The immunofluorescence images show the localization of SAM68 in the corresponding wild type germ cells. (**E**) Real Time PCR analysis of miR-720, miR-142-3p and miR-29b in RNA purified from round spermatids of *Sam68* wild-type (black) or knockout (grey) mice. The values were normalized against U6 snRNA and expressed as fold increase with respect to the value of wild type cells.
doi:10.1371/journal.pone.0039729.g007

whereas only three miRNAs were down-regulated in *Sam68*$^{-/-}$ germ cells. Notably, a similar increase of more than 50 miRNAs was also observed in *Tdrd6* knockout testis [10], suggesting that SAM68 may play a similar role in this pathway. The function of most of the SAM68-modulated miRNAs is largely unknown. However, miR-29b was previously proposed to play a role in the modulation of genomic DNA methylation in female primordial germ cells, by negatively regulating the expression DNMT3a and DNMT3b [37]. Notably, miR-29b belongs to a family of miRNAs that are often down-regulated in human cancers, including hormone-resistant prostate cancer (PCa) [38,39], and increased ectopic expression of miR-29b suppressed the metastatic phenotype of PCa cells by repressing epithelial-mesenchymal transition (EMT) signalling [39]. Since SAM68 is frequently up-regulated in PCa, where it contributes to cell proliferation and survival [40,41], these observations suggest that it might regulate miR-29b also in cancer cells. In line with this hypothesis, recent observations indicate that SAM68 contributes to oncogenic transformation by promoting EMT [42]. Thus, it is possible that increased expression of SAM68 in PCa cells is required to suppress miR-29b expression, hence contributing to the aggressive phenotype of these cells.

The expression of miRNAs can be regulated at the post-transcriptional level by modulating nuclear and cytoplasmic processing events. For instance, the KH-type splicing regulatory protein KSRP binds to the terminal loop of its target miRNAs, thereby promoting their processing [28]. The function of KSRP is antagonized by another splicing factor: hnRNP A1. It was shown that hnRNP A1 competes with KSRP for binding to the conserved terminal loop of pri-let-7a-1 and inhibits its processing by DROSHA [27]. Interestingly, hnRNP A1 interacts with DROSHA [26] and with SAM68 [43] in somatic cells, and we found that these three proteins can be co-immunoprecipitated together in male germ cell extracts (Figure 7B). Noteworthy, SAM68 and hnRNP A1 cooperate in the regulation of splicing of at least two common targets [43,44]. Thus, although direct studies to test this possibility need to be performed in the near future, it is tempting to speculate that SAM68 participates to hnRNP A1-mediated processing of selected miRNAs.

In conclusion, our study identifies SAM68 as a novel CB component that transiently associates with this structure and provide evidence for the involvement of SAM68 in the miRNA pathway during spermatogenesis.

Materials and Methods

Cell isolation and culture

The *Sam68* knockout colony was maintained by crossing *Sam68* heterozygous mice. Genotyping of the mice was performed as described previously [45]. Testes from 40–60 day-old CD1 mice (Charles River Laboratories) and C57BL6 *Sam68* wild-type and knockout mice were used to obtain pachytene spermatocytes, secondary spermatocytes, and round spermatids by elutriation technique as described previously [20,46]. After elutriation, pachytene spermatocytes were cultured in minimum essential medium (Invitrogen) and supplemented with 0.5% BSA (Sigma-Aldrich), 1 mM sodium pyruvate, and 2 mM lactate at 32°C in a humidified atmosphere containing 95% air and 5% CO2. At the end of the incubation, cells were washed in phosphate buffered saline (PBS) and used for further experiments.

Immunofluorescence analysis

Mouse germ cells were fixed in 4% paraformaldehyde (PFA) and washed three times in PBS. Cells were permeabilized with 0.1% Triton X-100 (Sigma-Aldrich) for 10 min and then incubated for 1 h in 0.5% BSA. Cells were washed three times in PBS and incubated for 2 h at room temperature (RT) with antibodies against SAM8 (1:1000, Santa Cruz Biotechnology), MVH (1:500; Abcam) or MILI (1:200, Abcam), followed by 1 h incubation with cy3-conjugated anti-mouse IgGs (Alexa Fluor) or FITC-conjugated anti-rabbit IgGs (Alexa Fluor). After washes, slides were mounted with Mowiol reagent (EMD) and analyzed by microscopy at RT as described [22,47]. Images were taken from a fluorescent microscope (Axioskop; Carl Zeiss, Inc.) using a Pan-Neofluar 40×/0.75 objective lens, and from an inverted microscope (DMI6000B; Leica) using a Pan-Neofluar 40×/0.75 objective lens. Images were acquired as TIFF files using an RT slider camera (Diagnostic Instruments) and the IAS2000 software (Biosistem 82) or LIF software (Leica). Photoshop and Illustrator softwares (Adobe) were used for composing the panels.

Immunoprecipitation experiments

Isolated mouse germ cells were washed in PBS and homogenized in lysis buffer [100 mM NaCl, 10 mM MgCl2, 30 mM Tris-HCl, pH 7.4, 1 mM DTT, and protease inhibitor cocktail (Sigma-Aldrich)] supplemented with 0.5% Triton X-100. Soluble extracts were separated by centrifugation at 10000 *g* for 10 min, pre-cleared for 2 h on protein A–Sepharose beads (Sigma-Aldrich) in the presence of rabbit IgGs (5 μg) and 0.05% BSA. After centrifugation for 1 min at 1000 *g*, supernatant fractions were incubated with rabbit anti-SAM68, anti-DROSHA (Abcam) or control IgGs (5 μg) for 3 h at 4°C under constant rotation. After washing, the beads were eluted in SDS sample buffer for Western blot analysis with anti-MVH antibody (1:500).

Chromatoid body immunoprecipitation

Testes from adult C57BL6 *Sam68* wild-type and knockout mice were digested in PBS containing 0.5 mg/ml of collagenase for 60 minutes at room temperature. Digested tubules were filtered through 100 μm filter (BD biosciences) and then centrifuged for 5 minutes at 300 *g*, 4°C. After two washes in PBS, cells were crosslinked in 0.1% PFA for 20 min. The reaction was stopped by adding 0.25 M glycine, pH 7. Cells were washed in PBS, resuspended in RIPA buffer [150 mM NaCl, 50 mM Tris-HCl, pH 7.5, 1 mM DTT, 1% Nonidet P40, 0.5% sodium deoxycholate, 1:200 Riboblock (Fermentas) and protease inhibitor cocktail (Roche)] and sonicated with Bioruptor UCD-200 sonicator (6 cycles of 30 s with 30 s intervals). The cell lysate was centrifuged for 10 minutes at 500 *g*. The pellet containing the CBs was filtered and resuspended in RIPA buffer and used for immunoprecipitation [6]. Cell lysates were pre-cleared with Dynabeads protein G (Invitrogen) for 30 minutes, and then added to Dynabeads protein G coupled with rabbit polyclonal anti-MVH antibody (Abcam, ab13840) or rabbit-polyclonal anti-ACROSIN (Santa Cruz, sc-67151) antibody. Tubes were incubated overnight at 4°C under rotation. Beads were rinsed, resuspended in RIPA buffer and the crosslinks were reversed in the same buffer (for RNA analysis) or in SDS sample buffer (for protein analysis) at 70°C for 45 minutes.

Electron microscopy

Small pieces of testis were cut, fixed in 5% glutaraldehyde and treated with a potassium ferrocyanide-osmium fixative. The samples were embedded in epoxy resin (Glycidether 100, Merck), sectioned, stained with 5% uranyl acetate and 5% lead citrate, and visualized on a JEOL 1200 EX transmission electron microscope.

Mass spectrometric analysis

Proteins were shortly separated with NuPAGE Novex Gel System (Invitrogen) followed by in-gel digestion with Trypsin (Promega) and the extraction of peptides. The peptides were analyzed with LC-MS/MS using an Agilent 1200 series nanoflow system (Agilent Technologies) connected to a LTQ Orbitrap mass-spectrometer (Thermo Electron, San Jose, CA, USA) equipped with a nanoelectrospray ion source (Proxeon, Odense, Denmark).

Microarray analysis

RNA from isolated male germ cells (spermatocytes, secondary spermatocytes and round spermatids) from adult *Sam68*$^{+/+}$ (n = 4) and *Sam68*$^{-/-}$ (n = 4) mice was extracted kit (QIAGEN). RNA samples were tagged for labeling with Cy3 and Cy5 dyes, respectively using QIAzol lysis reagent and the MIRNeasy mini, by using the miRCURY Labeling Kit (Exiqon) for use with Exiqon miRCURY LNA Array (v 10.0). The array consists of probes for the mature forms of all miRNA present in the miRBase 14.0 release of the miRNA registry. Probes corresponds to 1891 mature miRNAs, each represented twice on the microarray. The locked-nucleic acid miRNA probes are highly sensitive and optimized to minimize cross-hybridization between similar mature miRNAs. Two biological replicates for each sample were analysed. For each sample, 4 μg of total RNA was labeled and hybridized to the microarray. Sample RNA quality control was performed using Bioanalyser2100. Microarray data were normalized using the global Lowess (Locally Weighted Scatterplot Smoothing) regression algorithm (Exiqon).

Real time PCR

Validation of selected miRNA expression levels was performed using the Taqman® miRNA Expression Assays (Applied Biosystem). RNA was reverse-transcribed using specific miRNA stem-loop primers and the Taqman® miRNA reverse transcription kit (Applied Biosystems). Mature miRNA expression was measured with Taqman® microRNA assays (Applied Biosystems) according to the manufacturer's instructions and normalized for the expression level of the snRNP U6 RNA.

Acknowledgments

The authors wish to thank Dr Stéphane Richard for providing the *Sam68* knockout mice, Dr Federica Barbagallo for critical reading of the manuscript and Dr. Massimo De Felici for the generous gift of the anti-MVH antibody.

Author Contributions

Conceived and designed the experiments: MPP RG NK CS. Performed the experiments: VM OM MPP SC CS. Analyzed the data: RG NK CS. Contributed reagents/materials/analysis tools: RG NK CS. Wrote the paper: VM OM NK CS.

References

1. Paronetto MP, Sette C (2010) Role of RNA-binding proteins in mammalian spermatogenesis. Int J Androl 33:2–12.
2. Meikar O, Da Ros M, Korhonen H, Kotaja N (2011) Chromatoid body and small RNAs in male germ cells. Reproduction 142:195–209.
3. Benda C (1891) Neue mitteilungen uber die entwickelung der genital-drusen und die metamorphose der samenzellen (histogenese der spermatozoen). Verhandlungen der berliner physiologischen gesellschaft. Arch Anat Physiol 549–552.
4. Parvinen M (2005) The chromatoid body in spermatogenesis. Int J Androl 28:189–201.
5. Kotaja N, Sassone-Corsi P (2007) The chromatoid body: a germ-cell-specific RNA-processing centre. Nat Rev Mol Cell Biol 8:85–90.
6. Meikar O, Da Ros M, Liljenbäck H, Toppari J, Kotaja N (2010) Accumulation of piRNAs in the chromatoid bodies purified by a novel isolation protocol. Exp Cell Res 316:1567–75.
7. Toyooka Y, Tsunekawa N, Takahashi Y, Matsui Y, Satoh M, et al. (2000) Expression and intracellular localization of mouse Vasa-homologue protein during germ cell development. Mech Dev 93:139–49.
8. Deng W, Lin H (2002) Miwi, a murine homolog of piwi, encodes a cytoplasmic protein essential for spermatogenesis. Dev Cell 2:819–30.
9. Tsai-Morris CH, Sheng Y, Lee E, Lei KJ, Dufau ML (2004) Gonadotropin-regulated testicular RNA helicase (GRTH/Ddx25) is essential for spermatid development and completion of spermatogenesis. Proc Natl Acad Sci U S A 101:6373–8.
10. Vasileva A, Tiedau D, Firooznia A, Müller-Reichert T, Jessberger R (2009) Tdrd6 is required for spermiogenesis, chromatoid body architecture, and regulation of miRNA expression. Curr Biol 19:630–9.
11. Tanaka T, Hosokawa M, Vagin VV, Reuter M, Hayashi E, et al. (2011) Tudor domain containing 7 (Tdrd7) is essential for dynamic ribonucleoprotein (RNP) remodeling of chromatoid bodies during spermatogenesis. Proc Natl Acad Sci U S A 108:10579–10584.
12. Kotaja N, Lin H, Parvinen M, Sassone-Corsi P (2006) Interplay of PIWI/Argonaute protein MIWI and kinesin KIF17b in chromatoid bodies of male germ cells. J Cell Sci 119:2819–2825.
13. Sud BN (1961) The chromatoid body in spermatogenesis. Quarterly Journal of Microscopy Science 102: 273–292.
14. Paniagua R, Nistal M, Amat P, Rodríguez MC (1986) Ultrastructural observations on nucleoli and related structures during human spermatogenesis. Anat Embryol (Berl) 174:301–306.
15. Kotaja N, Bhattacharyya SN, Jaskiewicz L, Kimmins S, Parvinen M, et al. (2006) The chromatoid body of male germ cells: similarity with processing bodies and presence of Dicer and microRNA pathway components. Proc Natl Acad Sci U S A 103:2647–2652.
16. Ventelä S, Toppari J, Parvinen M (2003) Intercellular organelle traffic through cytoplasmic bridges in early spermatids of the rat: mechanisms of haploid gene product sharing. Mol Biol Cell 14:2768–2780.
17. Nguyen Chi M, Chalmel F, Agius E, Vanzo N, Khabar KS, et al. (2009) Temporally regulated traffic of HuR and its associated ARE-containing mRNAs from the chromatoid body to polysomes during mouse spermatogenesis. PLoS One 4: e4900.
18. Paronetto MP, Messina V, Bianchi E, Barchi M, Vogel G, et al. (2009) Sam68 regulates translation of target mRNAs in male germ cells, necessary for mouse spermatogenesis. J Cell Biol 185:235–249.
19. Paronetto MP, Messina V, Barchi M, Geremia R, Richard S, et al. (2011) Sam68 marks the transcriptionally active stages of spermatogenesis and modulates alternative splicing in male germ cells. Nucleic Acids Res. 39:4961–4974.
20. Paronetto MP, Zalfa F, Botti F, Geremia R, Bagni C, et al. (2006) The nuclear RNA-binding protein Sam68 translocates to the cytoplasm and associates with the polysomes in mouse spermatocytes. Mol Biol Cell 17:14–24.
21. Henao-Mejia J, Liu Y, Park IW, Zhang J, Sanford J, et al. (2009) Suppression of HIV-1 Nef translation by Sam68 mutant-induced stress granules and nef mRNA sequestration. Mol Cell 33:87–96.
22. Henao-Mejia J, He JJ (2009) Sam68 relocalization into stress granules in response to oxidative stress through complexing with TIA-1. Exp Cell Res 315:3381–3395.
23. Busà R, Geremia R, Sette C (2010) Genotoxic stress causes the accumulation of the splicing regulator Sam68 in nuclear foci of transcriptionally active chromatin. Nucleic Acids Res 38:3005–3018.
24. Kotaja N, Kimmins S, Brancorsini S, Hentsch D, Vonesch JL, et al. (2004) Preparation, isolation and characterization of stage-specific spermatogenic cells for cellular and molecular analysis. Nat Methods 1:249–254.
25. Kuramochi-Miyagawa S, Kimura T, Ijiri TW, Isobe T, Asada N, et al. (2004) Mili, a mammalian member of piwi family gene, is essential for spermatogenesis. Development 131:839–849.
26. Guil S, Cáceres JF (2007) The multifunctional RNA-binding protein hnRNP A1 is required for processing of miR-18a. Nat Struct Mol Biol 14:591–596.
27. Michlewski G, Cáceres JF (2010) Antagonistic role of hnRNP A1 and KSRP in the regulation of let-7a biogenesis. Nat Struct Mol Biol 17:1011–1018.
28. Trabucchi M, Briata P, Garcia-Mayoral M, Haase AD, Filipowicz W, et al. (2009) The RNA-binding protein KSRP promotes the biogenesis of a subset of microRNAs. Nature 459:1010–1014.
29. Wu H, Sun S, Tu K, Gao Y, Xie B, et al. (2010) A splicing-independent function of SF2/ASF in microRNA processing. Mol Cell 38:67–77.
30. Bielli P, Busà R, Paronetto MP, Sette C (2011) The RNA-binding protein Sam68 is a multifunctional player in human cancer. Endocr Relat Cancer 18: R91-R102.
31. Subramanyam D, Blelloch R (2011) From microRNAs to targets: pathway discovery in cell fate transitions. Curr Opin Genet Dev 21:498–503.
32. Yokota S (2008) Historical survey on chromatoid body research. Acta Histochem Cytochem 41:65–82.

33. Chuma S, Hosokawa M, Tanaka T, Nakatsuji N (2009) Ultrastructural characterization of spermatogenesis and its evolutionary conservation in the germline: germinal granules in mammals. Mol Cell Endocrinol. 306:17–23.
34. Onohara Y, Fujiwara T, Yasukochi T, Himeno M, Yokota S (2010) Localization of mouse vasa homolog protein in chromatoid body and related nuage structures of mammalian spermatogenic cells during spermatogenesis. Histochem Cell Biol 133:627–639.
35. Sette C, Messina V, Paronetto MP (2010) Sam68: a new STAR in the male fertility firmament. J Androl 31:66–74.
36. Ginter-Matuszewska B, Kusz K, Spik A, Grzeszkowiak D, Rembiszewska A, et al. (2011) NANOS1 and PUMILIO2 bind microRNA biogenesis factor GEMIN3, within chromatoid body in human germ cells. Histochem Cell Biol 136:279–287.
37. Takada S, Berezikov E, Choi YL, Yamashita Y, Mano H (2009) Potential role of miR-29b in modulation of Dnmt3a and Dnmt3b expression in primordial germ cells of female mouse embryos. RNA 15:1507–1514.
38. Porkka KP, Pfeiffer MJ, Waltering KK, Vessella RL, Tammela TL, et al. (2007) MicroRNA expression profiling in prostate cancer. Cancer Res 67:6130–6135.
39. Ru P, Steele R, Newhall P, Phillips NJ, Toth K, et al. (2012) MicroRNA-29b Suppresses Prostate Cancer Metastasis by Regulating Epithelial-Mesenchymal Transition Signaling. Mol Cancer Ther 11:1166–1173.
40. Busà R, Paronetto MP, Farini D, Pierantozzi E, Botti F, et al. (2007) The RNA-binding protein Sam68 contributes to proliferation and survival of human prostate cancer cells. Oncogene 26:4372–4382.
41. Paronetto MP, Cappellari M, Busà R, Pedrotti S, Vitali R, et al. (2010) Alternative splicing of the cyclin D1 proto-oncogene is regulated by the RNA-binding protein Sam68. Cancer Res 70:229–239.
42. Valacca C, Bonomi S, Buratti E, Pedrotti S, Baralle FE, et al. (2010) Sam68 regulates EMT through alternative splicing-activated nonsense-mediated mRNA decay of the SF2/ASF proto-oncogene. J Cell Biol 191:87–99.
43. Paronetto MP, Achsel T, Massiello A, Chalfant CE, Sette C (2007) The RNA-binding protein Sam68 modulates the alternative splicing of Bcl-x. J Cell Biol 176:929–939.
44. Pedrotti S, Bielli P, Paronetto MP, Ciccosanti F, Fimia GM, et al. (2010) The splicing regulator Sam68 binds to a novel exonic splicing silencer and functions in SMN2 alternative splicing in spinal muscular atrophy. EMBO J 29:1235–1247.
45. Richard S, Torabi N, Franco GV, Tremblay GA, Chen T, et al. (2005) Ablation of the Sam68 RNA binding protein protects mice from age-related bone loss. PLoS Genet 1: e74.
46. Sette C, Barchi M, Bianchini A, Conti M, Rossi P, et al. (1999) Activation of the mitogen-activated protein kinase ERK1 during meiotic progression of mouse pachytene spermatocytes. J Biol Chem 274:33571–33579.
47. Paronetto MP, Giorda E, Carsetti R, Rossi P, Geremia R, et al. (2004) Functional interaction between p90Rsk2 and Emi1 contributes to the metaphase arrest of mouse oocytes. EMBO J 23:4649–4659.

Aknowledgements

Ringrazio il Professor Delle Fave per avermi dato la possibilità di svolgere questo dottorato permettendomi di intraprendere questa interessante linea di ricerca.
Ringrazio il mio tutor, il Professor Sette per i suoi insegnamenti e per avermi seguito costantemente durante tutto il mio percorso.
Ringrazio il Dottor Capurso per le sue preziose indicazioni.
Ringrazio il Professor Geremia, il Professor Rossi, Susanna, Paola, Donatella e Marco per i loro utili consigli.
Ringrazio infine tutte le mie colleghe e colleghi, di Tor Vergata e del Santa Lucia, per il sostegno e la collaborazione.